# High Temperature Superconducting Microwave Switch

by
Michael M. Neel
*G & C Systems Division*

**December 1996**

**NAVAL AIR WARFARE CENTER WEAPONS DIVISION**
**CHINA LAKE, CA 93555-6100**


# Naval Air Warfare Center Weapons Division

## FOREWORD

This report presents the design, construction and testing of a High Temperature Superconductive Microwave Switch. This work was performed at the Naval Air Warfare Center Weapons Division, China Lake, Calif., during fiscal year 1995 in support of High Temperature Superconducting Antenna program sponsored by the Office of Naval Research, Code 312, Washington, DC. This work was monitored initially by Dr. Don Liebenberg and subsequently by Dr. Deborah Van Vechten under fund document N0001496WX20379.

This report is a working document subject to change and was reviewed for technical accuracy by Donald R. Bowling.

Approved by
K. L. HIGGINS, *Head*
*Guidance and Control Systems Division*
15 December 1996

Under authority of
J. V. CHENEVEY
RAdm, U.S. Navy
*Commander*

Released for publication by
S. HAALAND
*Director for Research and Engineering*

NAWCWPNS Technical Publication 8335

Published by . . . . . Technical Information Division
Collation . . . . . Cover, 46 leaves
First printing . . . . . 55 copies

# REPORT DOCUMENTATION PAGE

*Form Approved*
*OMB No. 0704-0188*



| 1. AGENCY USE ONLY *(Leave blank)* | 2. REPORT DATE | 3. REPORT TYPE AND DATES COVERED |
|---|---|---|
| | December 1996 | Interim report—April 1995-June 1996 |

**4. TITLE AND SUBTITLE**
High Temperature Superconducting Microwave Switch

**5. FUNDING NUMBERS**
N0001496WX20379

**6. AUTHOR(S)**
Michael M. Neel

**7. PERFORMING ORGANIZATION NAME(S) AND ADDRESS(ES)**
Naval Air Warfare Center Weapons Division
China Lake, CA 93555-6100

**8. PERFORMING ORGANIZATION REPORT NUMBER**
NAWCWPNS TP 8335

**9. SPONSORING/MONITORING AGENCY NAME(S) AND ADDRESS(ES)**
Dr. Deborah VanVechten
Code 312
Office of Naval Research
Washington, DC 22217-5660

**10. SPONSORING/MONITORING AGENCY REPORT NUMBER**

**11. SUPPLEMENTARY NOTES**

**12A. DISTRIBUTION/AVAILABILITY STATEMENT**
A Statement; public release; distribution unlimited.

**12B. DISTRIBUTION CODE**

**13. ABSTRACT** *(Maximum 200 words)*

(U) This report presents the design, construction, and testing of a high temperature superconducting microwave switch. The circuit is implemented in microstrip trasmission line geometry and utilizes voltage and/or current to create the switching action.

(U) Results of RF power limiting are also presented.

**14. SUBJECT TERMS**
Superconducting, Switch, Microstrip, Voltage Switching, Power Limiting, Laser Induced Switching

**15. NUMBER OF PAGES**
93

**16. PRICE CODE**

| 17. SECURITY CLASSIFICATION OF REPORT | 18. SECURITY CLASSIFICATION OF THIS PAGE | 19. SECURITY CLASSIFICATION OF ABSTRACT | 20. LIMITATION OF ABSTRACT |
|---|---|---|---|
| UNCLASSIFIED | UNCLASSIFIED | UNCLASSIFIED | UL |

## CONTENTS

Introduction ..... 3

Design of Microstrip Switch Circuit ..... 3

Steady-State Circuit Tests ..... 5

Heater Line Current and Microstrip Line Voltage Switching Tests ..... 5

Two-Millimeter Switch Circuit #1 ..... 10

Laser-Induced Switching Tests ..... 11

Pulsed Switching Tests ..... 11

Power Limiting Tests ..... 14

Conclusion ..... 15

References ..... 17

Appendixes:

A. Microstrip Circuit Design and Analysis ..... 19
B. Circuit and Circuit Housing Design ..... 35
C. Switch Insertion and Return Loss Data ..... 41
D. NRL Test Results on Conductus Circuits ..... 73
E. Laser Illuminated Switch Results ..... 83
F. Pulsed Switching Results ..... 85

## INTRODUCTION

During fiscal year 1994, work was begun on the design and fabrication of a superconducting microwave switch. This Naval Air Warfare Center Weapons Division (NAWCWPNS), China Lake, Calif., design incorporates a microstrip line section with narrow line width, and thin metallization that allows for switching the superconducting metal between the "normal" and superconducting states. Three different methods of producing the change in state are used, each of which provide unique advantages.

This report addresses the approach used to design and fabricate the switch and the final test results of the different configurations tested. These test results are compared to results shown in journal articles about similar devices. Conclusions about the possible superconducting mechanisms which allow for the change of state are drawn.

## DESIGN OF MICROSTRIP SWITCH CIRCUIT

The original concept for a microwave switch utilizing superconducting metals was published in 1991 (Reference 1). This paper addressed the design and testing of a coplanar waveguide switch. A subsequent paper in 1993 (Reference 2) addressed a further modification of this design, which provided improved switching speed. The NAWCWPNS program requirements for the High Temperature Superconductive (HTS) Antenna program at NAWCWPNS called for the use of a microstrip transmission line switch. This switch circuit is illustrated in simple fashion in Figure 1.

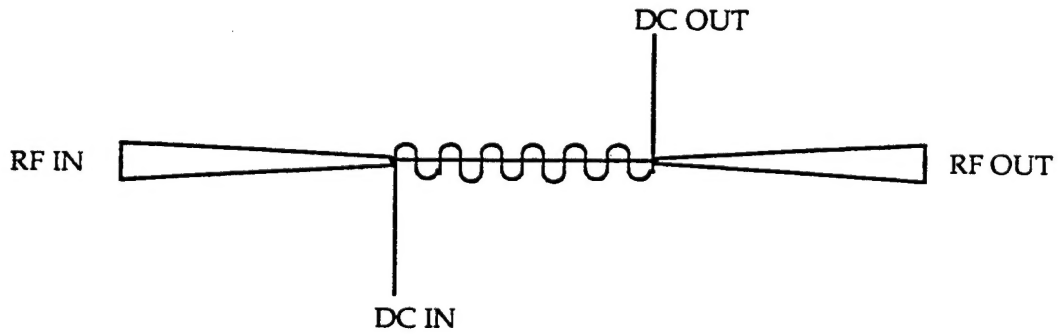


FIGURE 1. Superconducting Microstrip Switch (Simplified Illustration).

The microstrip line is made of 250-nanometer-thick yttrium-barium-copper oxide (YBCO) material deposited on a 0.020-inch-thick lanthanum aluminate substrate. The center section is 10-micrometer wide, and 1 to 3 millimeters long (depends on circuit version tested), with the metal thickness thinned to approximately 100 nanometer. The

microstrip line had a 0.50-micrometer-thick layer of polyimide deposited over it to serve as an insulator, on which the DC lines shown were deposited. This circuit followed the basic ideas presented in References 1 and 2 for inducing the switching mechanism in the superconductor, i.e., the use of DC current through the top level meandered line to heat the superconductive metal above its transition temperature.

The mechanical and thermal design of this center section is important in actually attaining switching of the superconductive metal from superconductive to "normal" state (which is about 100 times higher resistance than copper). In the previous referenced papers, the switching action was obtained by thinning the line thickness to about 100 nanometers. This allows the switching section to reach a high total resistance when it is either heated or pushed above the critical current. This high resistance produces a reflective switching action.

The other factor of switching that is affected by the thermal design of the circuit is the heat sinking around the switching section. In Reference 2, the substrate was thinned down, which gave a seven times better switching speed (from 3.5 to 0.5 microseconds). In order to allow the circuit to switch, the heat sinking under the narrow microstrip line section has to be poor. This allows the DC lines to heat up the microstrip when current is induced.

These factors were taken into account during the design of the circuit and housing, which was performed jointly by J.S. Martens (working at Conductus Inc., Sunnyvale, CA during this time period) and the Naval Air Warfare Center Weapons Division, China Lake, CA.

The basic microstrip line design analysis was performed initially at Conductus Inc. The results indicated a range of practical values for the length of the narrow switching section from 1 to 3 millimeters. This was based on estimated values of room temperature resistivity of 200 micro-ohm-centimeters and Superconducting conductivity of $3.9 * 10^9$ mho/meter, and metal compound thicknesses of 20 to 200 nanometers. These values gave a baseline of parametric performance about which to order the circuit geometry.

This initial design was verified with an EM analysis program, IE3D from Zeland Software, Fremont, CA. All six of the different designs were analyzed and verified to agree within reason with the somewhat estimated design from Conductus, and to follow the expected variations from shorter line sections to longer line sections. (The detailed microstrip design and analysis of Conductus Inc. and NAWCWPNS is in Appendix A.) These analyses performed indicated the use of a 2 to 3 millimeter-long switch section to be the most likely to give good cutoff in the "off" state and good match in the "on" state.

The circuit was defined to fit on a 1-centimeter chip, allowing a practical chip size and about 15 chips on each wafer. This circuit was designed to fit in the center of a "holder" circuit, which would allow convenient connector mounting and provide for the interchange of circuit chips in the same housing. The circuit and housing design are illustrated in Appendix B. The main design feature of the housing is the cutout under the microstrip Superconducting chip. The chip is held in place by small clamps, with a 0.050-inch mounting ledge around the perimeter. Most of the chip is not in direct contact with the metal housing, providing for poor heat sinking to allow the circuit line to heat up.

## STEADY-STATE CIRCUIT TESTS

Once the circuits were fabricated and mounted in the housing, a series of steady-state switching tests were performed. These tests were done to investigate the use of three separate switching mechanisms. One method was to heat the circuit by means of DC current in the overlaid lines above the microstrip line. The other was to induce a voltage across the microstrip line, similar to the method in Reference 3. The last method was to illuminate the microstrip line with a medium-power laser spot. The first two methods were used at the facilities at NAWCWPNS. The laser switching tests were performed at the Naval Research Laboratories (NRL), Washington, D.C.

## HEATER LINE CURRENT AND MICROSTRIP LINE VOLTAGE SWITCHING TESTS

During the planning for the switching tests, it was noted that the tests could be done more efficiently if the heater current and induced voltage switching tests were done together. These tests were set up to allow for a combination of switching conditions to show parametric curves of cut-off level versus voltage and current. A simple illustration of these conditions is shown in Figure 2.

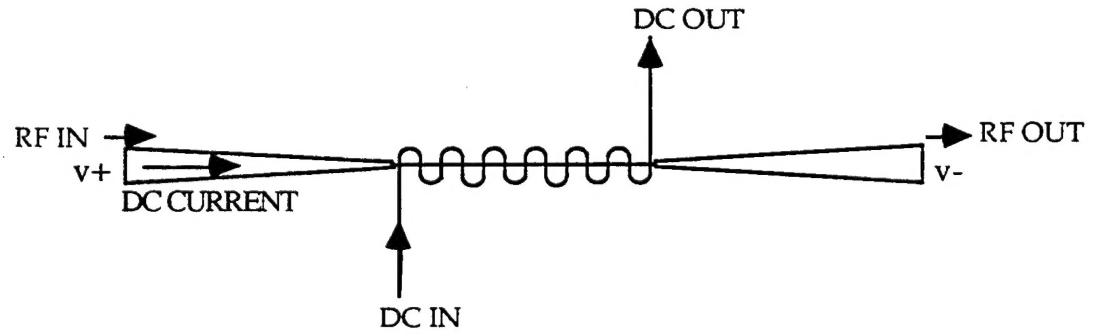


FIGURE 2. Superconducting Microstrip Heater Current and Voltage Switching Methods.

A test matrix for these tests was set up to investigate changes due to circuit temperature (with no heater current or line voltage) and at a fixed temperature with different combinations of heater current and line voltage. This matrix is shown in Table 1.

TABLE 1. Switch Test Condition Matrix.

| Test # | Temp (kelvin) | Heater current (ma) | Line voltage (volts) |
|---|---|---|---|
| 1 | 100 | 0 | 0 |
| 2 | 90 | 0 | 0 |
| 3 | 80 | 0 | 0 |
| 4 | 77 | 0 | 0 |
| 6 | 77 | 5 | 0 |
| 7 | 77 | 10 | 0 |
| 8 | 77 | 15 | 0 |
| 9 | 77 | 0 | 5 |
| 10 | 77 | 0 | 10 |
| 11 | 77 | 0 | 15 |
| 12 | 77 | 5 | 5 |
| 13 | 77 | 10 | 5 |
| 14 | 77 | 15 | 5 |
| 15 | 77 | 5 | 10 |
| 16 | 77 | 10 | 10 |
| 17 | 77 | 15 | 10 |
| 18 | 77 | 5 | 15 |
| 19 | 77 | 10 | 15 |
| 20 | 77 | 15 | 15 |

These tests should indicate the relative quality of the HTS circuit (Tests 1 through 4 indicating the transition of the HTS compound) and provide three parametric curves of heater current and line voltage versus switching cut-off level. The test equipment block diagram for these tests is illustrated in Figure 3.

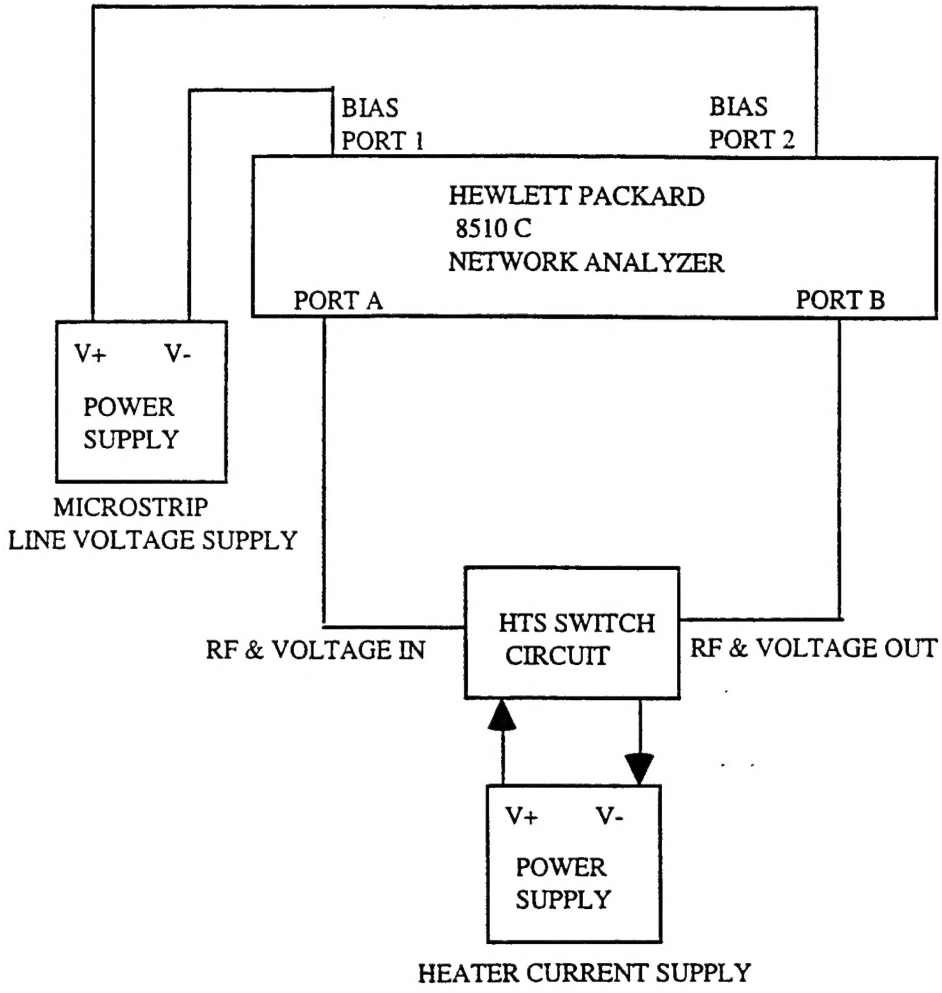


FIGURE 3. Test Equipment Setup for Heater Current and Line Voltage Switching.

The circuit was cooled by placing it on an aluminum stand inside a foam Dewar, which was filled with liquid nitrogen. The circuit housing has a connection for a temperature sensor to indicate the circuit housing temperature.

Tests 1 through 4 were performed by calibrating the network analyzer at the coaxial cable ends with a full two-port calibration, using open-short-load calibration standards and then connecting to the circuit. The Dewar was then filled to the appropriate level to bring the circuit to the desired temperature.

Tests 6 through 20 were performed by using TRL calibration standards. Each TRL standard was placed in the Dewar and brought to 77 K before calibrating. In this way most of the effects of the housing, connectors, and wire connections should be removed.

All the tests were done over the 500 MHz to 2.0 GHz frequency range, using a stepped sweep of 201 points.

Three different circuits were tested. Two circuits with a 3-millimeter-long switching circuit section (3 millimeter #1, and 3 millimeter #2) and one with a 2-millimeter-long switching circuit section. It was noted during the tests that the room temperature resistances of these circuits were quite different from each other. This indicates a difference in either the quality of the Superconductor compound or the thickness of the switching sections. (The frequency versus insertion and return loss test data and measured room temperature resistances is contained in Appendix C.) The parametric curves of insertion loss (S21) versus heater current and line voltage are illustrated in Figures 4, 5 and 6.

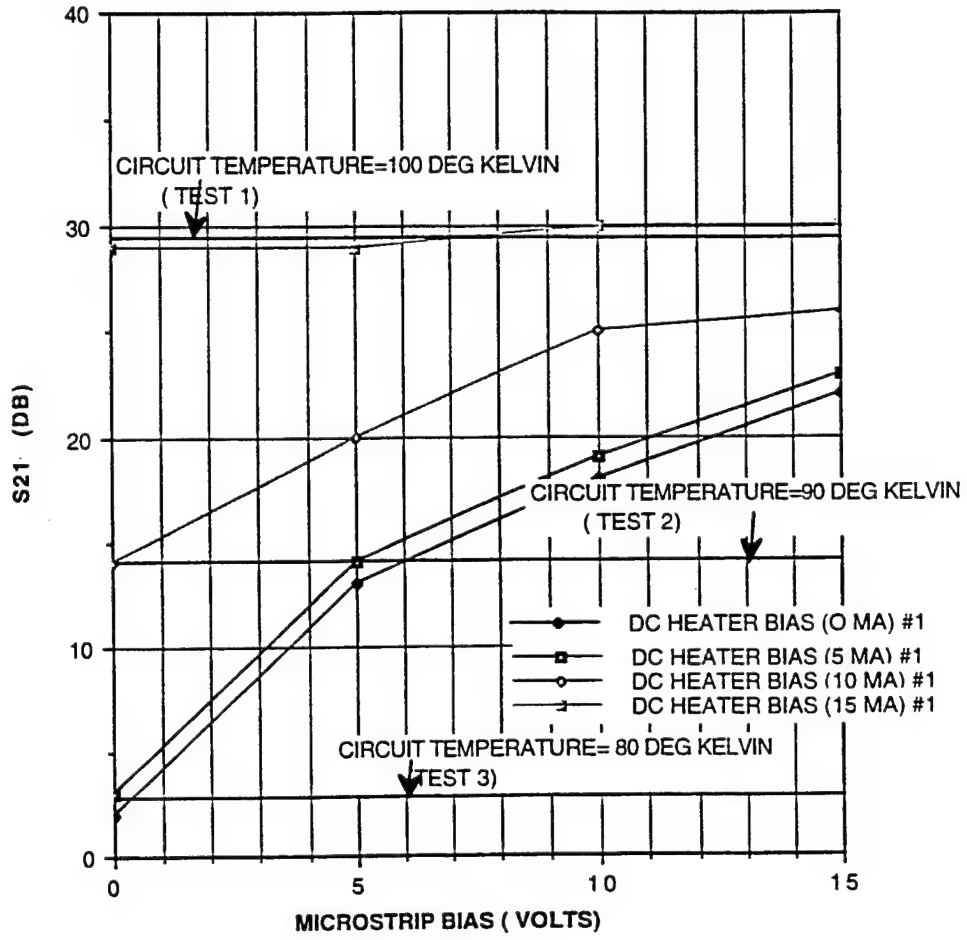


FIGURE 4. Three-Millimeter Switch Section (#1) With 40-Micrometer Pitch DC Heater Lines (77 K).

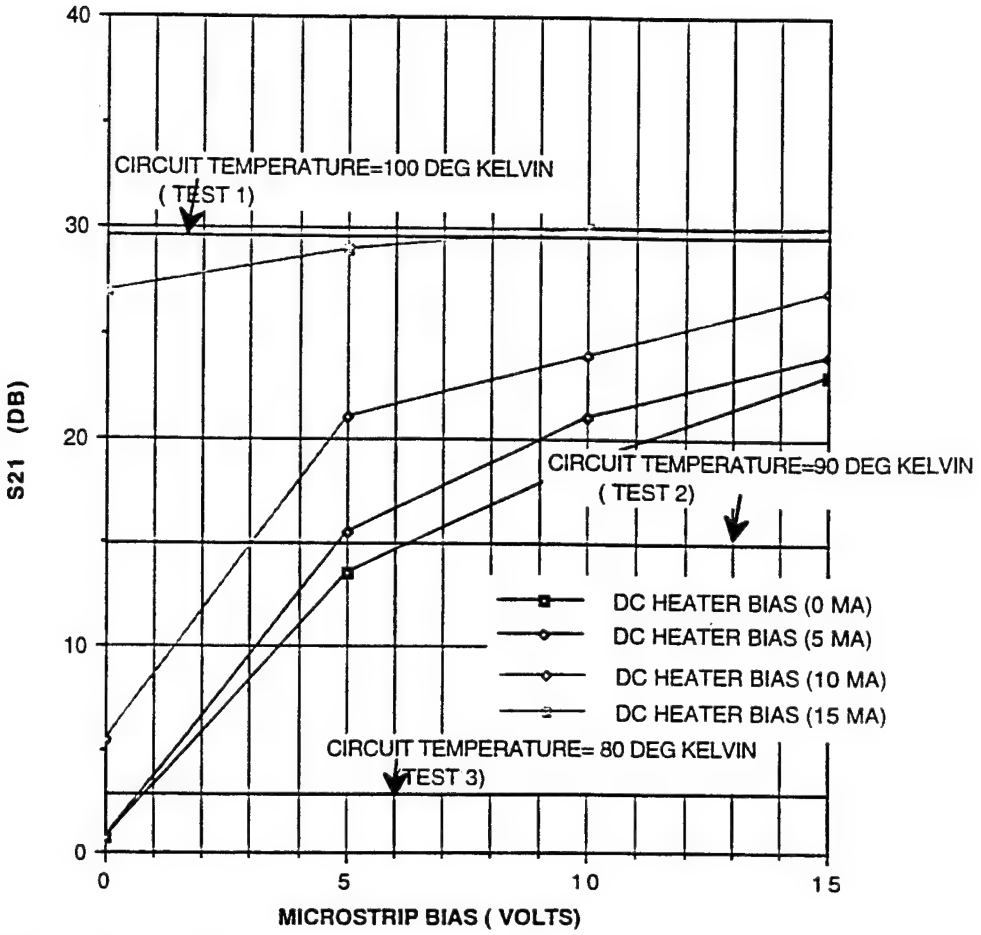


FIGURE 5. Three-Millimeter Switch Section (#2) With 40-Micrometer Pitch DC Heater Lines (77 K).

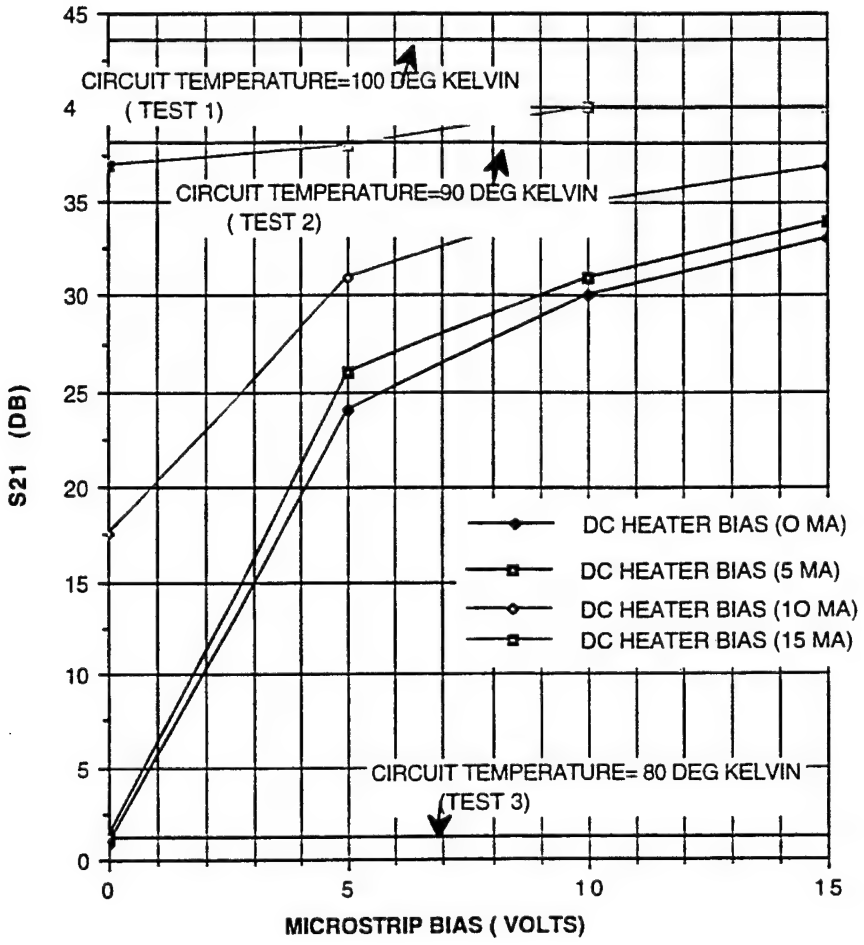


FIGURE 6. Two-Millimeter Switch Section With 40-Micrometer Pitch DC Heater Lines (77 K).

## 2 MILLIMETER SWITCH CIRCUIT #1

These results indicate a maximum cut-off level of 30 dB for the 3-millimeter circuits and 40 dB for the 2-millimeter section. The difference between the 3-millimeter-long and 2-millimeter-long circuits runs contrary to the simulated analysis and to reasonably expected results. The reason for the change is the higher room temperature resistance. The 2-millimeter circuit had a 6.8 K ohm resistance as compared to 4.0 K ohm for the 3-millimeter circuits. This difference indicates a circuit that would have a higher resistance when either warmed up to a higher temperature or is pushed past its maximum current capacity level.

The change in state for the induced voltage switching is also quite different for the 2-millimeter switch. The minimum cut-off for the 3-millimeter switches is 13 dB at 5 volts, and 23 dB for the 2-millimeter switch.

The possible reasons for the higher resistance in the 2-millimeter circuit are that the material itself was of poorer quality or the center region was thinner (verified as a possibility by NRL tests, Appendix D). Either of these conditions would cause the circuit to have a higher resistance and more insertion loss when switched to the "normal" state.

## LASER-INDUCED SWITCHING TESTS

The previous tests demonstrated two electrical methods of inducing the superconducting compound to switch to a high resistance state. The other method available was to illuminate the switching section with a medium-power laser. This should induce an initial non-thermal response in the compound to begin a switching action, and a thermal longer term effect to retain the "normal" state.

This work was done primarily by Valerie Browning and Jeffrey Pond of NRL. Identical circuits were used for the laser switching tests, without the DC heater lines overlaid. In addition, detailed tests of the superconductor compound quality were performed. These tests confirmed the large variation of the compounds from circuit to circuit. (Report is contained in Appendix D.)

The laser induced switching tests were performed over the 50 MHz to 5 GHz frequency range. The laser power was set to six different levels, with the circuit at two different temperatures. (These test results are shown in Appendix E.) They indicate a cut-off level of about 20 dB maximum for the highest laser power. A slight change can be seen between the 77 K tests and the 75 K tests. The composite circuit resistance was also measured for the different laser powers. It indicates a very linear change versus laser power.

These tests demonstrate the feasibility of switching a superconductor to the "normal" state using laser illumination.

## PULSED SWITCHING TESTS

In addition to steady-state switching, the pulsed switching response of the circuits was investigated. The response of pulsed heater current similar to References 1 and 2 and pulsed line voltage similar to Reference 3 was tested. The test setup is illustrated in Figure 7.

In these tests, an RF crystal detector was used to show the switched RF response on an oscilloscope. The heater current is induced through the same heater lines as the previous tests. The microstrip line voltage is induced through bias tees at each end of the circuit. The amplifier boosts the output RF power to the detector to provide an easily seen RF response to an oscilloscope. The current breakout box was a short series wire that provided a place to utilize a current probe to measure the series current to the circuit.

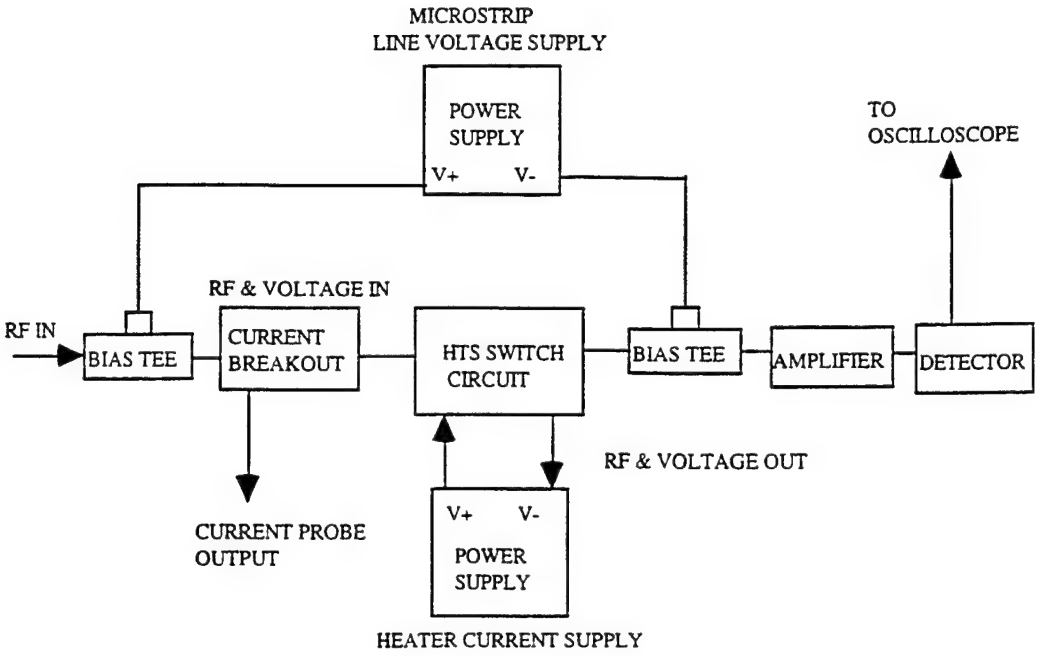


FIGURE 7. Test Equipment Setup for Heater Current and Line Voltage Switching.

The pulsed heater current switching test results were much different from those obtained by J.S. Martens. The observed switching time was on the order of 1 second or more. This was not surprising since this switching mechanism uses heating of the entire length of the switching section to produce the change of state. In this case, the package thermal design is a large contributor to the switching speed and the thermal design issues are not well understood at this time. It is guessed that the differences in package design between the work of J.S. Martens and our circuit is the cause of the large difference in switching speeds.

The transmission line voltage method of switching (where voltage is imposed across the transmission line itself) has not had published results shown previously. The work in Reference 3 shows DC measurements of current versus voltage and transmission loss for various bias voltages, which indicated the strong possibility of series voltage switching but did not show any pulsed switching test results.

Initial tests indicated that switched pulse rise/fall times of nanoseconds were possible. This is a speed improvement of 1000 over previous results using heater lines to induce switching.

Due to the fast switching speeds expected, the test setup was examined carefully to find the rise/fall time measurement limitations. (Pulsed switching test results are in Appendix F.) The pulse generator used had a rated rise/fall time of 1 nanosecond. Possible sources of high time constant are the detector, bias tees, and amplifier. The detector and amplifier induced rise/fall times were tested by connecting the pulse generator to the amplitude modulation input of the RF generator and measuring the output pulse rise/fall time. This was found to be 5 nanoseconds.

The overall rise/fall time of the test circuit was checked by connecting everything except the switch circuit and measuring the rise/fall time. This was also found to be 5 nanoseconds. Thus, the fastest rise/fall time that could be expected to be measured with the equipment used was 5 nanoseconds.

The circuit with a 2-millimeter long switching section was cooled to 77 K in a foam Dewar filled with liquid nitrogen. The RF input power was set to -10 dBm. Voltage pulses were applied through the bias tees and initially set to a 50-nanosecond pulse width and a 100-nanosecond period. The pulse amplitude was set to various values and the detected RF waveform observed on an oscilloscope. It was found in general that the rise/fall time of the output pulsed RF was about 8 nanoseconds. The interesting aspects of the tests were in the changes in pulse shape and switched "on" level observed. The best conditions noted were at a switching pulse amplitude of 0.5 volt. The output pulse shape was clean, with a detected "on " level of 8 millivolts. As the switching pulse amplitude was raised, the switched "on" edge of the output pulse showed more ringing type response and the "on" level decreased. With a switching pulse amplitude of 5 volts, no power is transmitted through the switch. This indicates a change in basic circuit state. The low-amplitude switching pulse serves to push the superconductor into the "normal" state without sinking excess heat into the surroundings. The higher voltages create more heat, which eventually creates a steady state condition that will keep the superconductor in the "normal" state. The input voltages and currents were measured using a current probe attached to the input bias line. These measurements indicated that the power dissipated in the circuit and the resistance of the switching section. Tables 2, 3, and 4 summarize the pulsed tests.

TABLE 2. Voltage and Current Measurements
(50-nanosecond pulse width, 1-microsecond period).

| Pulse Amplitude (Volts) | Peak Current ( ma) | Avg. Current (ma) | Resistance (ohms) | Power Dissipated (mw) |
|---|---|---|---|---|
| 0.94 | 9 | 4.5 | 208 | 4.2 |
| 0.7 | 7 | 4 | 175 | 2.8 |
| 0.5 | 4.8 | 3.2 | 156 | 1.6 |

TABLE 3. Detected RF Switching Times.

| Pulse amplitude (volts) | Detected RF cut off time (ns) | Detected RF turn on time (ns) |
|---|---|---|
| 0.8 | 3 | 14 |
| 0.7 | 4 | 8 |
| 0.5 | 3 | 6 |
| 0.4 | 3 | 4 |

TABLE 4. Pulse Cut Off Characteristics
(50-nanosecond pulse width, 100-nanosecond period).

| Pulse amplitude (volts) | Detector "on" level (mv) | Peak-to-peak output voltage (mv) | Detected RF turn on time ( ns) | Pulse ring characteristics |
|---|---|---|---|---|
| 0.45 | 7 | 40 | 4 | |
| 0.5 | 8 | 60 | 7 | small |
| 1.0 | 6 | 80 | 6 | moderate |
| 2.0 | 4 | 120 | 14 | large |
| 3.0 | 2 | 140 | 20 | very large |
| 5.0 | none | | | |

From the above data, it is seen that as the switching pulse voltage amplitude is raised above 0.5 volt, that the dissipated power rises. This raises the local heating and begins to sink more heat into the substrate. A similar effect was noted when the pulse period was decreased or the incident RF power was increased. In order to attain nanosecond switching times, the switch design must be done carefully to avoid too much power (DC or RF) being sunk into the switch. This limits the amount of cutoff that can be attained. From tests of insertion loss versus voltage bias, 0.5 volt bias gave about 10 dB of cutoff. With careful design using multiple biased sections, it appears that a switch that can provide a 40-dB on/off ratio and nanosecond switching times is possible.

## POWER LIMITING TESTS

From previous tests at NRL and NAWCWPNS, the effect of switch cutoff from incident RF power was noticed. A test was performed to measure the RF power limiting capability of this switch design. The input and output power was measured for a range of input power from -20 to +32 dBm. The measured data are illustrated in Figure 8.

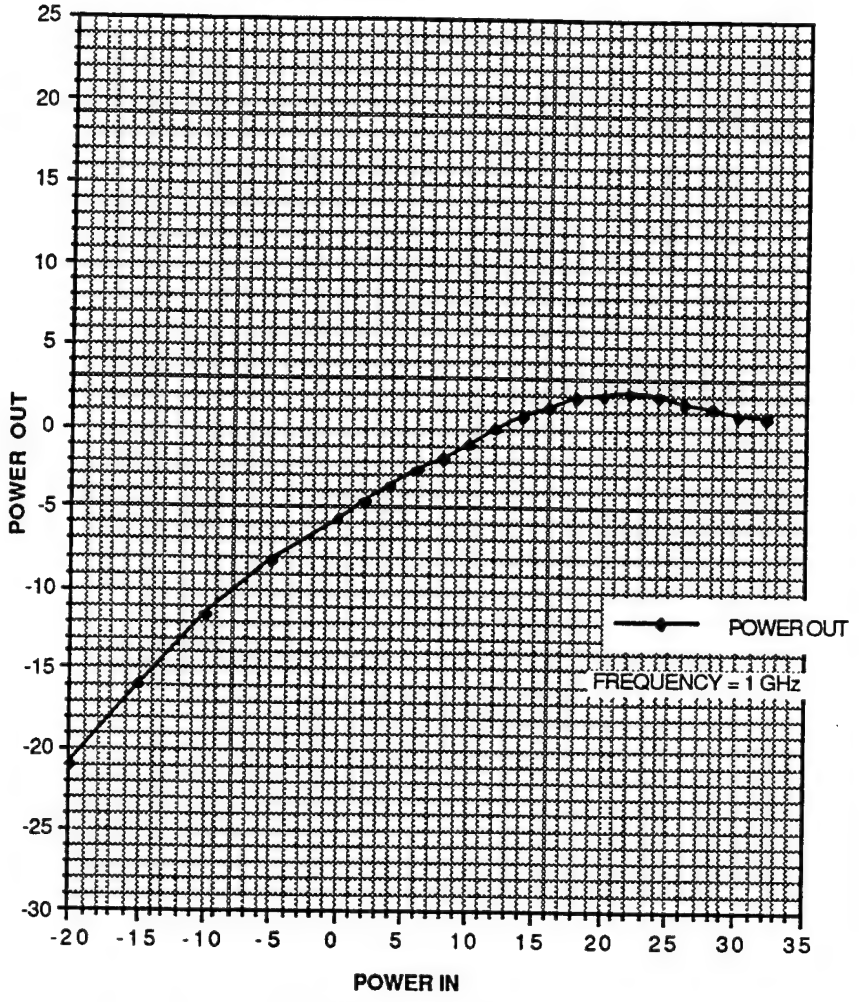


FIGURE 8. Two-Millimeter Switch #1 Power Limiting.

This data indicate a linear response up to -10 dBm input power. At that power, the slope of the curve starts to change and continues to change until the input power reaches +20 dBm, where the output power does not exceed +2 dBm. This seems to be an effective power-limiting capability and can undoubtedly be tailored for different responses by changes in the switch geometry. The simplicity of the circuit presents excellent possibilities for insertion into receiver circuits that are already utilizing HTS materials.

## CONCLUSION

A HTS switch controllable by a series voltage bias, heater line current or laser light is demonstrated. Proper design of the voltage bias can produce nanosecond switching times.

Pulsed laser illumination is also believed to be capable of yielding similar results. As a result of the circuit geometry used, this device will also work as a power limiter with proven limiting ability up to 2 watts input power.

This device is useful in HTS circuit and antenna applications which require fast switching speeds and simple circuitry.

## REFERENCES

1. J. S. Martens, et al. "A Reflective Microwave Switch Made of Tl-Ca-Ba-Cu-O for Signal Control Applications," *Microwave and Guided Wave Letters*, Vol. 1, No. 10 (October 1991), pp. 291-93.

2. J. S. Martens, et al. "HTS Based Switched Filter Banks and Delay Lines," *IEEE Transactions on Applied Superconductivity*, Vol. 3, No. 1 (March 1993), pp. 2824-27.

3. G. Darcy Poulin, et al. "A Superconducting Microwave Switch," 1994 Applied Superconductivity Conference, Boston, Mass.

# Appendix A

## MICROSTRIP CIRCUIT DESIGN AND ANALYSIS

### CONDUCTUS INC.

Design and Simulation Document
Account 7005-000 on Customer PO N68936-94-M-G473
Thermal Switch Test Circuits

Per request, six designs of thermal switches for use on YBCO were generated using 3 permutations on active area geometry and two permutations on control line geometry. The designs and the rationale for their selection are presented below along with small signal simulation results in the low microwave frequency regime. The design and simulations cover only the active region, its feed lines and the control structure and does not include pads, wire bonds, or other external items.

### ZEROTH ORDER DESIGN ISSUES

One of the base desires is to get an extenction ratio (difference between on state and off state insertion losses) of 30 dB or higher while operating in the low Ghz range. Since the switches will be electrically small (a few mm at worst), the insertion loss in the off state will be dominated by the normal state resistance of the bridge. A first place to start then is the minimum number of squares (length divided by width) for the bridge.

Recall that for a simple impedance Z inserted in a transmission line, the S-parameters are given by

$$S_{11} = S_{22} = \frac{Z}{2Z_o + Z}$$

$$S_{121} = S_{21} = \frac{2Z_o}{2Z_o + Z}$$

where $Z_o$ is the characteristic impednace of the transmission environment (50 Ω in this case). If we assume Z in the on-state is 0, Z in the off state is primarily resistive, and we wish $|S_{21}|$ in the off state to be 30 dB lower ($|S_{21}| = 0.032$), then Z must be at least 3025 Ω.

It is possible to arrive at this through multiple switches or some clever $\lambda/4$ switch spacing but we will neglect that posibility for the time being. This is a very conservative design goal.

Assumptions

Temperature during the off state will be between 120 and 160K. This will be dependent on packaging and the cryogenic approach used during testing but was typical in previous work. Excellent heat sinking of the substrate is probably not a good idea since the heater line will then not be able to provide enough heat to switch the circuit. Some heat sinking is of course required (it could be extremely small) or the switch will never return to the on state.

In this temperature range, a lower bound on resistivity is about 100 μΩ-cm although it appears a better value for reasonable YBCO is about 200 μΩ-cm. Poor YBCO and some other materials may have values an order of magnetude higher. The trade-off with those materials is an increase in on state insertion loss and a reduction in power handling capability.

The entire active area goes normal in the off state. This is not guaranteed but is somewhat likely since there is positive feedback involved once one section goes normal.

Using the above resistivity and resistance goal, we see

$$\frac{L}{W} > 1.51t$$

where t is the film thickness (in the switch region) in nm, L is the active area length, and W is the active area width. If t is 200 nm, then the active area should be 300 squares while if t is 20 nm, the active area shoud be about 30 squares. If W is restricted to 10 μm (minimum based on present design rules), then

$$L(\mu m) > 15.1t$$

where t is still the thickness in nm giving a range on minimum L of 300 to 3000 μm depending on film thickness and degree of safety margin desired.

## THE DESIGN BASE

The overall design is shown in Figure A-1. As is discussed in the next section, the parameters to be varied will be somewhat limited. The design information here is limited to the active region.

Not to scale, control line not shown in top drawing

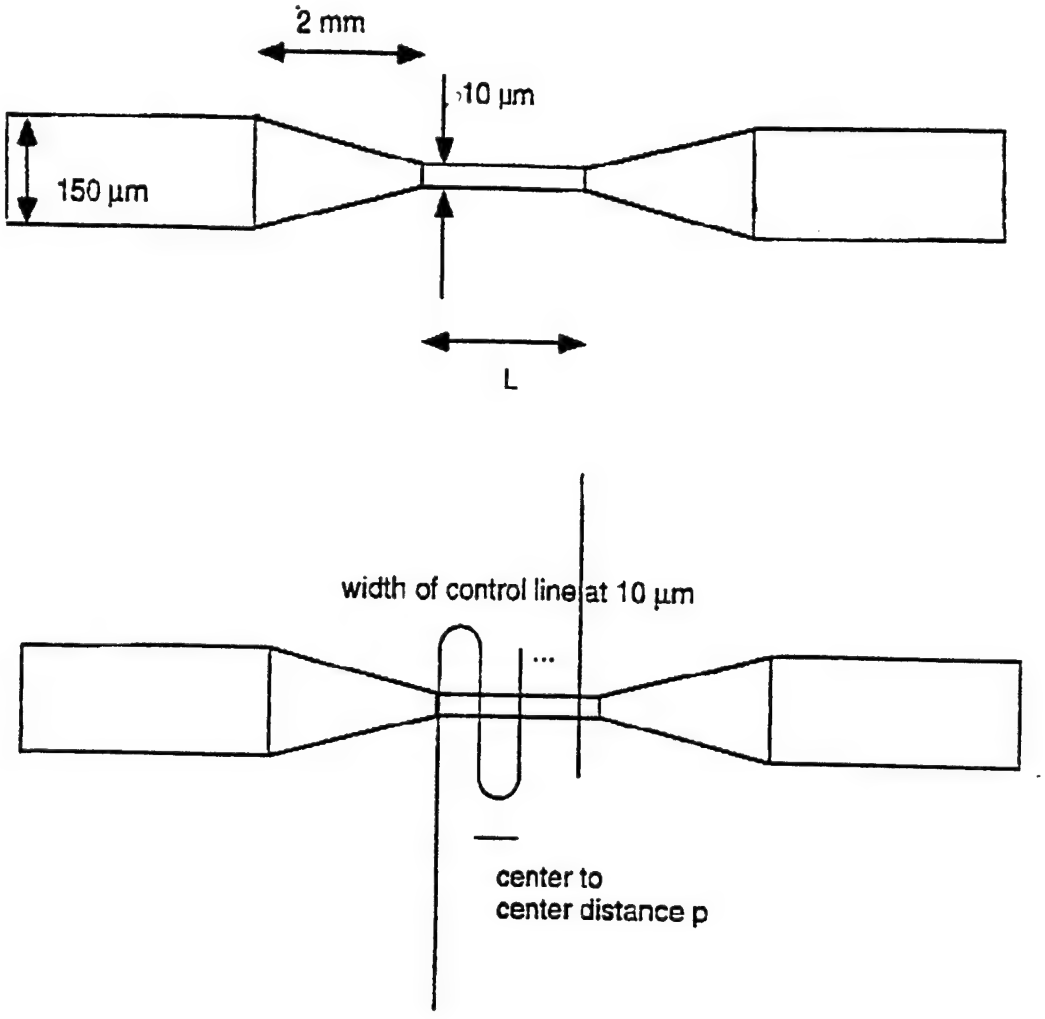


FIGURE A-1. Number of Meanders Fixed by L and P.

## Three Bridge Configurations

One set of permutations is to fix the width at 10 µm and vary only the length over this range of values (e.g., 300 µm, 0.95 and 3 mm). The remaining variable is then the taper length where the goal is to minimize the RF disruption caused by the presence of a narrow active region. Since at 1 Ghz, the wavelength on $LaAlO_3$ (microstrip form) exceeds 7.5 cm, it is not realistic to expect a multi-$\lambda$ transformer. Since the active region is itself electrically small, we can take some liberties. To keep even the largest bridge comfortable on a $cm^2$ chip, use a taper length of 2 mm for all designs.

## Control Line Configurations

In all cases, the meandering control line should cover the entire active area. The permutation variable is the dgree of coverage. Again assume a 10 μm control line width and use two different line pitches as illustrated in Figure A-2. The straight length in all cases should be a minimum of 70 μm with a circular arc at each end maintaining the 10 μm linewidth. The pitch (defined as the spacing from the center of one straight section to the center of the next straight section) can be 40 and 80 μm for the two permutations.

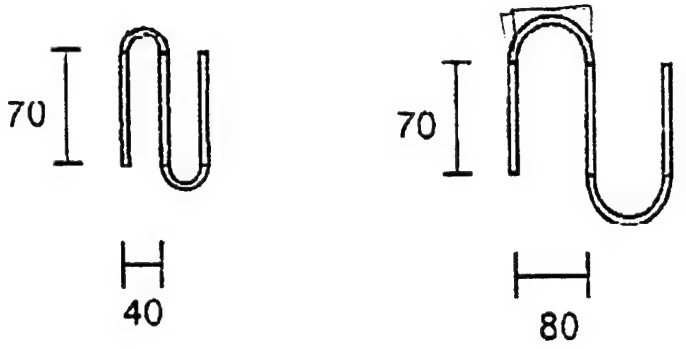


FIGURE A-2. Schematic of the Control Line Geometry for Two Permutations. Dimensions are in microns. Only three straight sections are shown here. In the actual designs, enough straight sections would be used to cover the active region.

The only remaining variables in the control line sectrion are in the material used and in how the feed is done. The pads for the feed must obviously be large to permit wire bonding and having narrow line before reaching the active area unnecessarily increases resistance. The line should be kept at at least 50 μm wide until within about 1 mm of the active region to minimize those effects.

Assuming that the control line resistance will be dominated by the meander section, then the approximate control line resistance is $X\rho$ (in $\Omega$) where X is in the following table (= 16/(wt) where l is the length of the meander section, w is 10 μm and t is the thickness). The length of the meander is scaled with the bridge length so that in all cases the meander covers, as close as is possible, the entire active region. The resistivity of the material was not known at the time this document was prepared. If gold (+ adhesion layer) is used, a reasonable value is 5 to 10 μΩ-cm and would probably be a factor of 3 higher for Mo.

| X | L = 0.3 mm | L = 0.95 mm | L = 3 mm |
|---|---|---|---|
| Ctd line pitch = 40 μm | 4.34 | 14.65 | 48.2 |
| Ctrl line pitch = 80 μm | 1.680 | 7.00 | 24.3 |

Depending on the actual control materials used, the power dissipation in the control line when applying a dc current $I_{ctl}$ is simply

$$P_{ctl} \approx I_{ctl}^2 X \rho$$

This should probably not exceed a few hundred mW to avoid the control line exploding BUT THAT IS NOT A GUARANTEED AVAILABLE POWER LEVEL. The exact limit will be dependent on packaging, cryo-engineering and the microstructure of the control line metalization. Experimental care is extremely important on this issue.

Simulation Results

The six scenarios were simulated with a plausible collection of parasitics to get a better picture of the S-parameters in the range of 0.5 to 2 Ghz. The dominant parasitics are the capacitance between the main line and the control line and the interaction between the time constants in the two sides of the circuit. The microstrip parasitcs are drawn from the usual reference (and in the simulation software). The capacitance between the control line and the hot line was teated as two lumped elements with a fringing capacitance estimated from an electrostatic model. A fringing parallel plate model was used including some contributions from ground plane linking (relevant because the dielectric constant of $LaAlO_3$ is so much higher that that of the interlevel polyimide dielectric). The inductance was calculated using a high impedance transmission line model with some reduction for the presence of other conducting bodies nearby. The resistance of the control line was calculated using no spreading terms but the simulation of the resistive active area did include penetration and spreading effects. No attempt was made at a full-wave simulation in light of the time constaints on this project.

Tables of the main changing circuit parameters are below: control linc inductance L1, control line resistance R1 (assuming 8 μΩ-cm, an Au average), and interlink capacitance C1. Some anomalous spreading capacitance was added to the calculated values and is based on previous experimental results.

| L1(nH) | Length - 0.3 | Length - 0.95 | Length = 3 |
|---|---|---|---|
| Pitch = 40 | 0.5 | 1.6 | 5.5 |
| Pitch = 80 | 0.15 | 0.75 | 2.7 |

| R1(Ω) | Length - 0.3 | Length - 0.95 | Length = 3 |
|---|---|---|---|
| Pitch = 40 | 35 | 117 | 384 |
| Pitch = 80 | 15 | 56 | 194 |

| C1(pF) | Length - 0.3 | Length - 0.95 | Length = 3 |
|---|---|---|---|
| Pitch = 40 | 0.18 | 0.46 | 1.46 |
| Pitch = 80 | 0.16 | 0.22 | 0.75 |

One example of the schematic used for simulations is shown in Figure A-3. The actual values change depending on which of the 6 designs is being simulated (Tline3, R1, L1, C1, C2, Tline1, and Tline2 all change). The switch state is controlled through Tline3. Note that Cap1 + Cap2 = C1 from the above table. L2, L3, R2, and R3 could change depending on how the drive circuit is done but the inductances will probably not be smaller than this which is most important (isolation reasons). The resistance R4 was used for some convergence control and to look at any spreading effects. As would be expected because of the low frequencies being used here, there were few errors induced by treating the normal active area as an RL circuit.

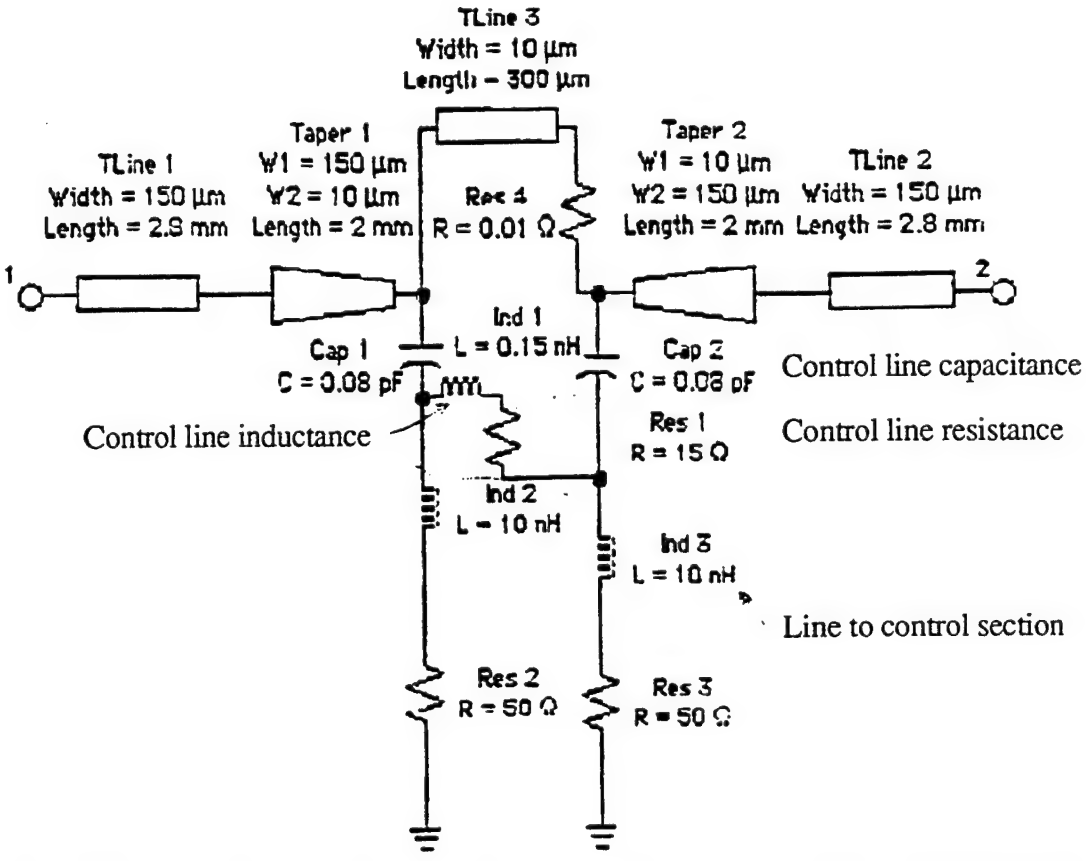


FIGURE A-3. Base Schematic for the Simulations. The parameters Tline3, C1, C2, L1, R1, Tline1, and Tline2 changes as the various permutations are simulated.

A microstrip model was used throughout (and all of the associated discontinuity models) using the substrate definition below. This is for one of the feed line sections and assumes worst case scenarios on roughness, effective rf loss and loss tangent. None of these figure strongly in these particular simulations anyway. The dielectric constant is only accurate on $LaAlO_3$ to 2 to 5% just from intra-wafer and inter-wafer variations. Again this does not enter strongly into these particular simulations.

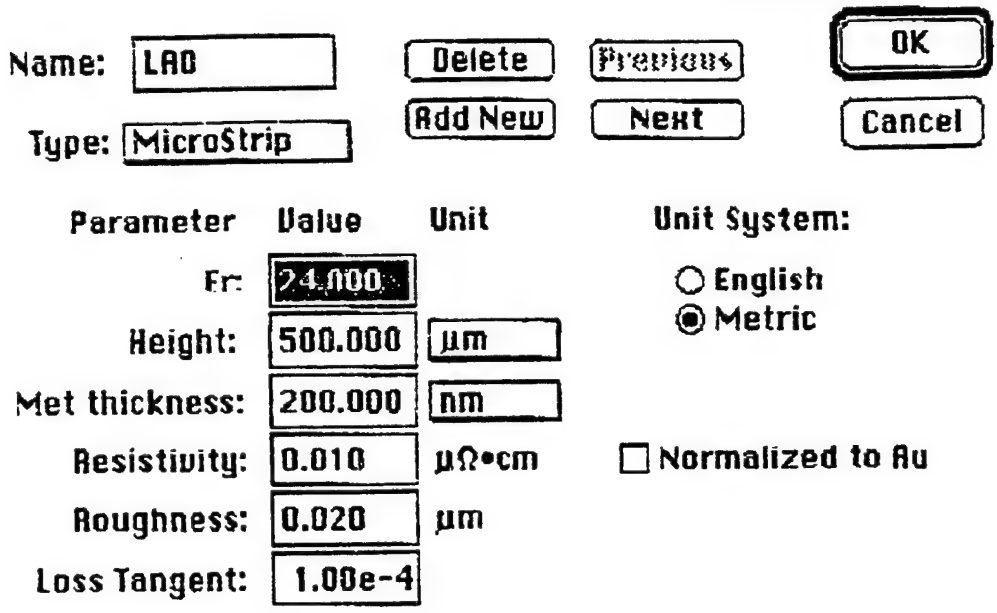


For each of the 6 permutations, the magnitude of $S_{11}$ and $S_{21}$ are plotted in Figure A-4. For each circuit, the simulations were run with the switch on, the switch off assuming a 200 nm film, and the switch off assuming a 20 nm film. The differences between the on state performance with the two film thicknesses was not significant under these small signal conditions. The active area length (in mm) and control line pitch (in µm) are printed in the upper left corner of each plot and this code 0.3 40 for example) will be used in the following discussion.

0.3-MILLIMETER SWITCH SECTION

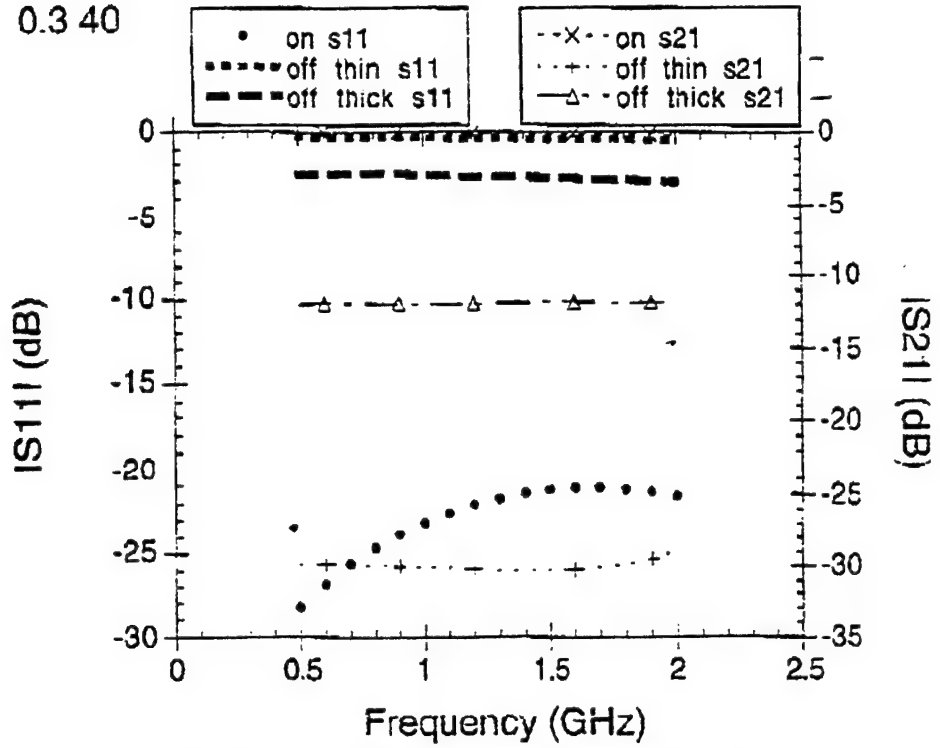


FIGURE A-4. 40-Millimeter Pitch Heater Line.

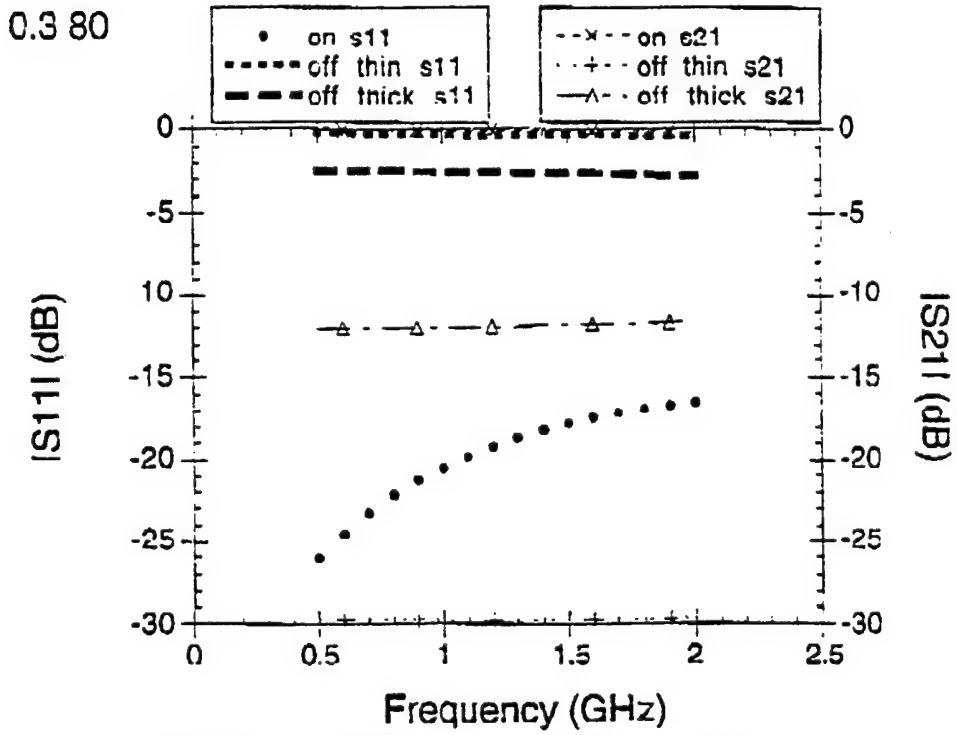


FIGURE A-5. 80-Millimeter Pitch Heater Line.

0.95-MILLIMETER SWITCH SECTION

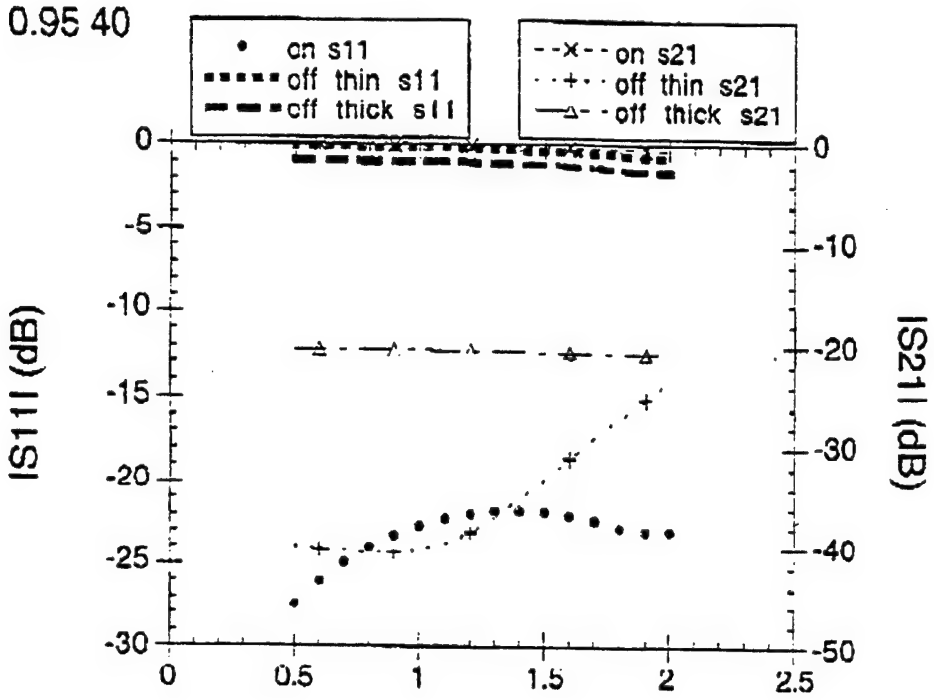


FIGURE A-6. 40-Millimeter Pitch Heater Line.

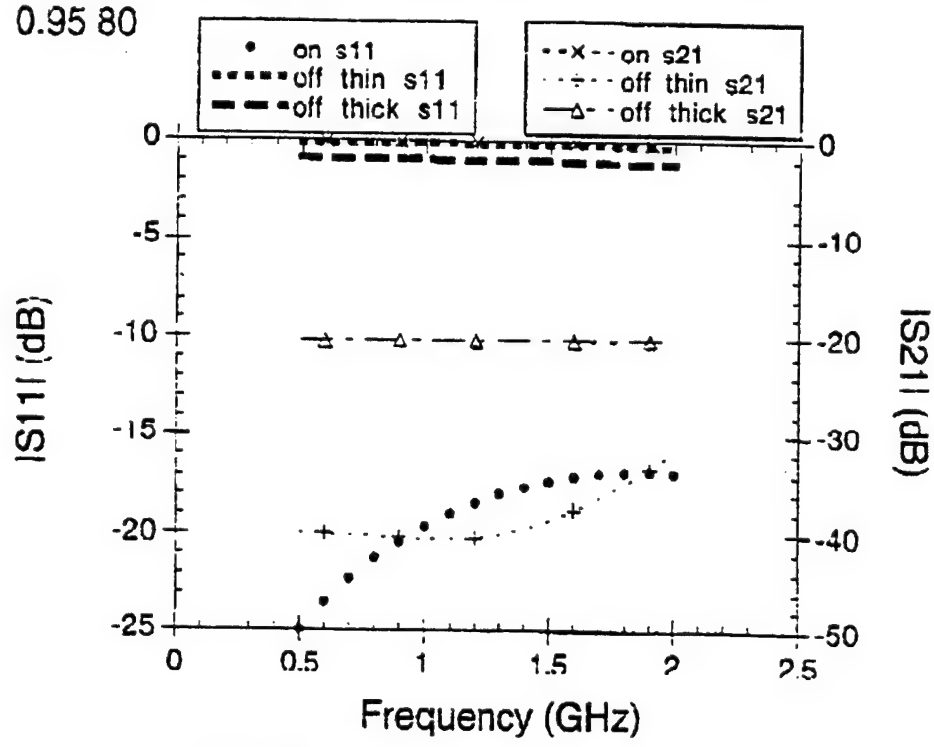


FIGURE A-7. 80-Millimeter Pitch Heater Line.

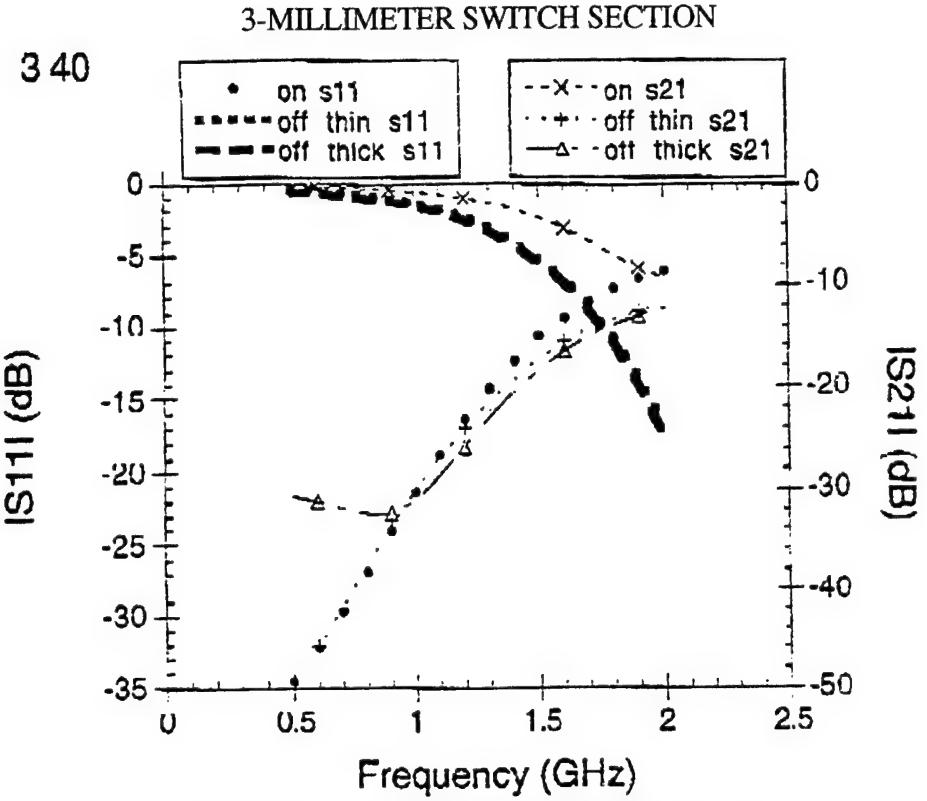


FIGURE A-8. 40-Millimeter Pitch Heater Line.

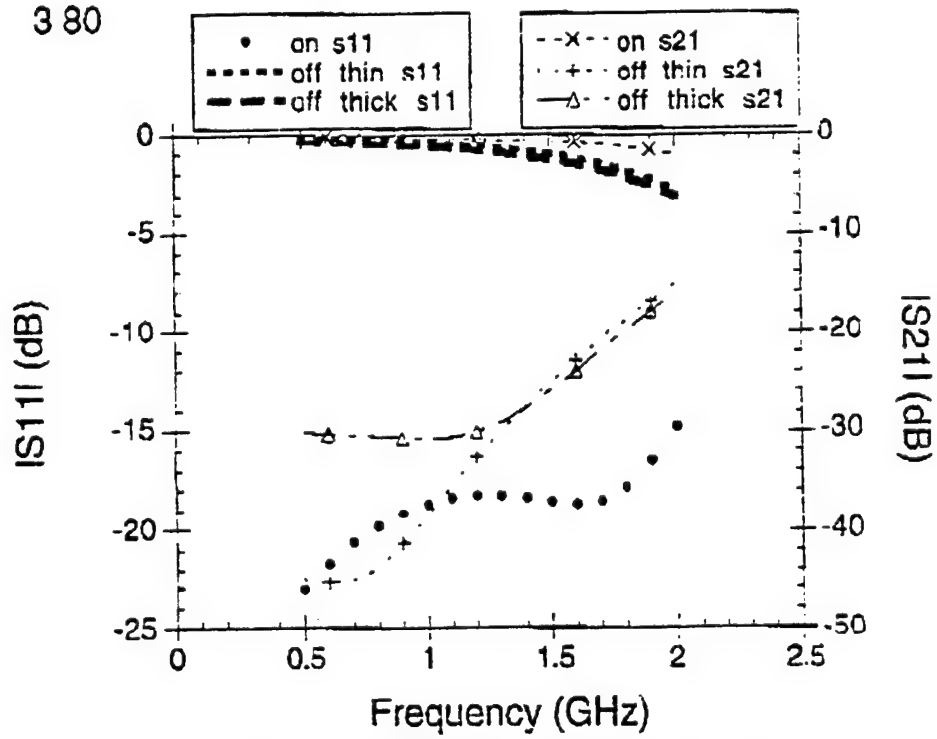


FIGURE A-9. 80-Millimeter Pitch Heater Line.

### Comments on Simulations

One can see that in all cases, the on state response is reasonable. In the 3 40 case, the $S_{11}$ is starting to get large above 1.5 Ghz and this is because the capacitance is the largest for that circuit. The off state response is only good for both film thicknesses in the 3 40 and 3 80 cases with respective frequency limits (based on -30 dB levels for $S_{21}$) of 1 and 1.5 GHz. The thin film off state is acceptable for all of the 0.3 and 0.95 simulations while the thick off response gets progressively worse for shorter active areas as would be expected. In a manufacturing environment this would be an interesting trade-off since the thinner active areas would be less reproducible while the responses are better. The off state $S_{21}$ values start rising for longer active areas because of control line coupling.

Do not forget that the simulations are fairly conservative, parasitics were overestimated by probably a 20 to 50% margin for safety. Also, do not forget the hidden trade-off on the control line pitches. The wider pitch 80 has obvious parasitic advantages from the above plots but will result in slower switching times and a higher switching current. The overall performance indications are summarized below.

| Design | On state performance | Thick off state performance | Thin off state performance |
|---|---|---|---|
| 0.3 40 | good | S21 = -12 | good |
| 0.3 80 | good | S21 = -12 | good |
| 0.95 40 | good | S21 = -20 | good < 1.75 Ghz |
| 0.95 80 | good | S21 = -20 | good |
| 3 40 | good < 1.5 Ghz | OK < 1 Ghz | OK < 1 GHz |
| 3 80 | good | OK < 1.5 Ghz | OK < 1.5 GHz |

## SUMMARY

A set of six thermal switch designs have been presented for use on reasonable quality YBCO. The main variations between the designs are in active area length and control line pitch. The 3 length variations cover a wide range to allow for possible experimentation in film thichness and process variability. It may be of interest to use a matrix of thinning (for example one wafer unthinned and one wafer thinned) to gain further information. All dimensions are fairly conservative and parasitics have been derated for simulation purposes. Simulations covered small signal behavior in the low microwave range over a pair of possible film thicknesses, which represent a reasonable range of possible values.

## NAWCWPNS CIRCUIT ANALYSIS

The following plots indicate tesults using a method of moments based planar circuit simulator from Zeland Software (IE3D), to calculate the switch circuit response. This

model includes all dielectric layers actually used in the circuit fabrications. These results (labeled "IE3D analysis") are compared to the analysis conducted at Conductus to provide a check on its validity, and to investigate the performance ranges expected.

## 0.95 MILLIMETER SWITCH SECTION

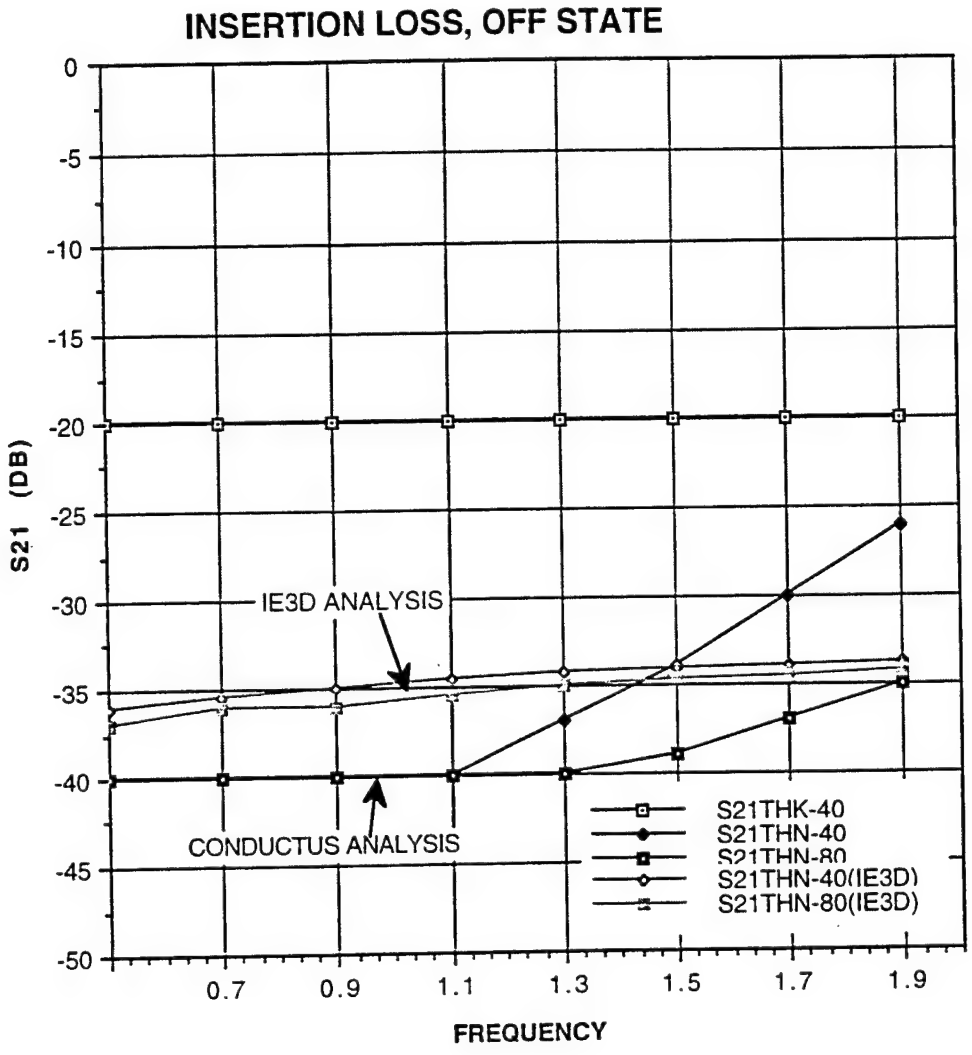

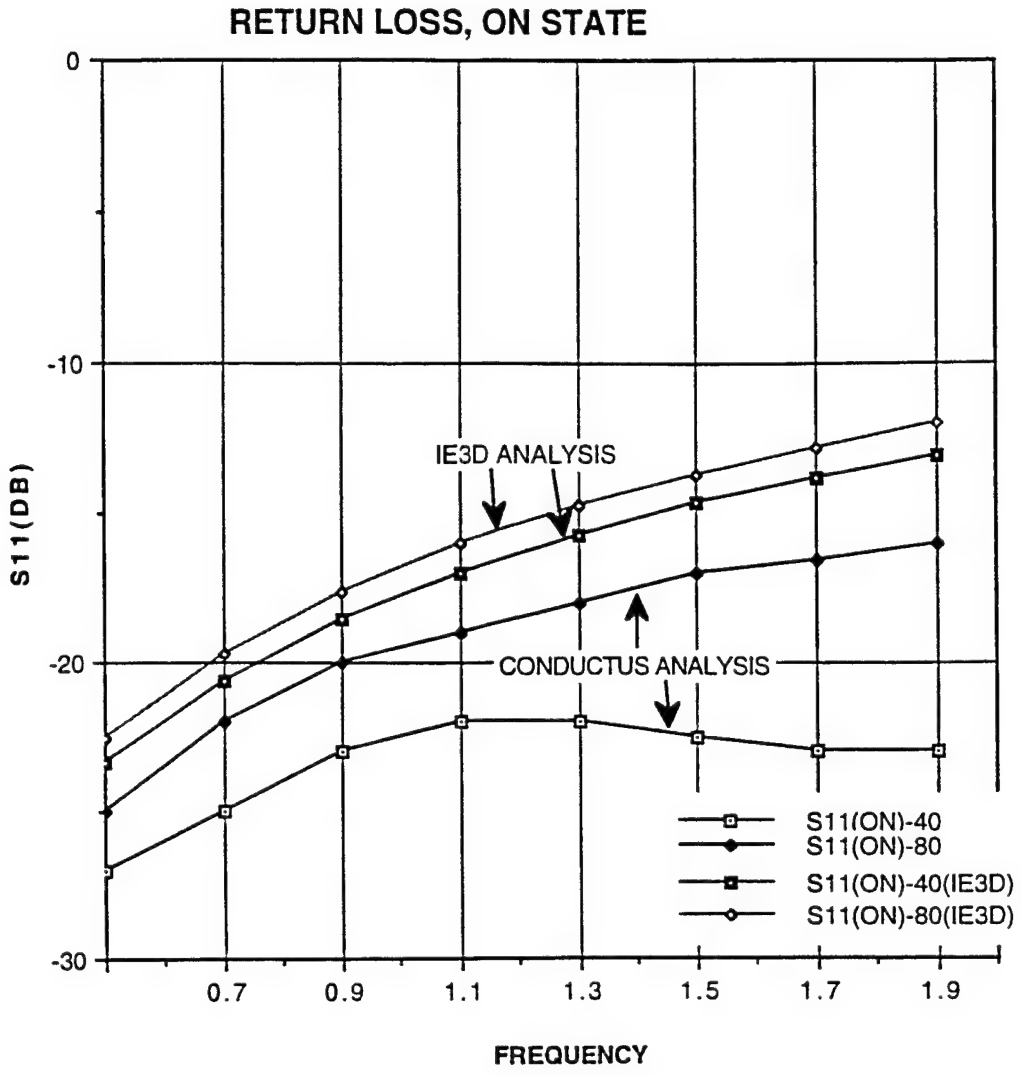
RETURN LOSS, ON STATE
0
-10
-20
-30
S11(DB)
IE3D ANALYSIS
CONDUCTUS ANALYSIS
S11(ON)-40
S11(ON)-80
S11(ON)-40(IE3D)
S11(ON)-80(IE3D)
0.7
0.9
1.1
1.3
1.5
1.7
1.9
FREQUENCY

## 3 MILLIMETER SWITCH SECTION

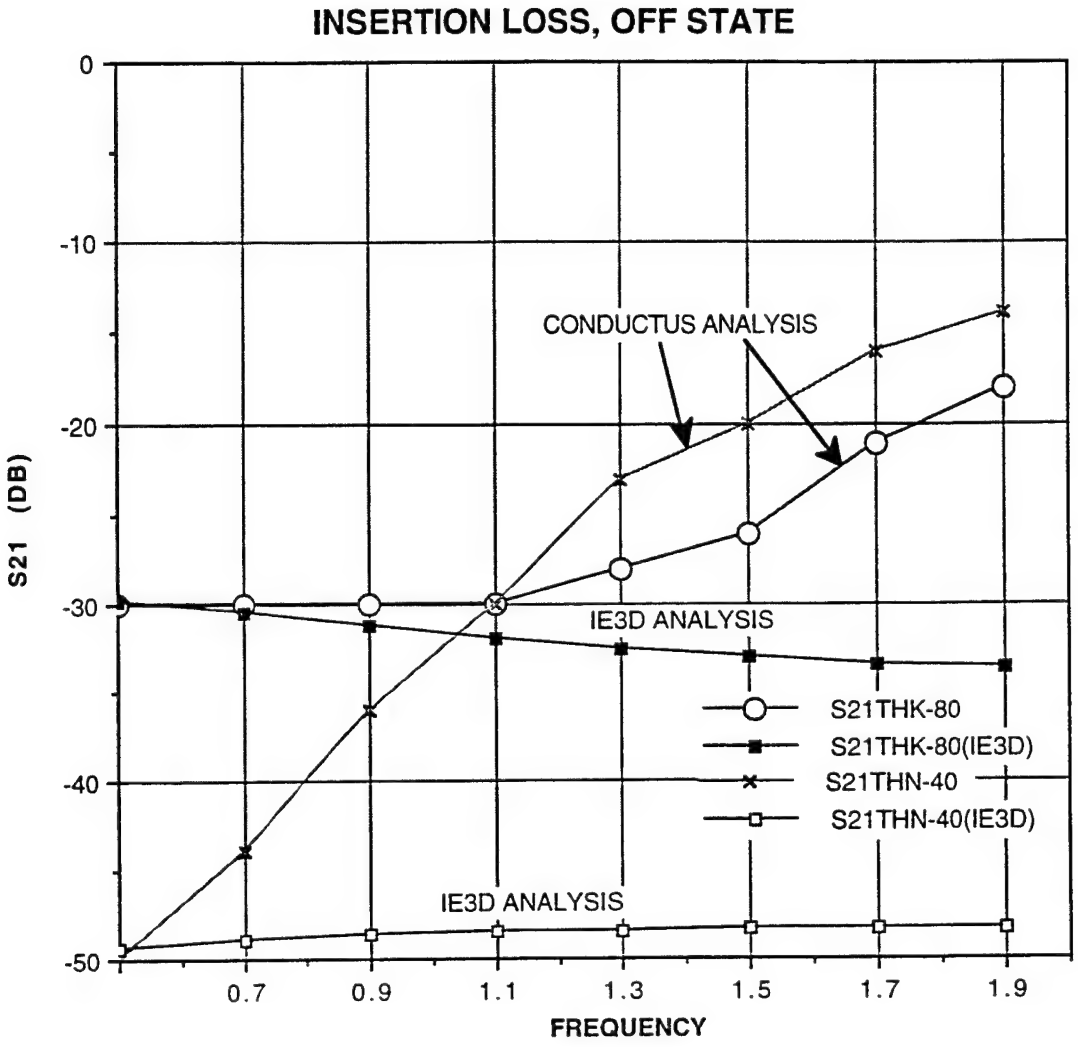

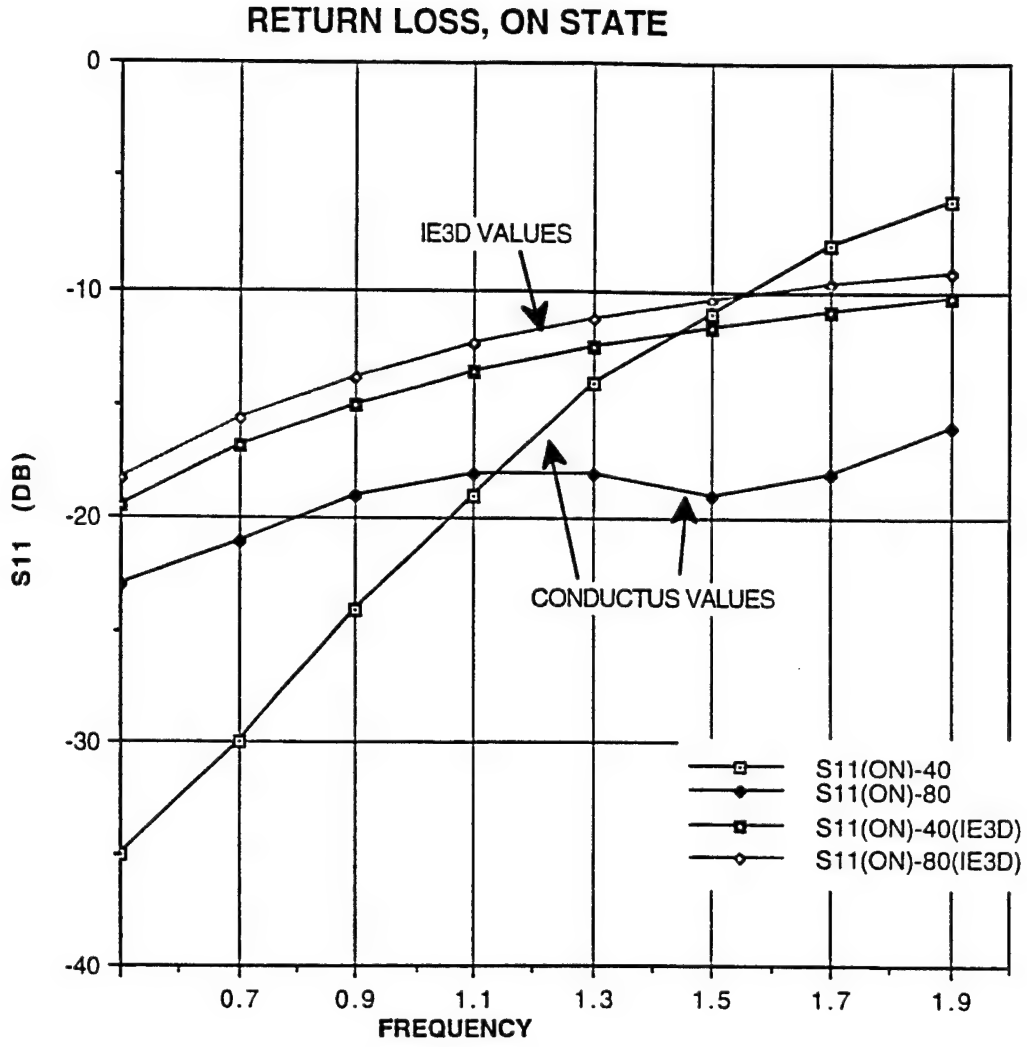
RETURN LOSS, ON STATE
0
-10
-20
-30
-40
S11 (DB)
IE3D VALUES
CONDUCTUS VALUES
0.7
0.9
1.1
1.3
1.5
1.7
1.9
FREQUENCY
S11(ON)-40
S11(ON)-80
S11(ON)-40(IE3D)
S11(ON)-80(IE3D)

# Appendix B

## CIRCUIT AND CIRCUIT HOUSING DESIGN

All holes centered Material: aluminum, gold plated

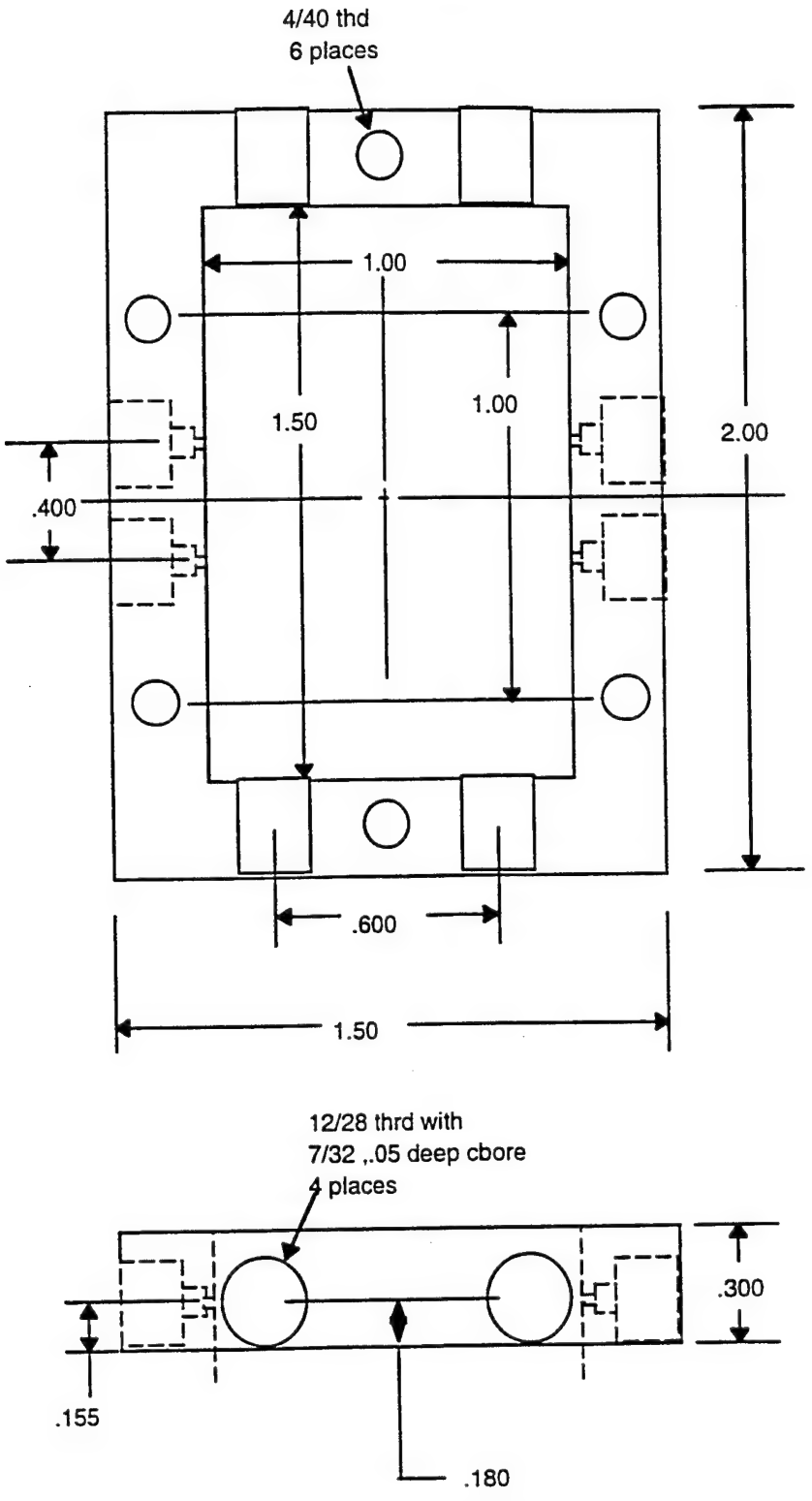


FIGURE B-1. Circuit Housing.

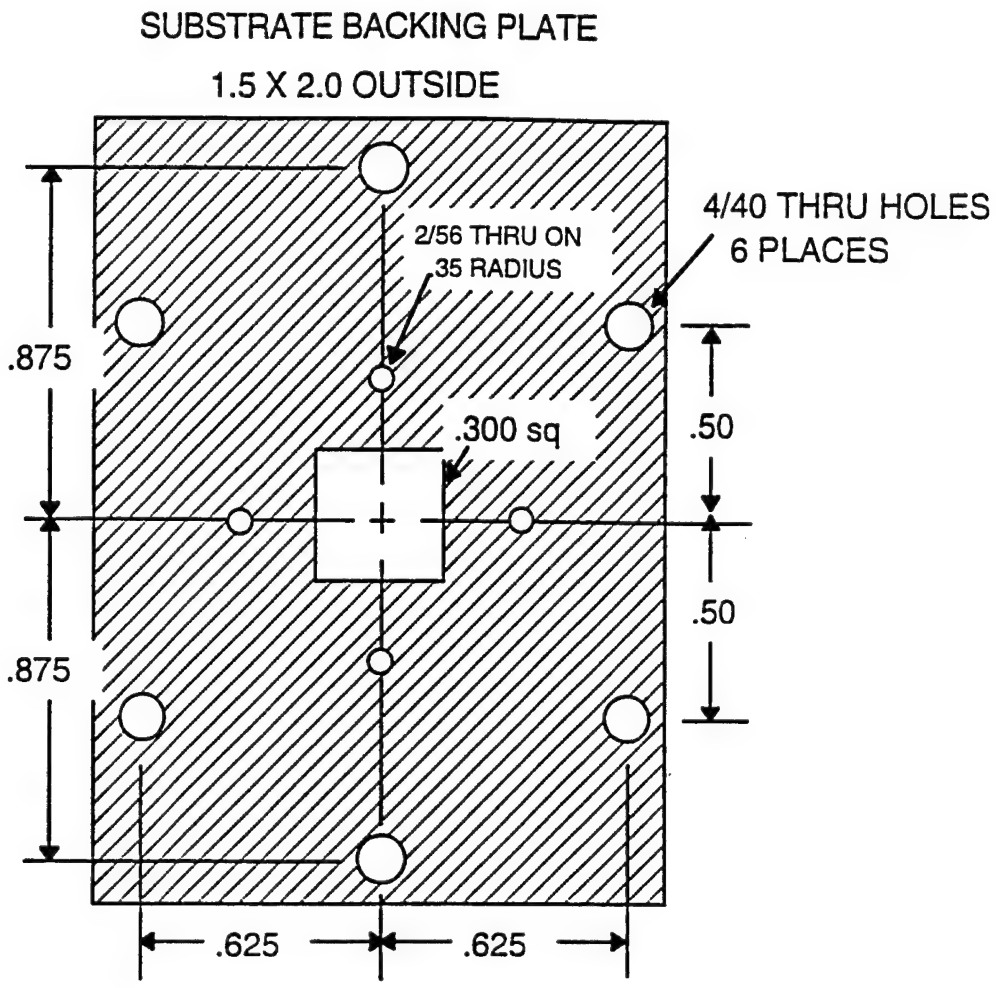


FIGURE B-2. Back Circuit Mounting Plate.

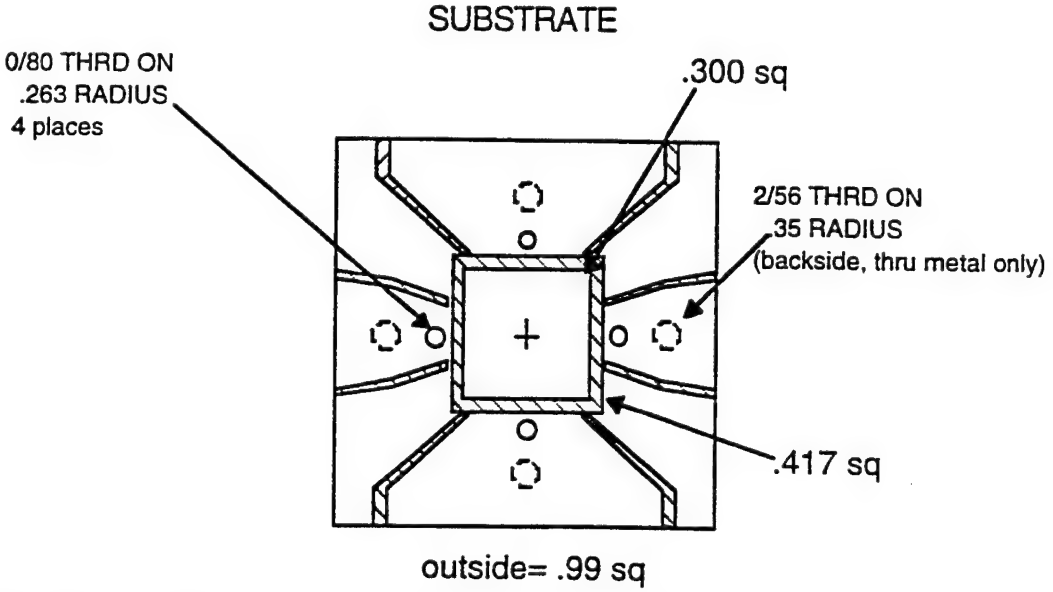


FIGURE B-3. Chip Interface Circuit (Roger's 6010LM on 0.125 Inch Aluminum).

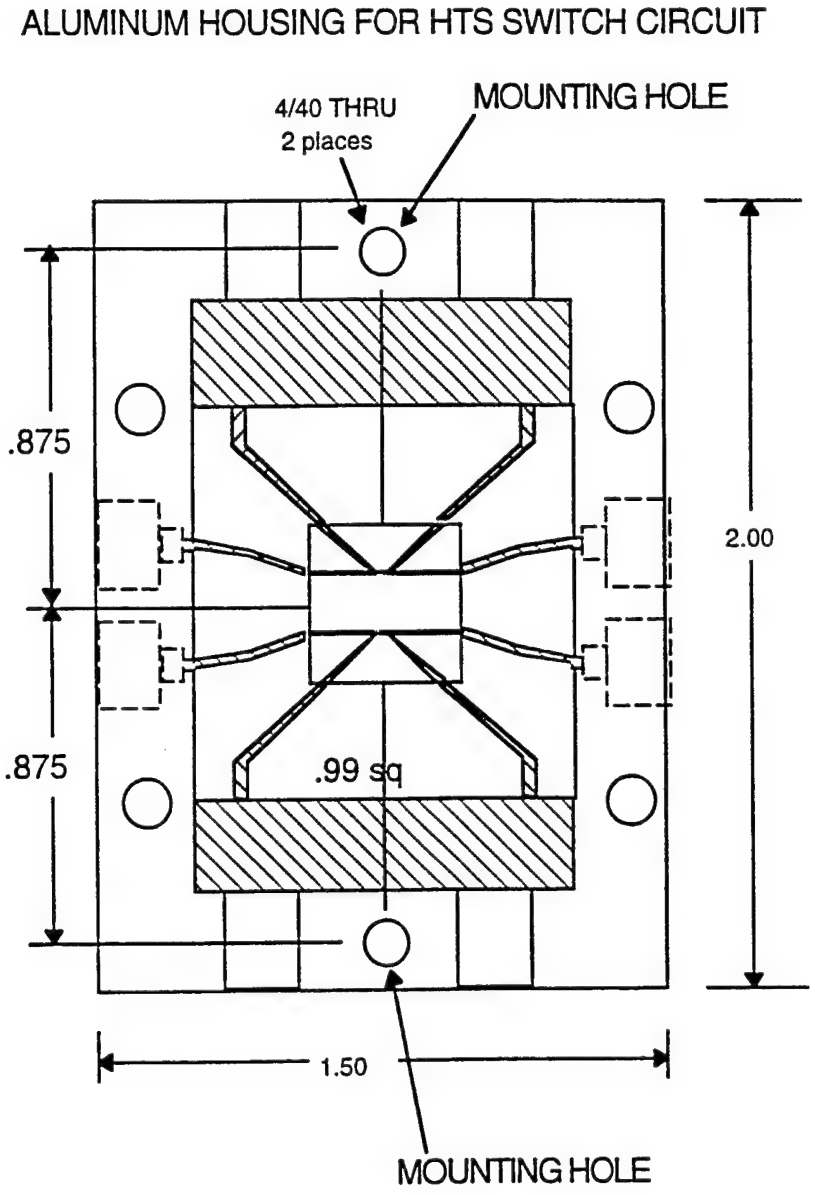


FIGURE B-4. Chip Holder Circuit and HTS Chip Mounted in Housing.

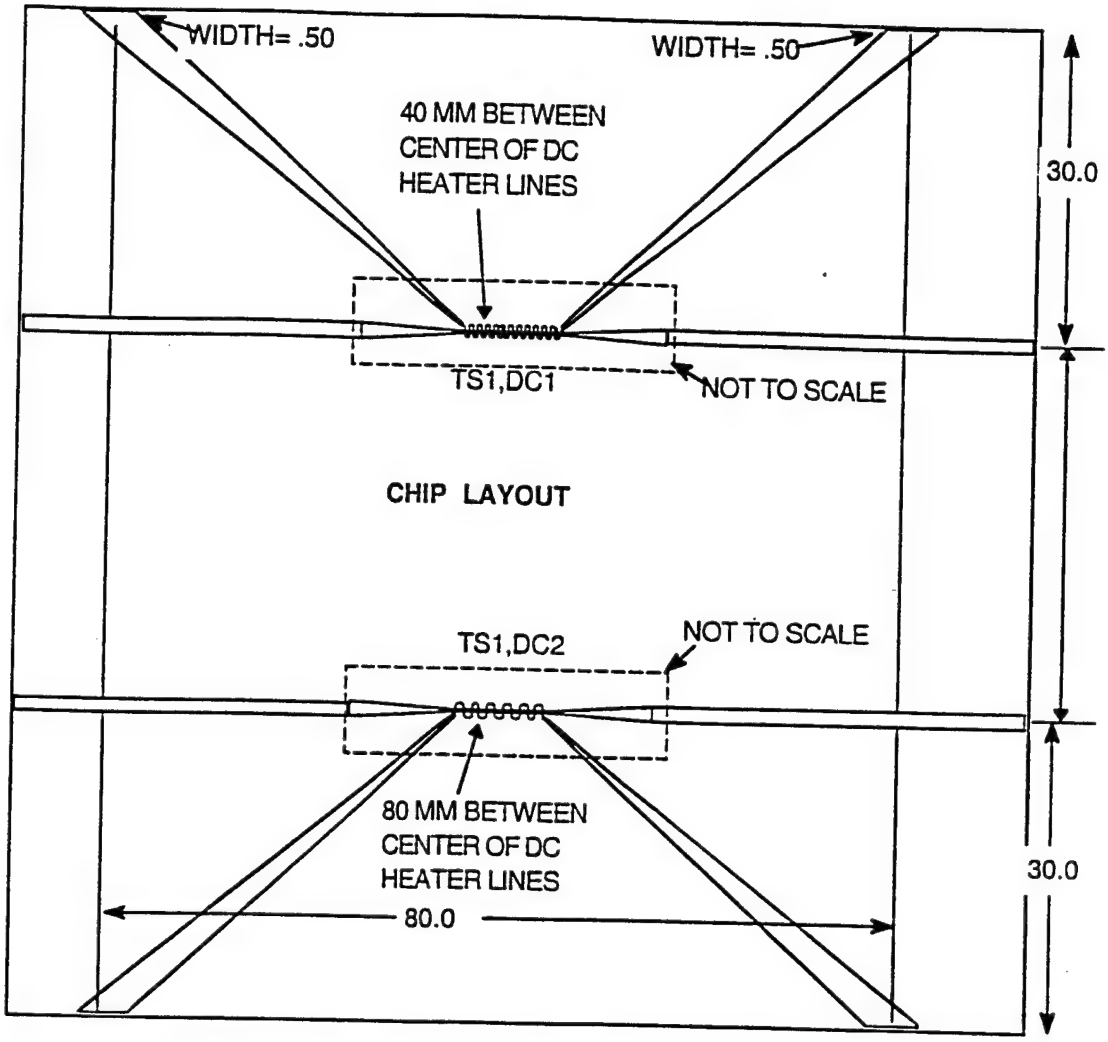


FIGURE B-5. Exploded View of Superconducting Circuit Chip.

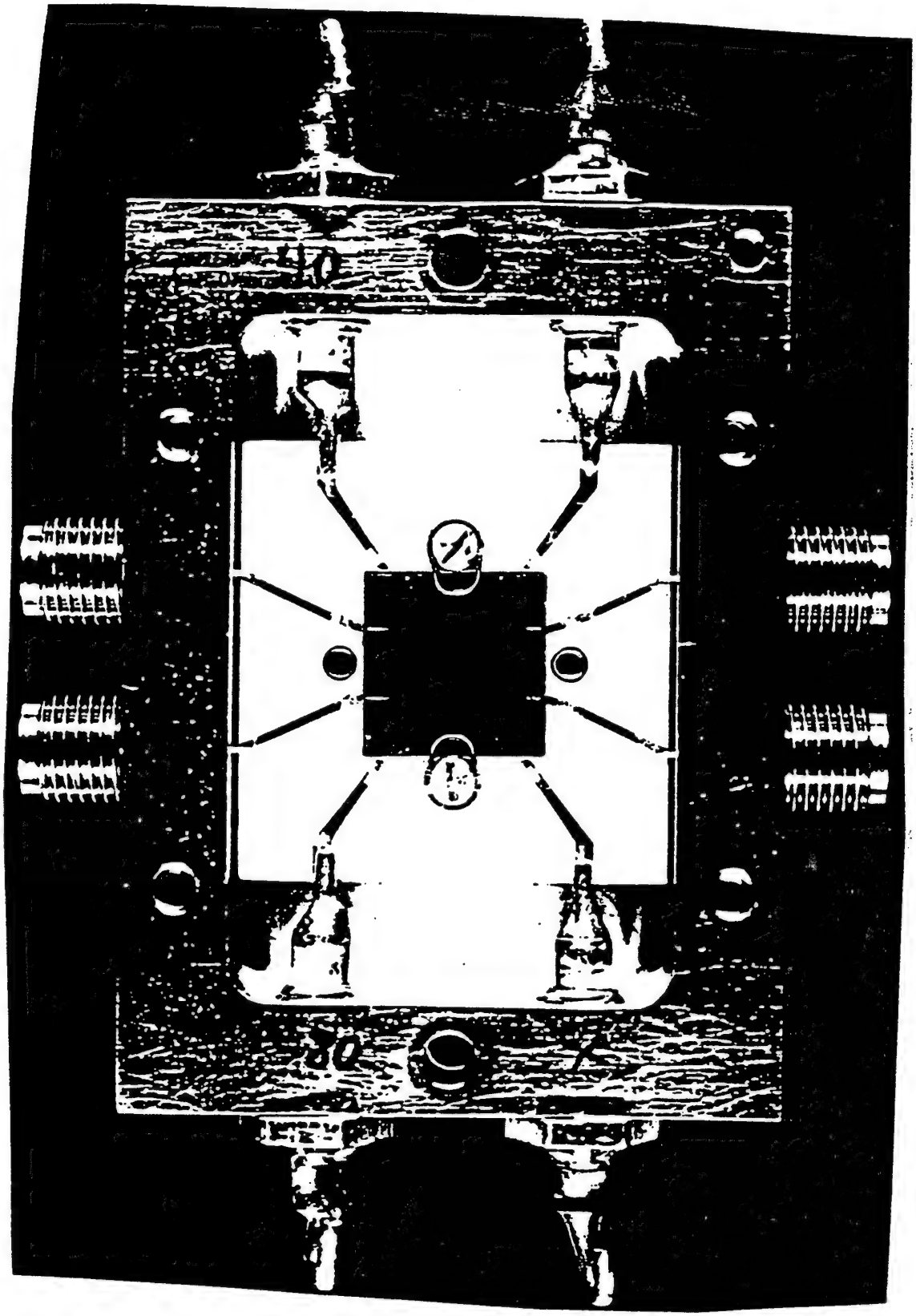

FIGURE B-6. Back Circuit Mounting Plate.

# Appendix C

## SWITCH INSERTION AND RETURN LOSS DATA 3-MM SWITCH #1 AND 2, AND 2-MM SWITCH #1

Switch Circuit Room Temperature Resistance

| Circuit no. | Switch, mm | Resistance (room temp.), K ohm |
|---|---|---|
| 1 | 3 | 4.5 |
| 2 | 3 | 4.0 |
| 1 | 2 | 6.8 |

Switch Test Condition Matrix

| Test # | Temp ( K) | Heater current (ma) | Line voltage (volts) |
|---|---|---|---|
| 1 | 100 | 0 | 0 |
| 2 | 90 | 0 | 0 |
| 3 | 80 | 0 | 0 |
| 4 | 77 | 0 | 0 |
| 6 | 77 | 5 | 0 |
| 7 | 77 | 10 | 0 |
| 8 | 77 | 15 | 0 |
| 9 | 77 | 0 | 5 |
| 10 | 77 | 0 | 10 |
| 11 | 77 | 0 | 15 |
| 12 | 77 | 5 | 5 |
| 13 | 77 | 10 | 5 |
| 14 | 77 | 15 | 5 |
| 15 | 77 | 5 | 10 |
| 16 | 77 | 10 | 10 |
| 17 | 77 | 15 | 10 |
| 18 | 77 | 5 | 15 |
| 19 | 77 | 10 | 15 |
| 20 | 77 | 15 | 15 |

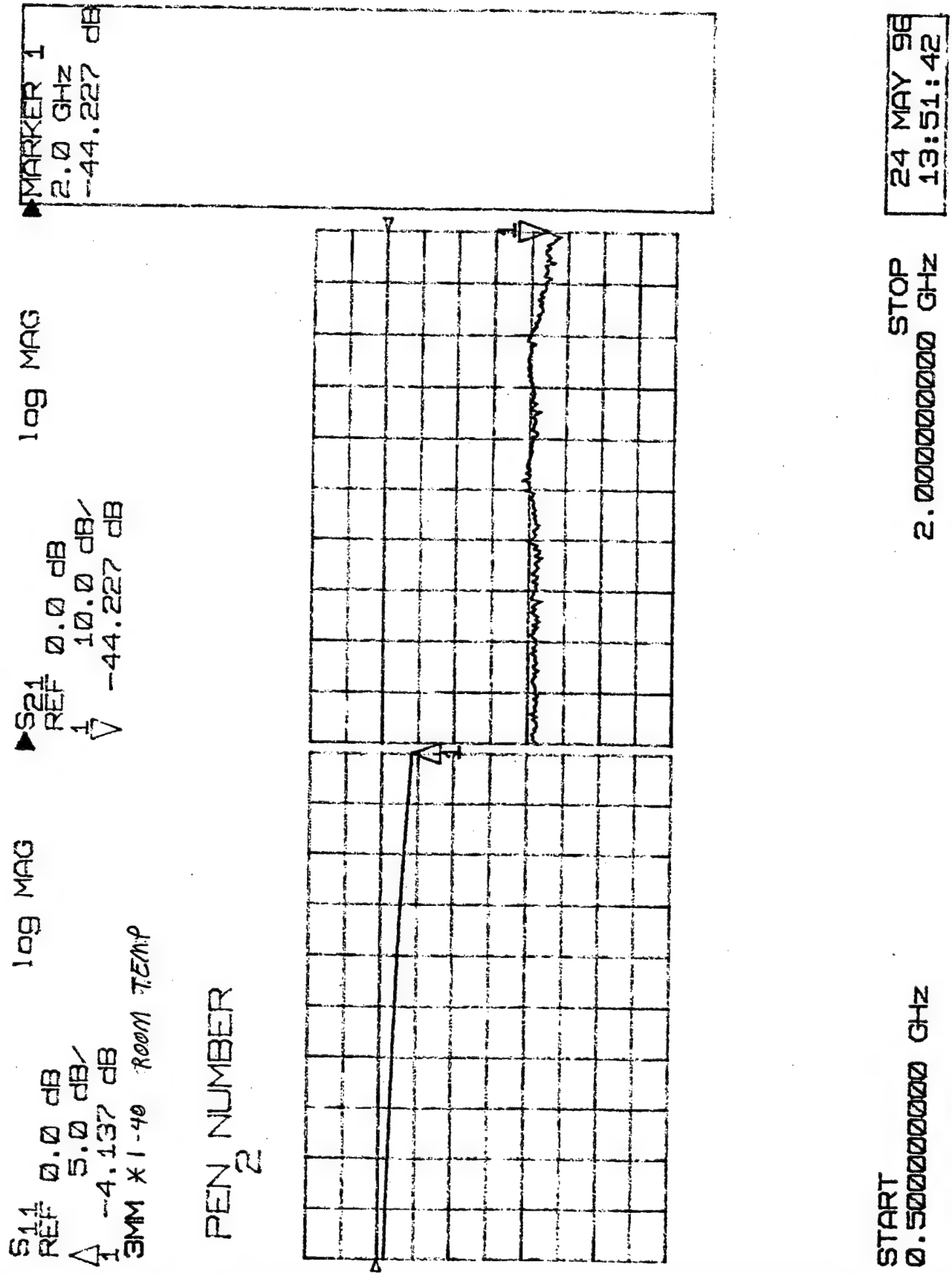
MARKER 1
2.0 GHz
-44.227 dB
log MAG
S21
REF 0.0 dB
10.0 dB/
-44.227 dB
log MAG
S11
REF 0.0 dB
5.0 dB/
-4.137 dB
3MM X1-40 ROOM TEMP
PEN NUMBER
2
START
0.500000000 GHz
STOP
2.000000000 GHz
24 MAY 96
13:51:42

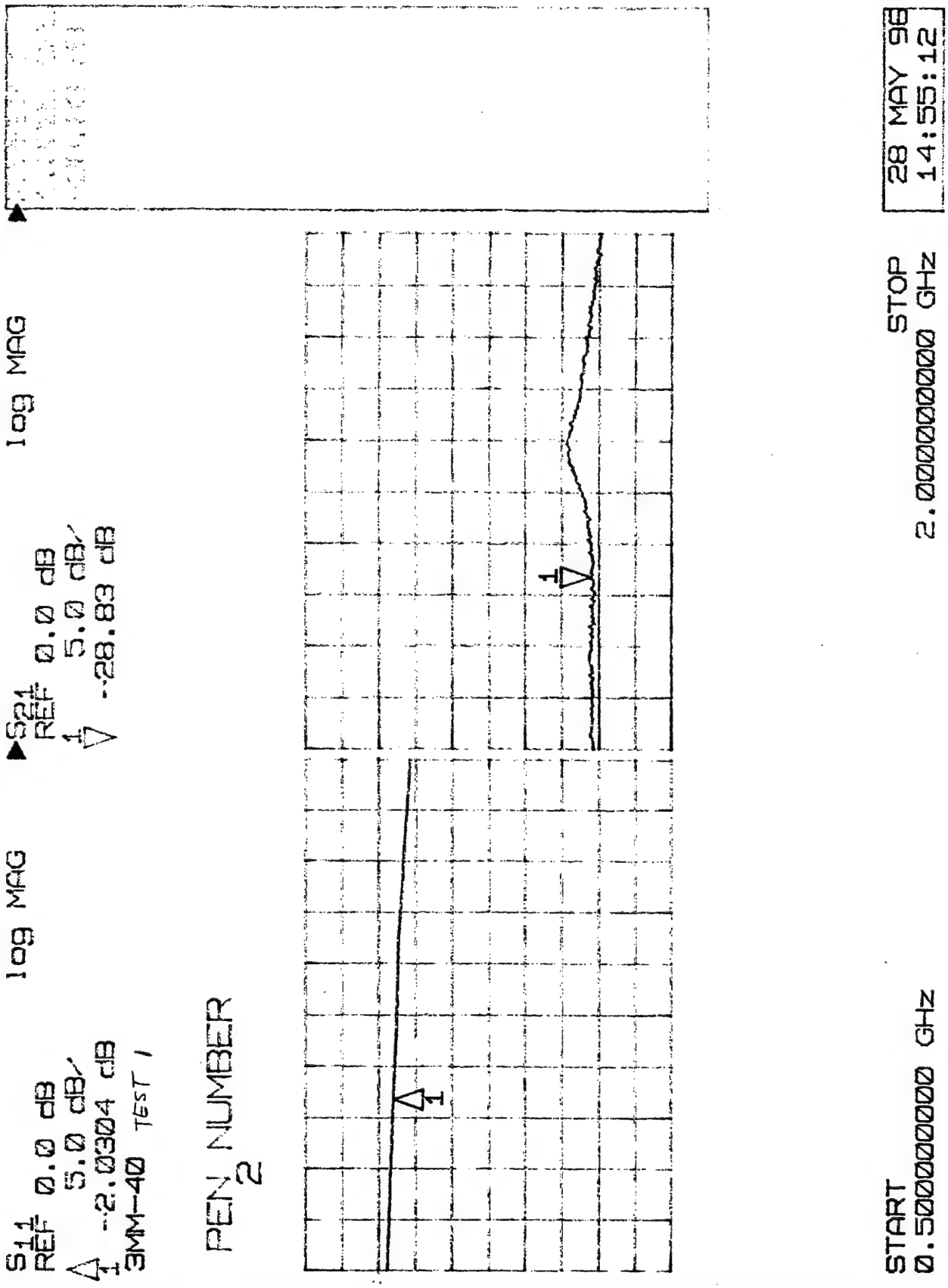
S11
REF 0.0 dB
5.0 dB/
1 -2.0304 dB
3MM-40 TEST 1
log MAG
S21
REF 0.0 dB
5.0 dB/
1 -28.83 dB
log MAG
C A PEN NUMBER 2
H
START
0.500000000 GHz
STOP
2.000000000 GHz
28 MAY 98
14:55:12

DC Λ - 200

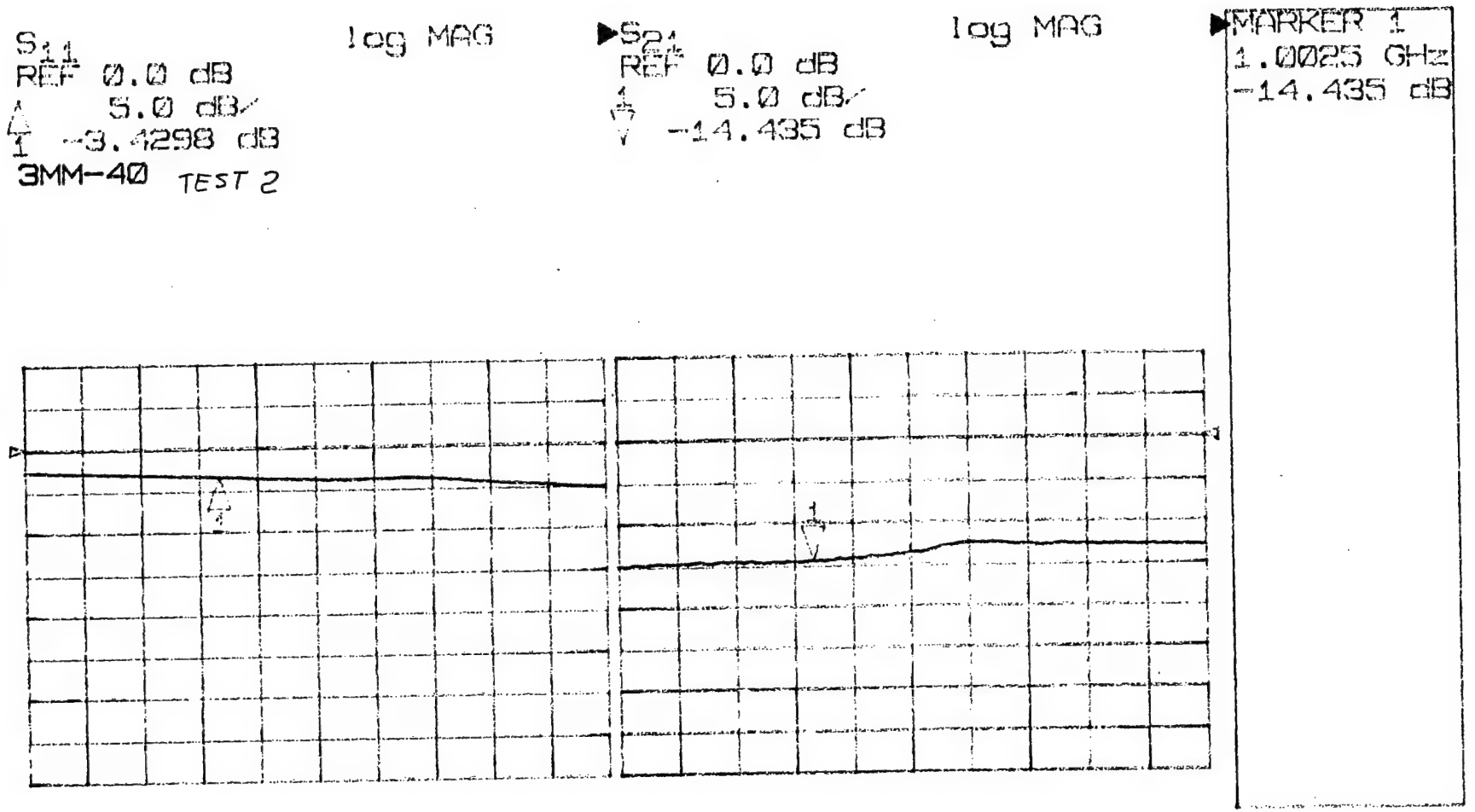
S11
log MAG
REF 0.0 dB
5.0 dB/
1 -3.4298 dB
3MM-40 TEST 2
S21
log MAG
REF 0.0 dB
5.0 dB/
1 -14.435 dB
MARKER 1
1.0025 GHz
-14.435 dB
START
0.500000000000 GHz
STOP
2.000000000000 GHz
28 MAY 98
15:04:57

DC R = 0.3 Ω

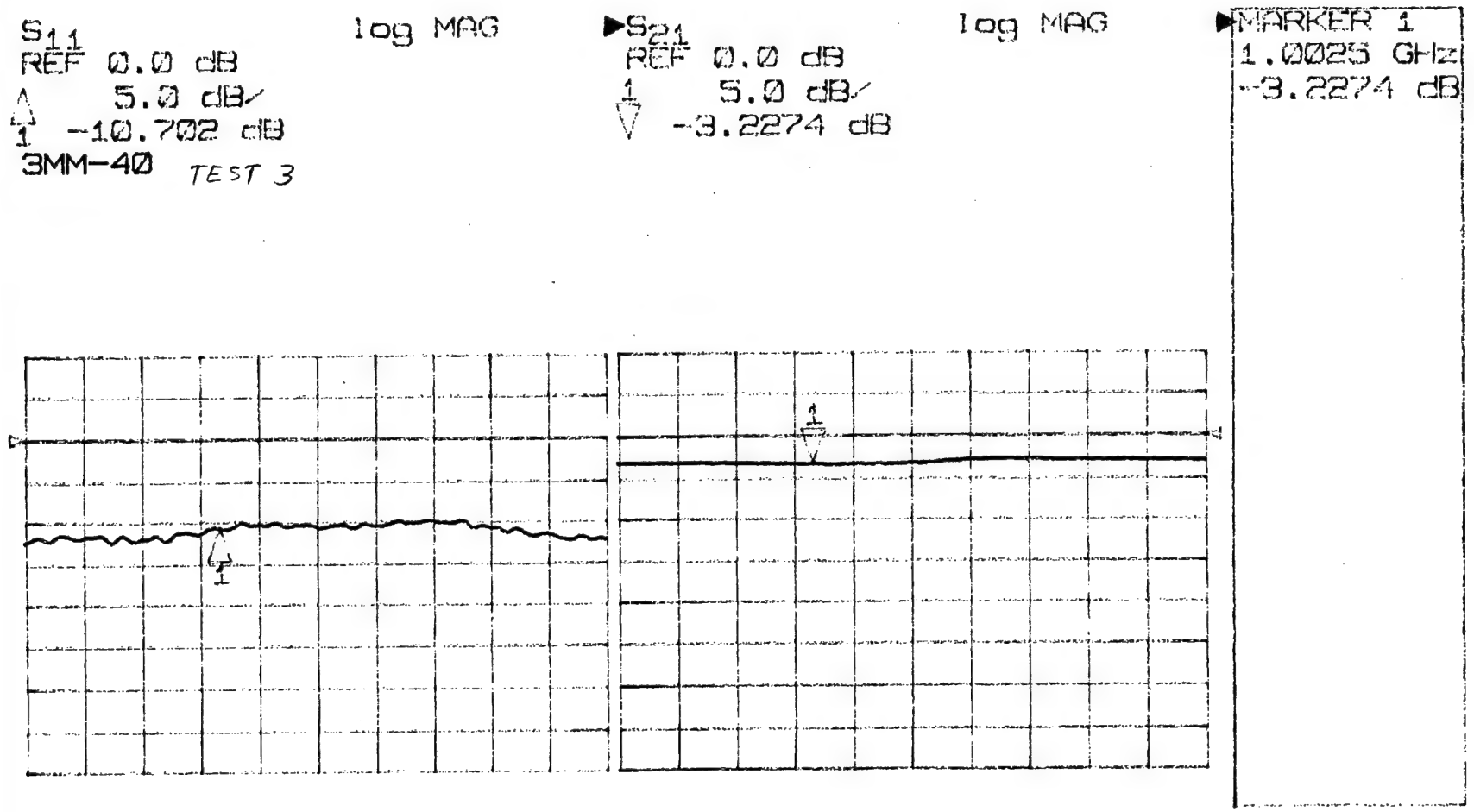


CAT I

45

NAWCWPNS TP 8335

DCR = .2Ω

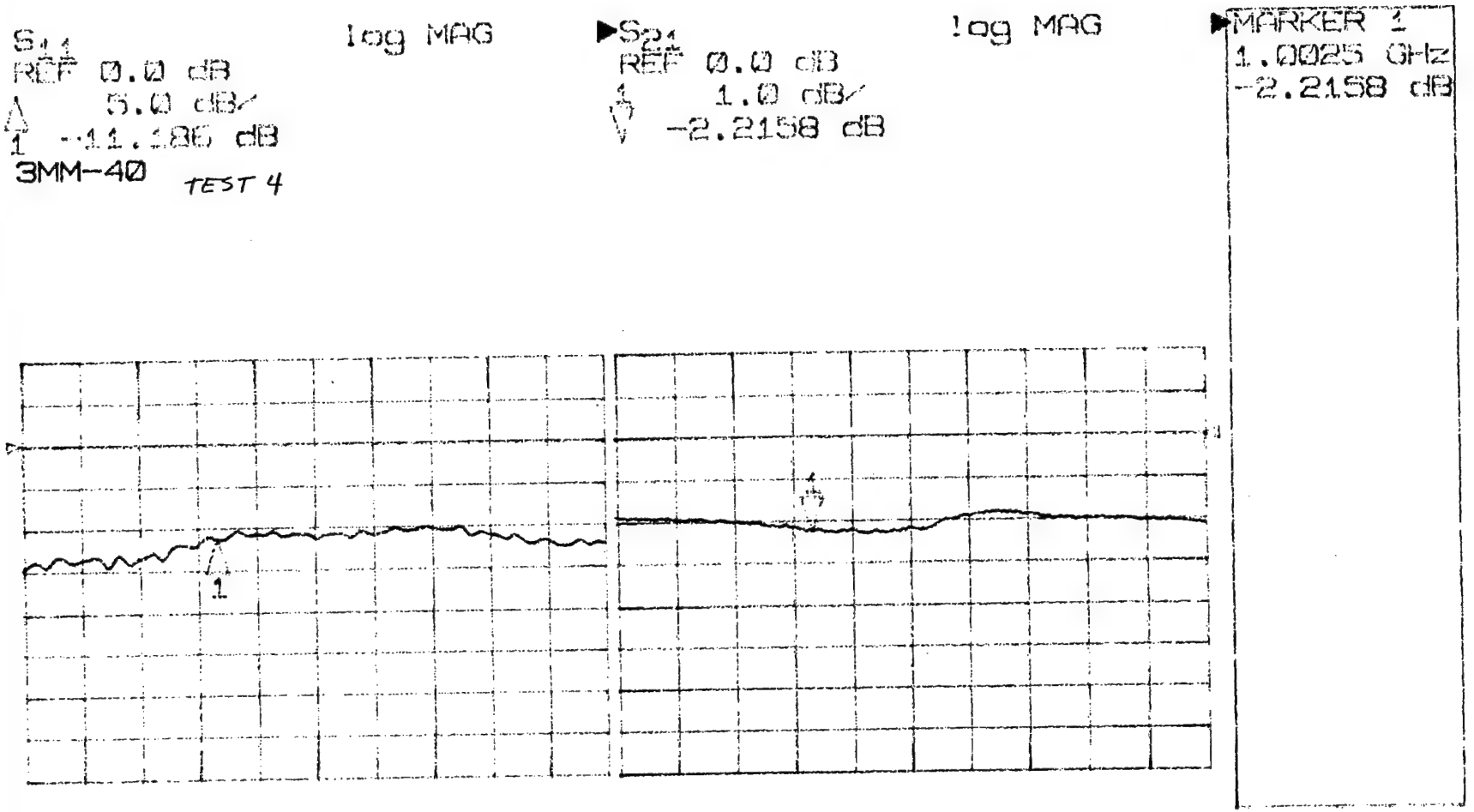
S11
log MAG
REF 0.0 dB
5.0 dB/
1 -11.186 dB
3MM-40
TEST 4
S21
log MAG
REF 0.0 dB
1.0 dB/
-2.2158 dB
MARKER 1
1.0025 GHz
-2.2158 dB
START
0.500000000000 GHz
STOP
2.000000000000 GHz
28 MAY 90
15:28:50

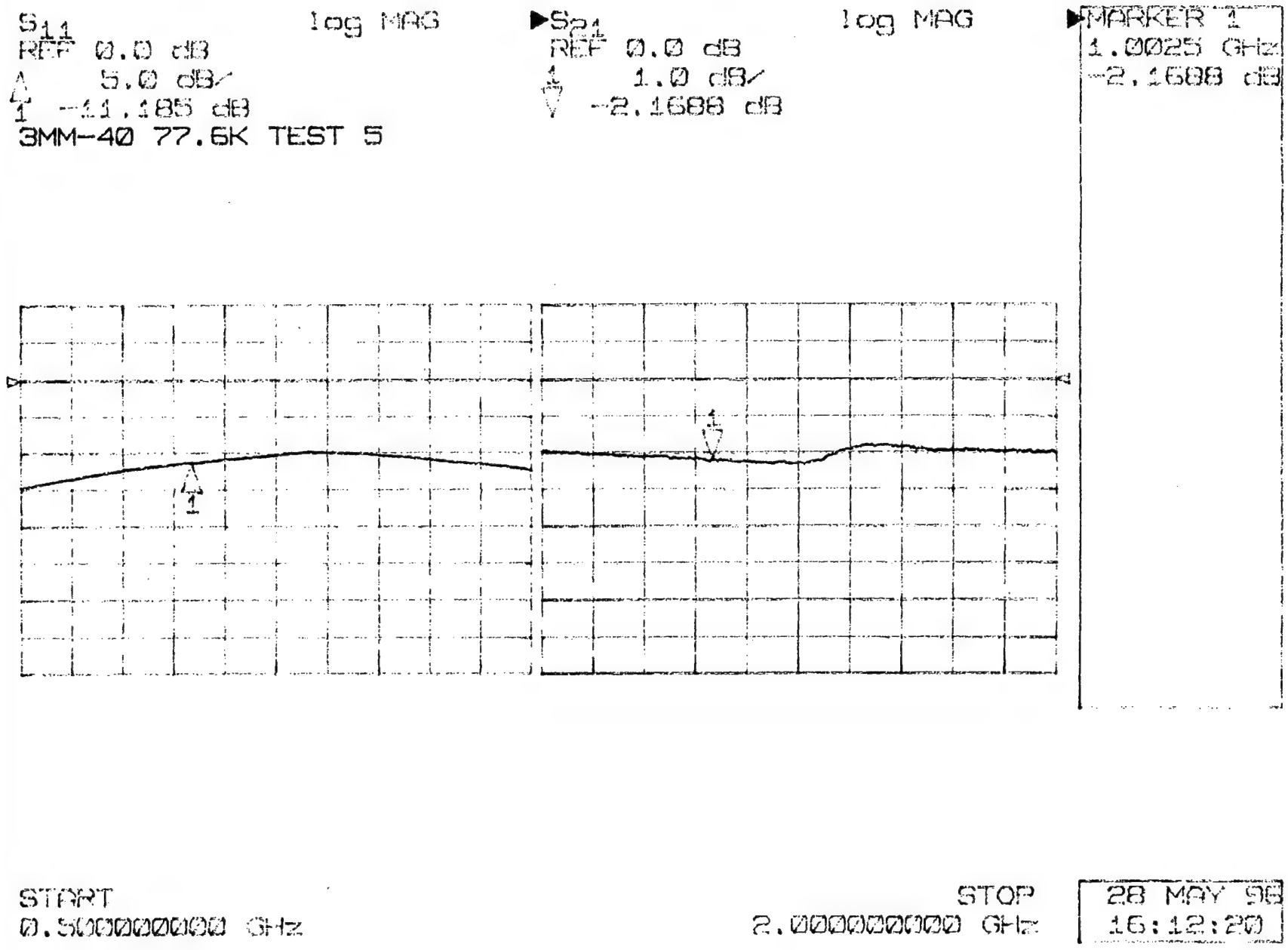
S11
log MAG
REF 0.0 dB
5.0 dB/
1 -11.185 dB
3MM-40 77.6K TEST 5
S21
log MAG
REF 0.0 dB
1.0 dB/
-2.1688 dB
MARKER 1
1.00025 GHz
-2.1688 dB
START
0.500000000000 GHz
STOP
2.000000000000 GHz
28 MAY 98
16:12:20

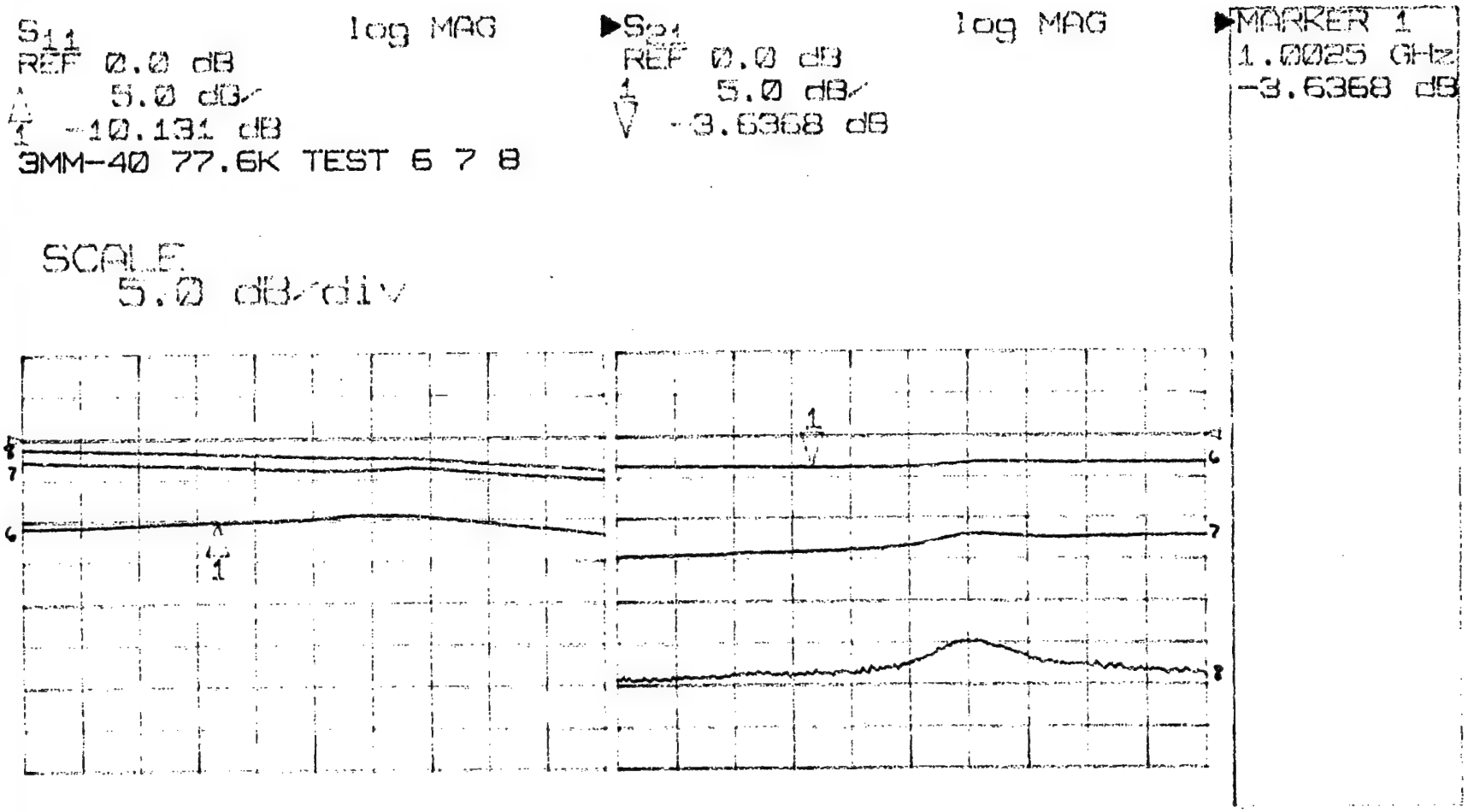
S11
log MAG
REF 0.0 dB
5.0 dB/
-10.131 dB
3MM-40 77.6K TEST 6 7 8
S21
log MAG
REF 0.0 dB
5.0 dB/
-3.6368 dB
MARKER 1
1.0025 GHz
-3.6368 dB
SCALE
5.0 dB/div
START
0.500000000000 GHz
STOP
2.000000000000 GHz
28 MAY 96
16:15:56

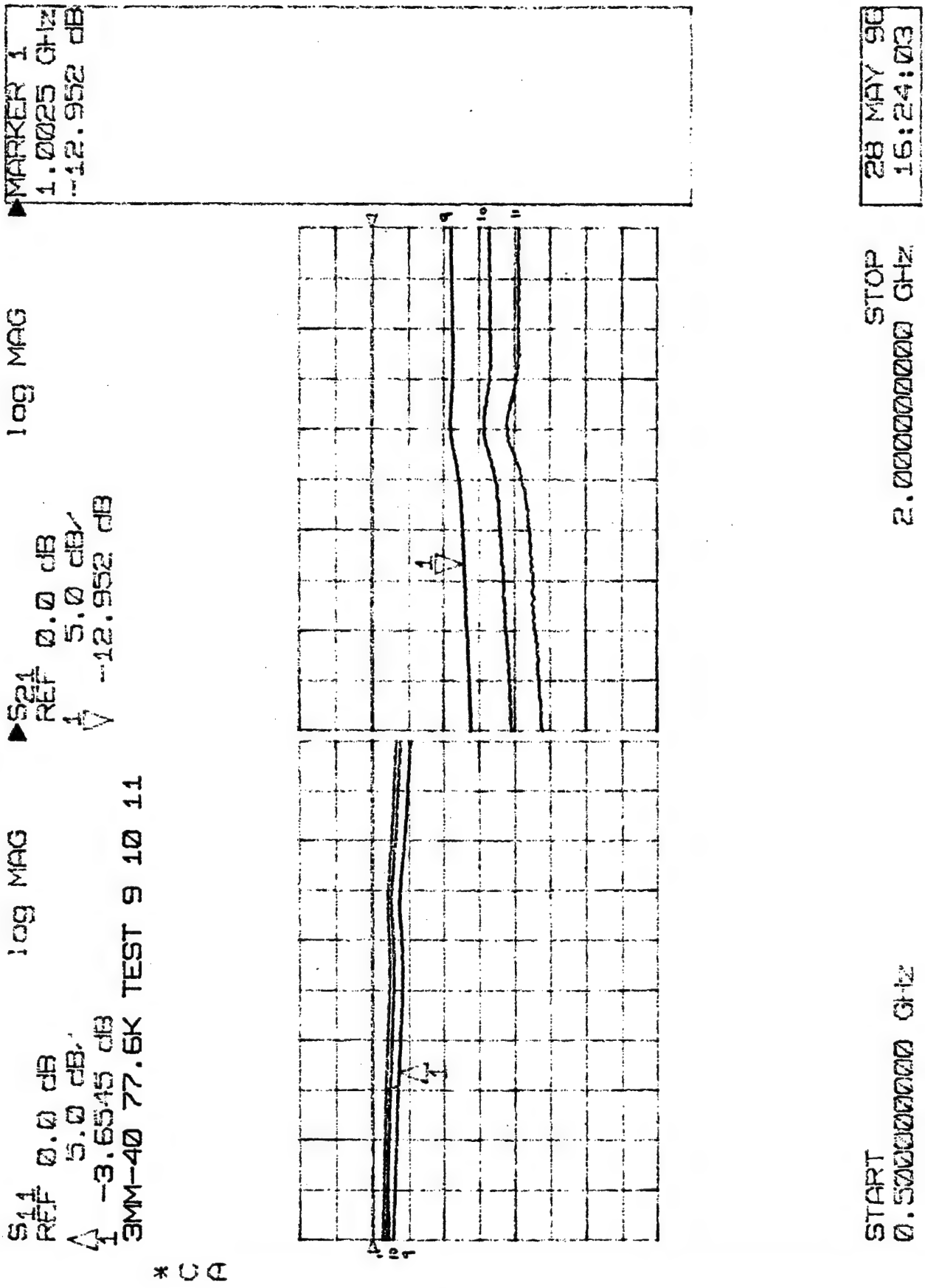
S11
REF 0.0 dB
5.0 dB/
1 -3.6545 dB
3MM-40 77.6K TEST 9 10 11
log MAG
S21
REF 0.0 dB
5.0 dB/
1 -12.952 dB
log MAG
MARKER 1
1.0025 GHz
-12.952 dB
START
0.500000000 GHz
STOP
2.000000000 GHz
28 MAY 98
15:24:03

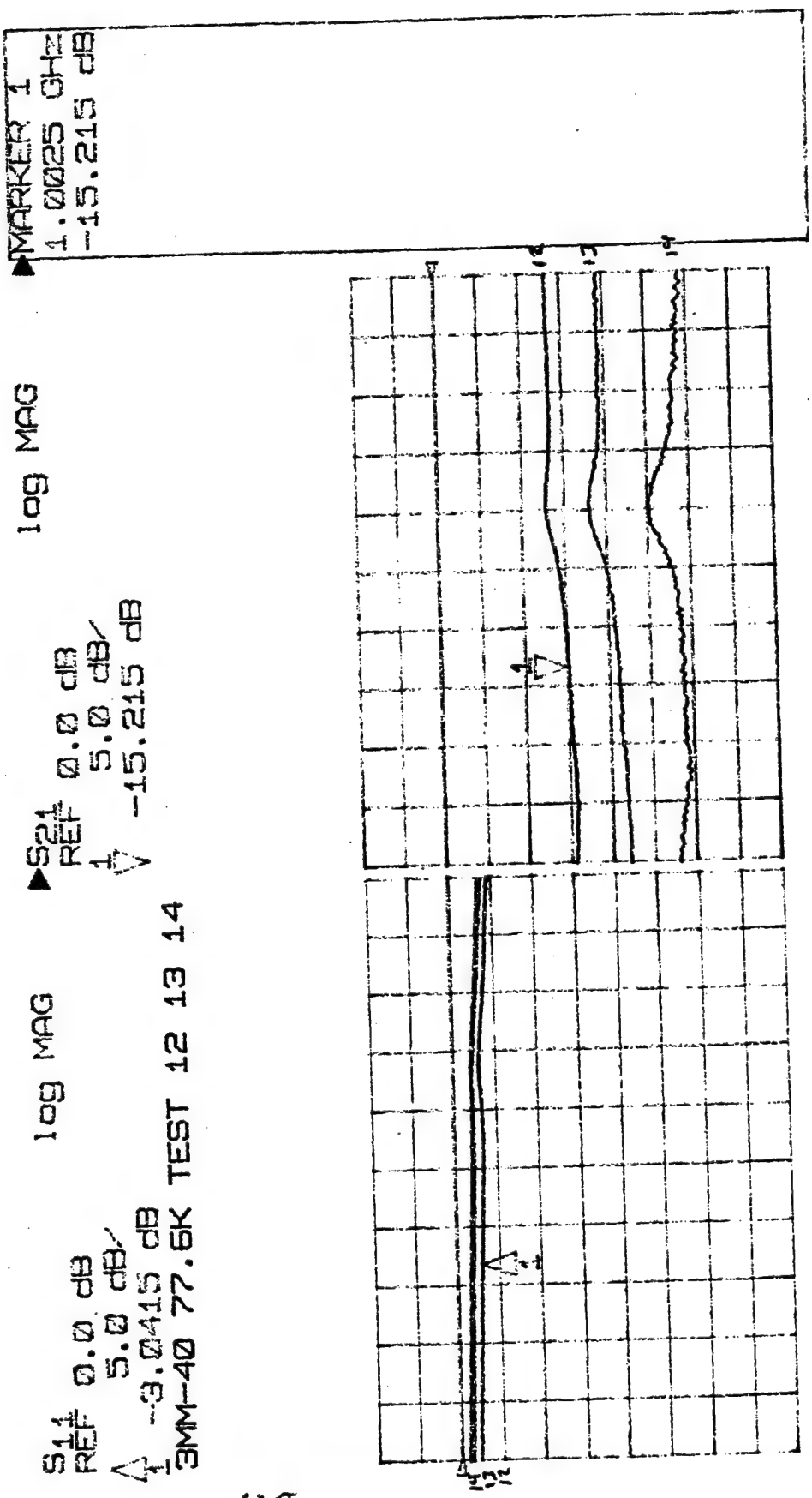
MARKER 1
1.0025 GHz
-15.215 dB
log MAG
S21
REF 0.0 dB
5.0 dB/
-15.215 dB
log MAG
S11
REF 0.0 dB
5.0 dB/
-3.0415 dB
3MM-40 77.6K TEST 12 13 14
START
0.500000000 GHz
STOP
2.000000000 GHz
28 MAY 96
16:30:43

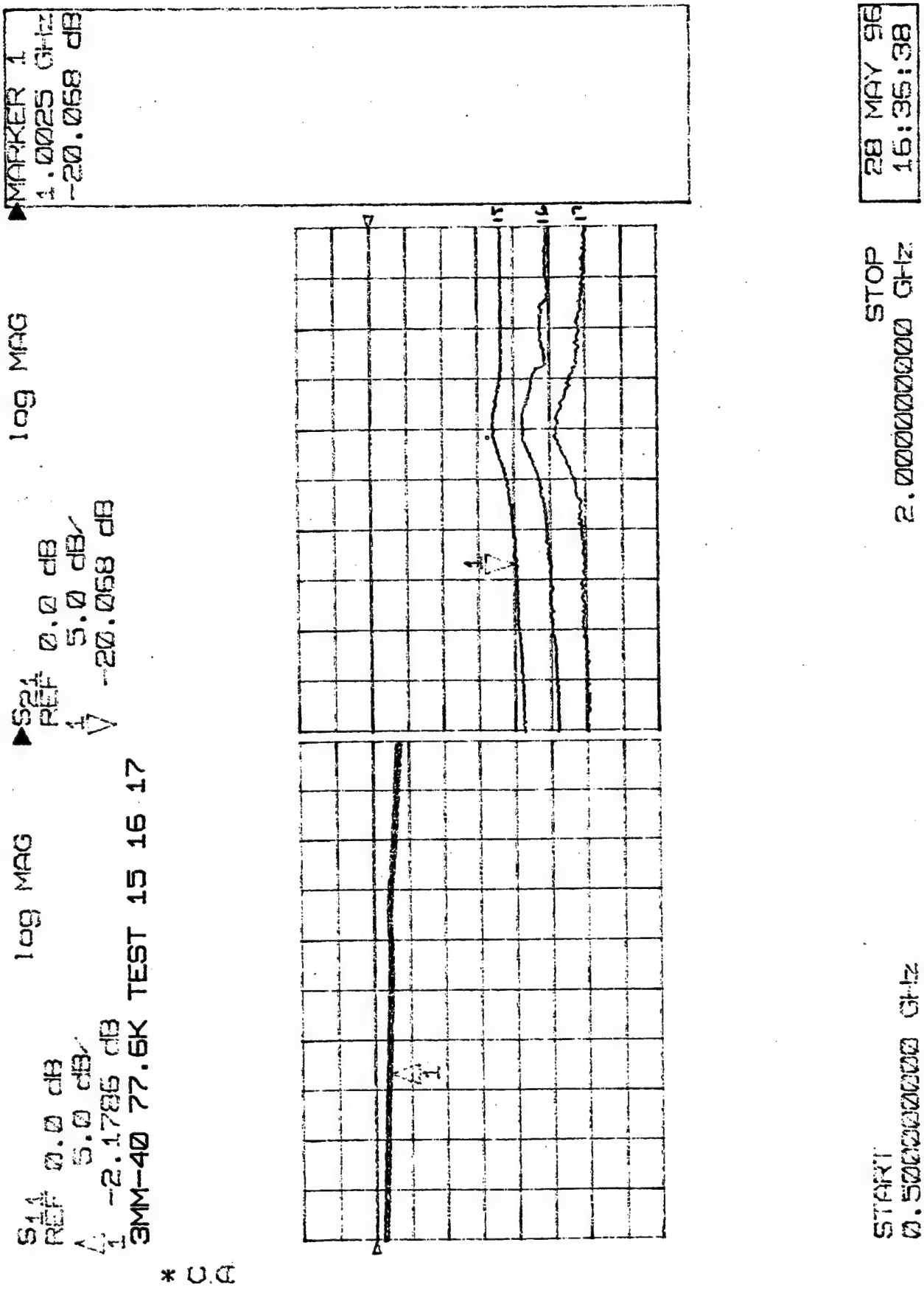
MARKER 1
1.0025 GHz
-20.058 dB
log MAG
S21
REF 0.0 dB
5.0 dB/
-20.058 dB
log MAG
S11
REF 0.0 dB
5.0 dB/
-2.17285 dB
3MM-40 77.6K TEST 15 16 17
* C.A
START
0.500000000 GHz
STOP
2.000000000 GHz
28 MAY 96
16:35:38

S11 log MAG
REF 0.0 dB
5.0 dB/
-1.8151 dB

S21 log MAG
REF 0.0 dB
5.0 dB/
-30.38 dB

MARKER 1
1.0025 GHz
-30.38 dB

3MM-40 77.6K TEST 15 16 17
18 19 20

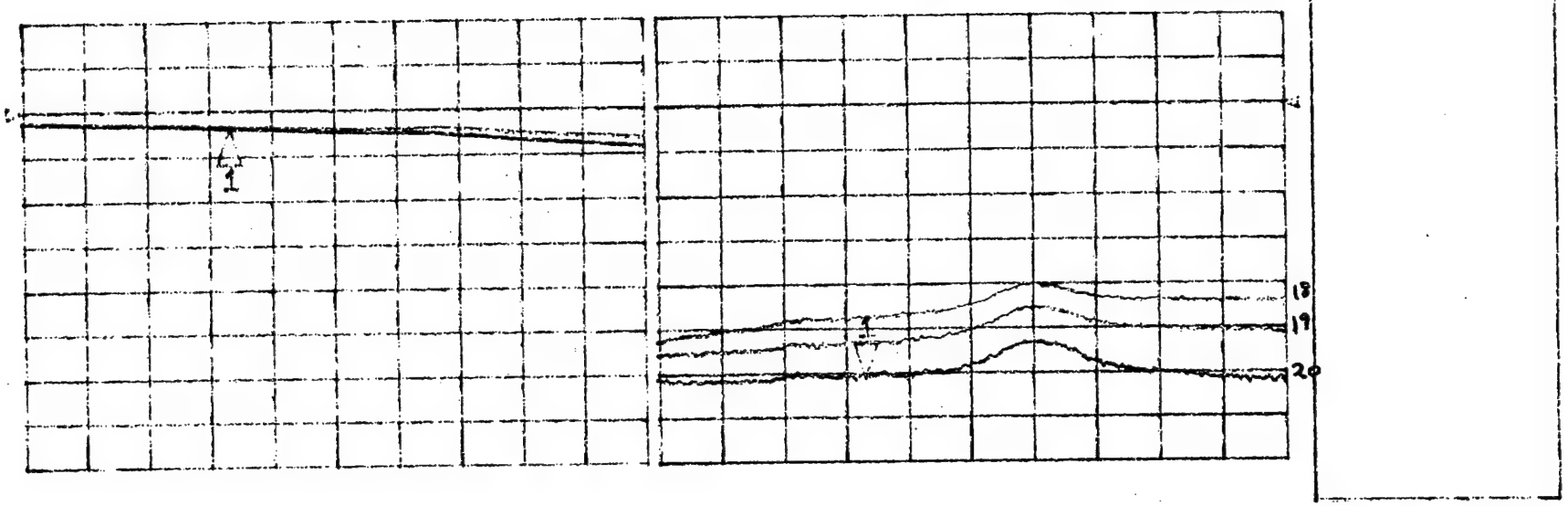


START
0.500000000000 GHz

STOP
2.000000000000 GHz

28 MAY 92
15:43:12

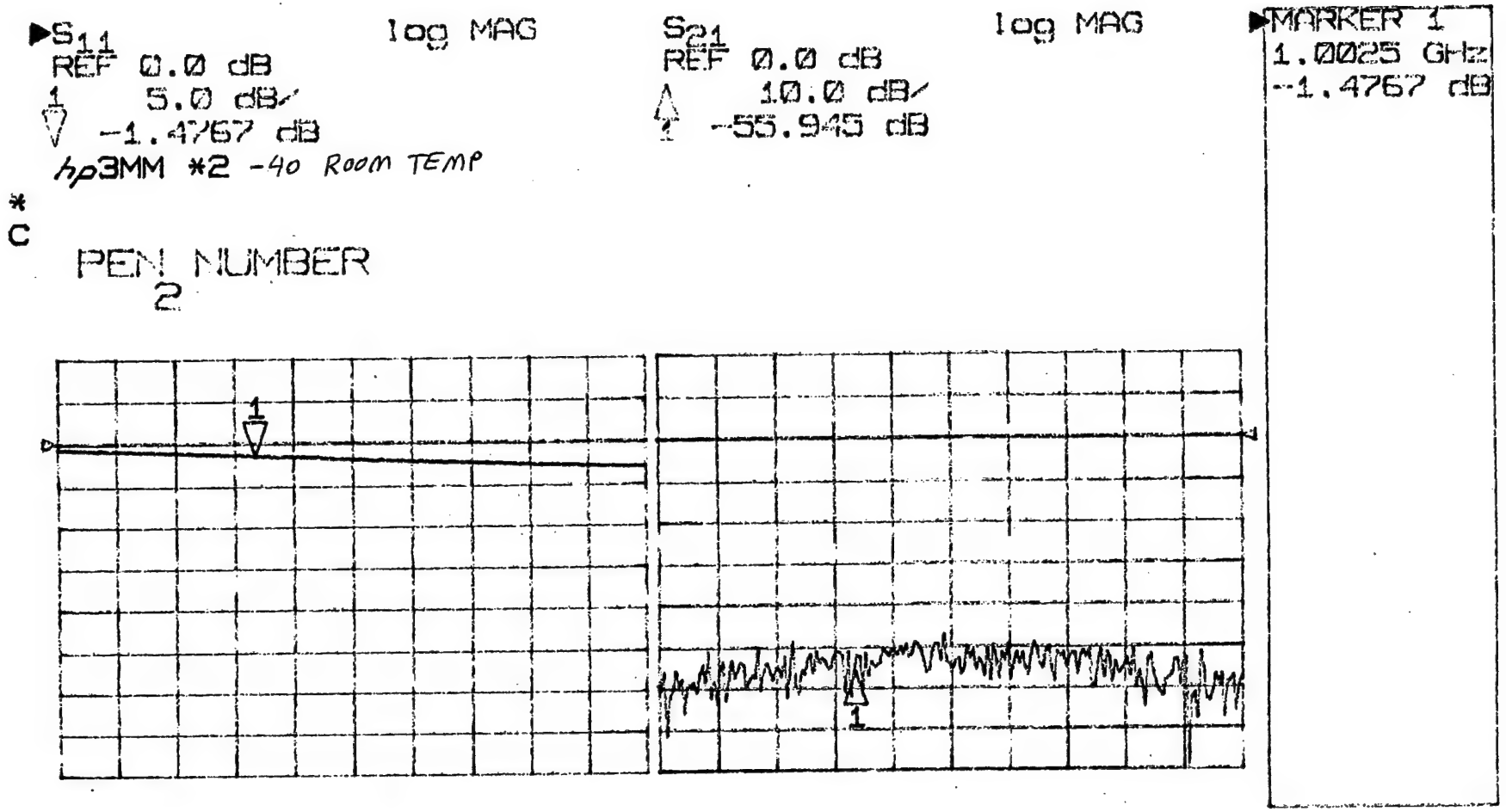
▶S11
log MAG
REF 0.0 dB
1 5.0 dB/
-1.4767 dB
hp3MM *2 -40 Room TEMP
C *
PEN NUMBER
2
S21
log MAG
REF 0.0 dB
10.0 dB/
-55.945 dB
▶MARKER 1
1.0025 GHz
-1.4767 dB
START
0.500000000 GHz
STOP
2.000000000 GHz
03 JUL 96
10:13:35

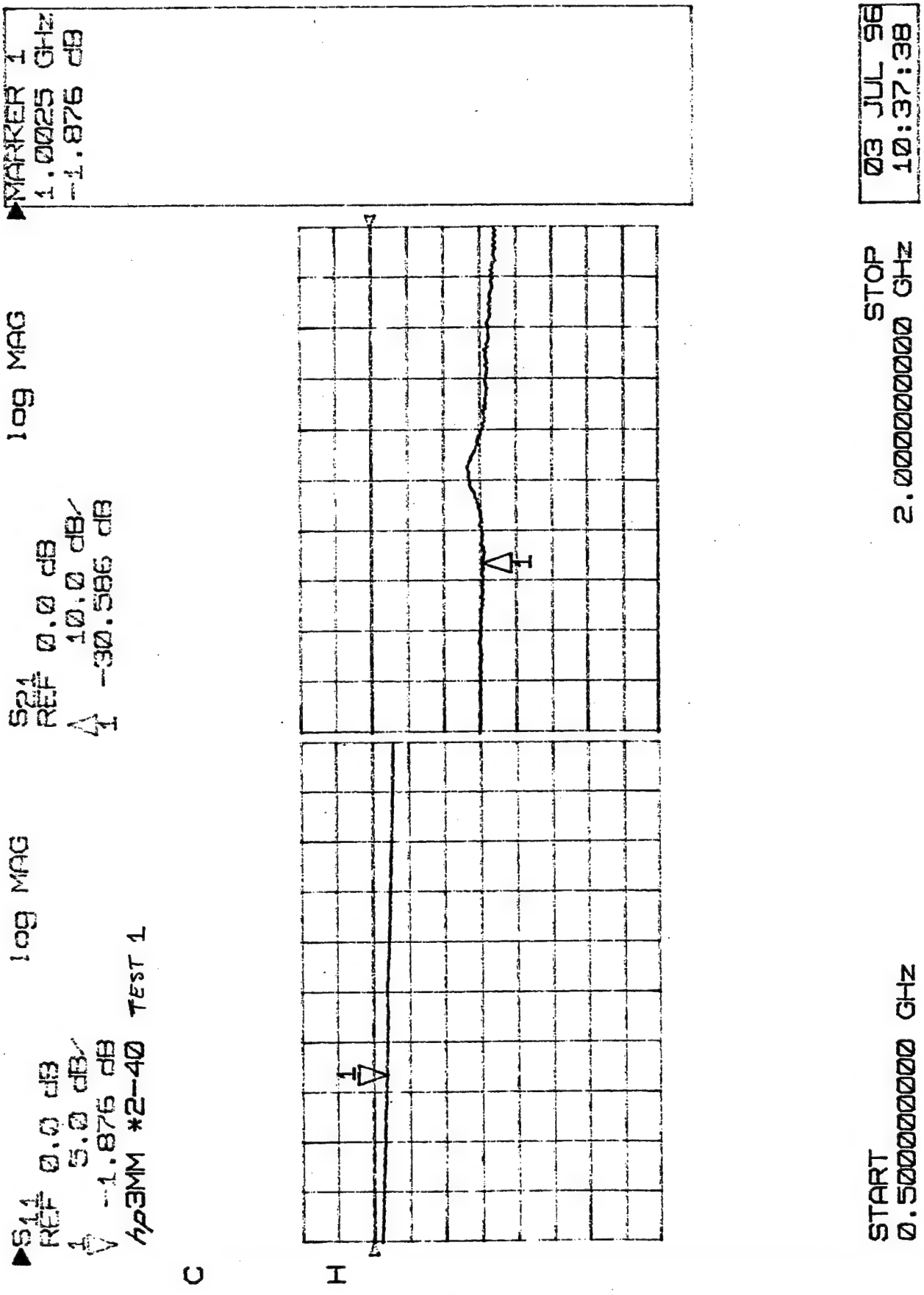
MARKER 1
1.0025 GHz
-1.876 dB
log MAG
S21
REF 0.0 dB
10.0 dB/
1 -30.586 dB
log MAG
S11
REF 0.0 dB
5.0 dB/
1 -1.876 dB
HP3MM *2-40 TEST 1
START
0.500000000 GHz
STOP
2.000000000 GHz
03 JUL 96
10:37:38

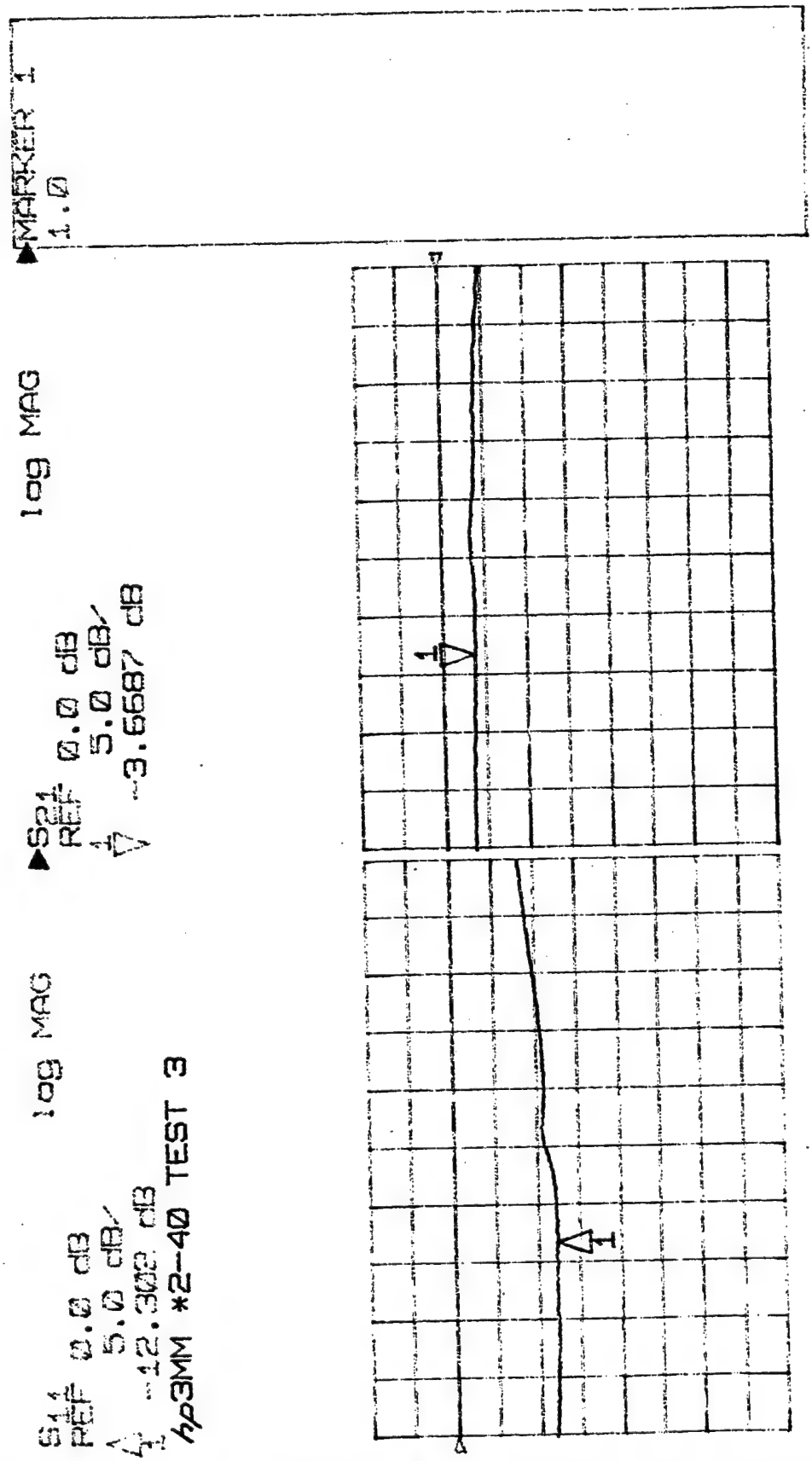
MARKER 1
1.0
log MAG
S21
REF 0.0 dB
5.0 dB/
-3.6687 dB
log MAG
S11
REF 0.0 dB
5.0 dB/
-12.3032 dB
hp3MM *2-40 TEST 3
START
0.500000000 GHz
STOP
2.000000000 GHz

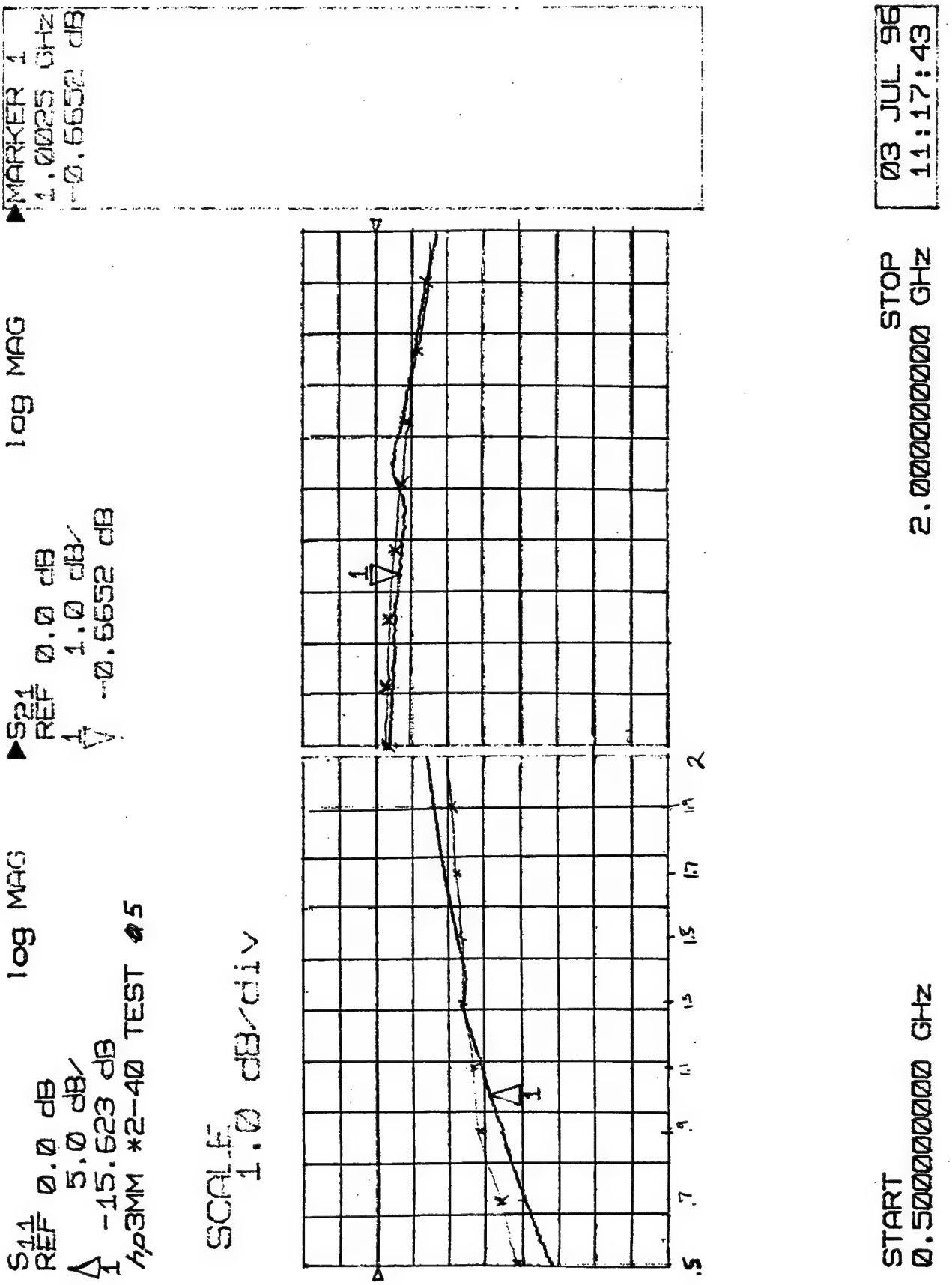
S11
REF 0.0 dB
5.0 dB/
-15.623 dB
#p3MM *2-40 TEST #5
log MAG
S21
REF 0.0 dB
1.0 dB/
-0.6552 dB
log MAG
MARKER 1
1.0025 GHz
-0.6552 dB
SCALE
1.0 dB/div
START
0.500000000 GHz
STOP
2.000000000 GHz
03 JUL 96
11:17:43

S11 log MAG
REF 0.0 dB
5.0 dB/
1 -14.794 dB
hp3MM *2-40 TEST 5 7 8

S21 log MAG
REF 0.0 dB
1 5 1.0 dB/
-0.6817 dB

MARKER 1
1.0025 GHz
-0.6817 dB

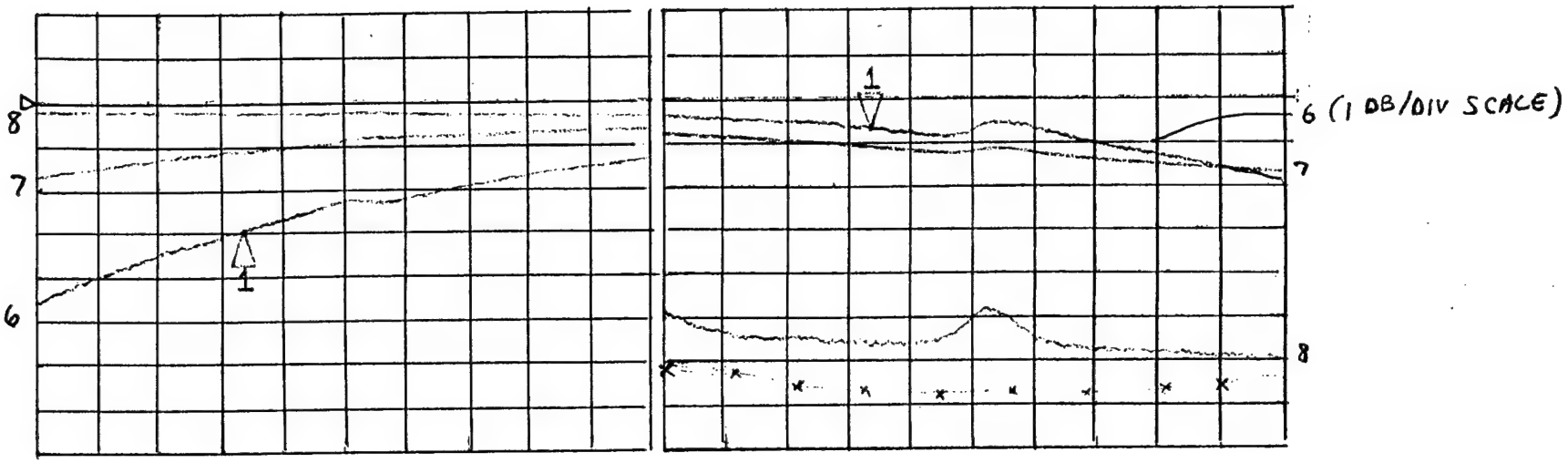


START
0.500000000000 GHz

STOP
2.000000000000 GHz

03 JUL 96
11:25:48

C

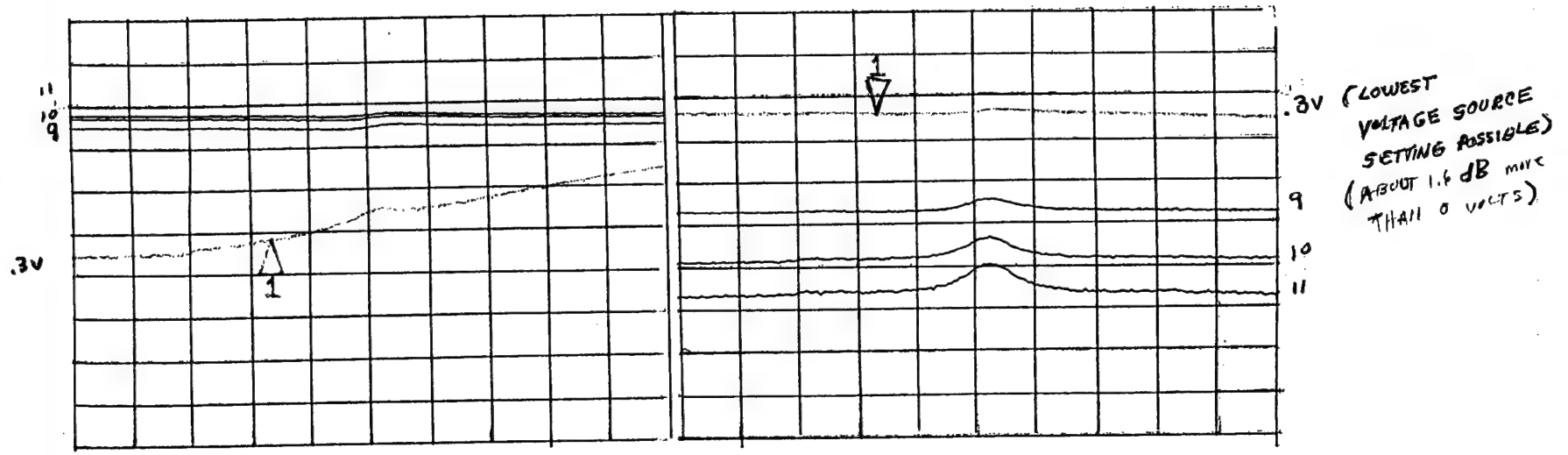
S11
REF 0.0 dB
Δ 5.0 dB/
1 -16.03 dB
hp3MM *2-40 TEST 9 10 11
log MAG
S21
REF 0.0 dB
1 5.0 dB/
2.2213 dB
MARKER 1
1.0025 GHz
-2.2213 dB
.3V
9
10
11
(LOWEST VOLTAGE SOURCE SETTING POSSIBLE) (ABOUT 1.6 dB more THAN 0 VOLTS)
START
0.500000000 GHz
STOP
2.000000000 GHz
03 JUL 96
11:31:05

S11 log MAG
REF 0.0 dB
5.0 dB/
1 -2.6458 dB
hp3MM *2-40 TEST 12 13 14

S21 log MAG
REF 0.0 dB
1 5.0 dB/
-15.87 dB

MARKER 1
1.0025 GHz
-15.87 dB

C

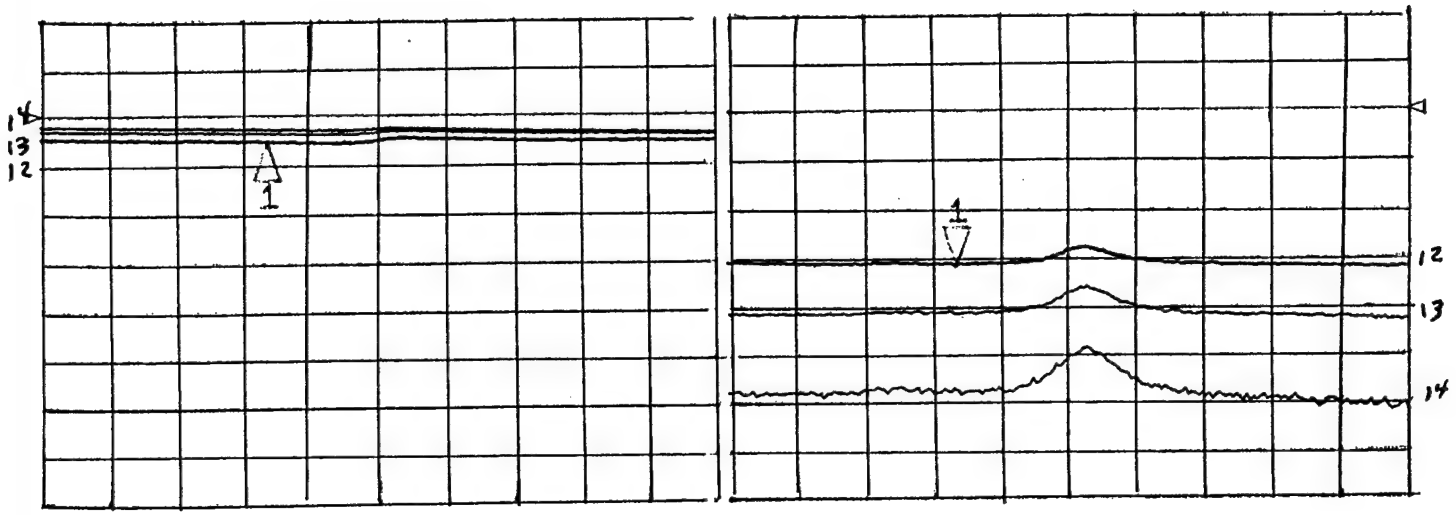


START
0.500000000000 GHz

STOP
2.000000000000 GHz

03 JUL 96
11:41:20

S11 log MAG
REF 0.0 dB
5.0 dB/
1 -1.8552 dB
hp3MM *2-40 TEST 15 16 17

▶S21 log MAG
REF 0.0 dB
1 5.0 dB/
-20.673 dB

▶MARKER 1
1.0025 GHz
-20.673 dB

*
C

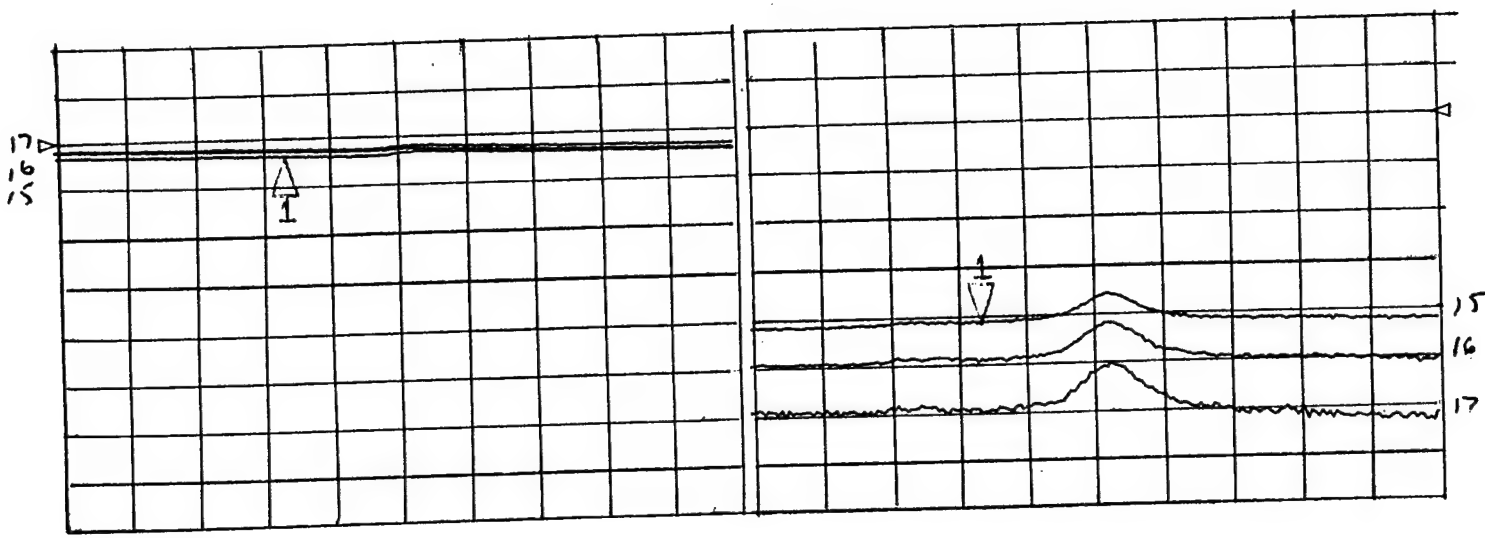


START
0.500000000 GHz

STOP
2.000000000 GHz

03 JUL 96
11:46:24

NAWCWPNS TP 8335

60

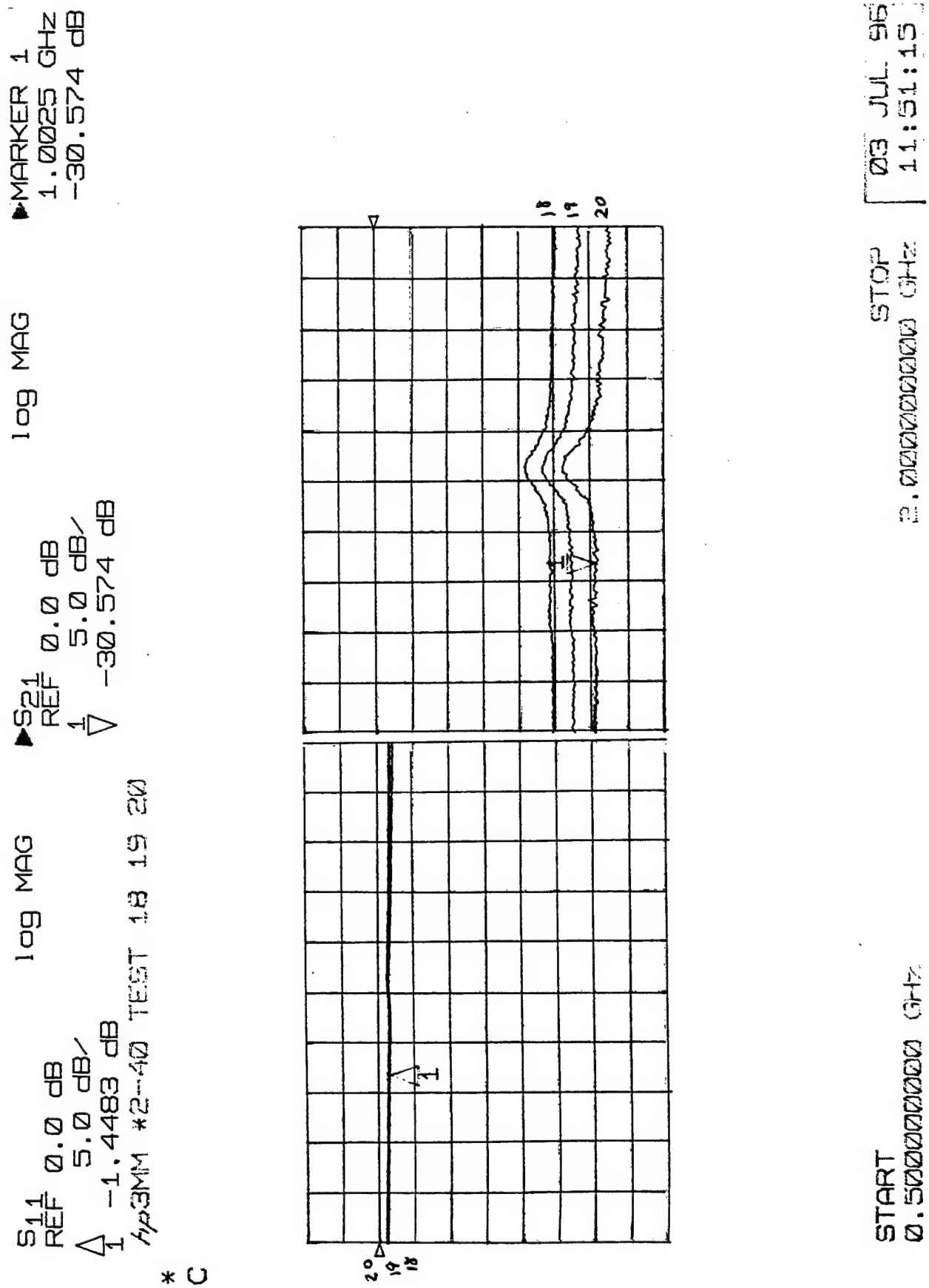
S11
REF 0.0 dB
5.0 dB/
1 -1.4483 dB
Hp83MM *2-40 TEST 18 19 20
log MAG
S21
REF 0.0 dB
5.0 dB/
1 -30.574 dB
log MAG
MARKER 1
1.0025 GHz
-30.574 dB
START
0.500000000 GHz
STOP
2.000000000 GHz
03 JUL 96
11:51:15

▶$S_{11}$ log MAG
REF 0.0 dB
5.0 dB/

$S_{21}$ log MAG
REF 0.0 dB
10.0 dB/

hp2MM *1-40 ROOM TEMP

C

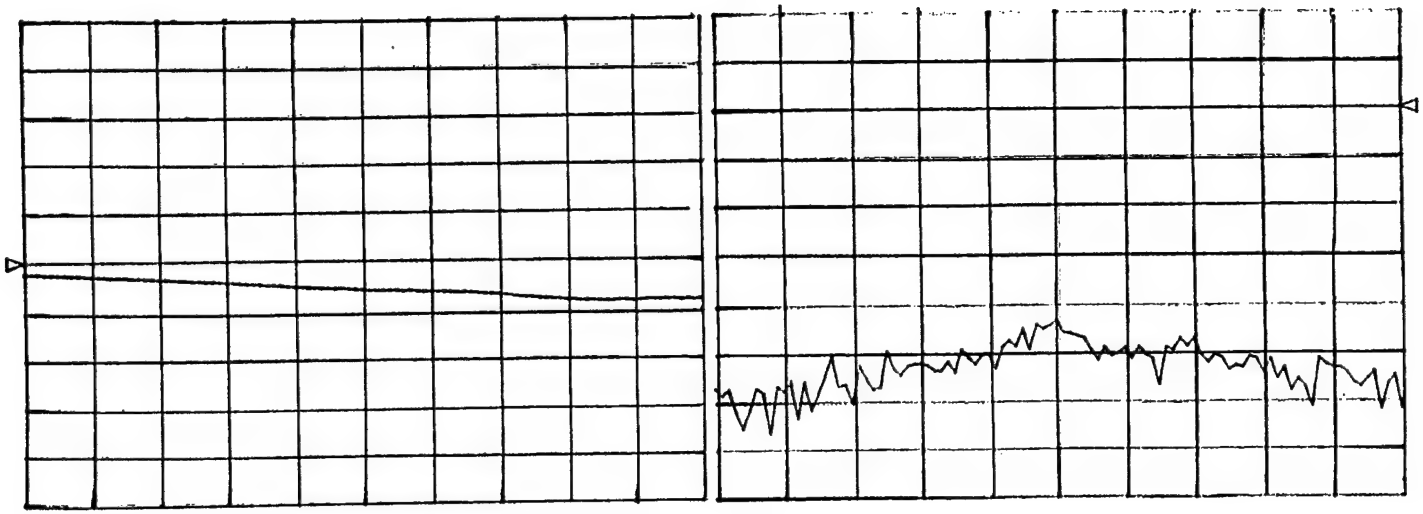

START
0.5000000000 GHz

STOP
2.0000000000 GHz

31 JUL 96
08:55:51

▶$S_{11}$ log MAG
REF 0.0 dB
5.0 dB/

$S_{21}$ log MAG
REF 0.0 dB
10.0 dB/

hp2MM *1-40 TEST 1

C

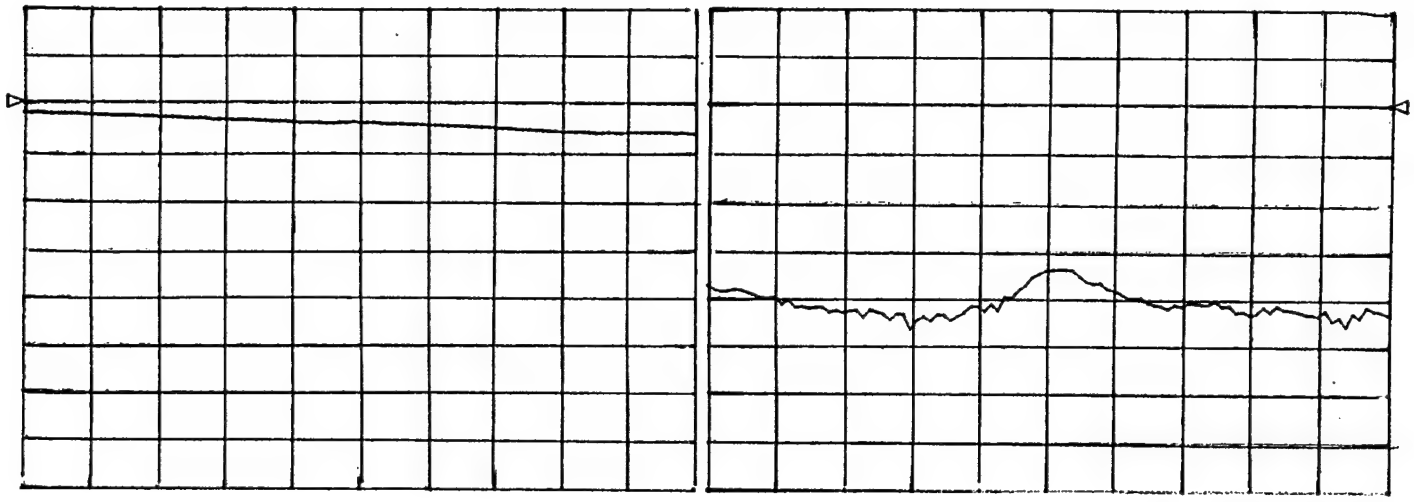

START
0.500000000 GHz

STOP
2.000000000 GHz

31 JUL 96
09:12:10

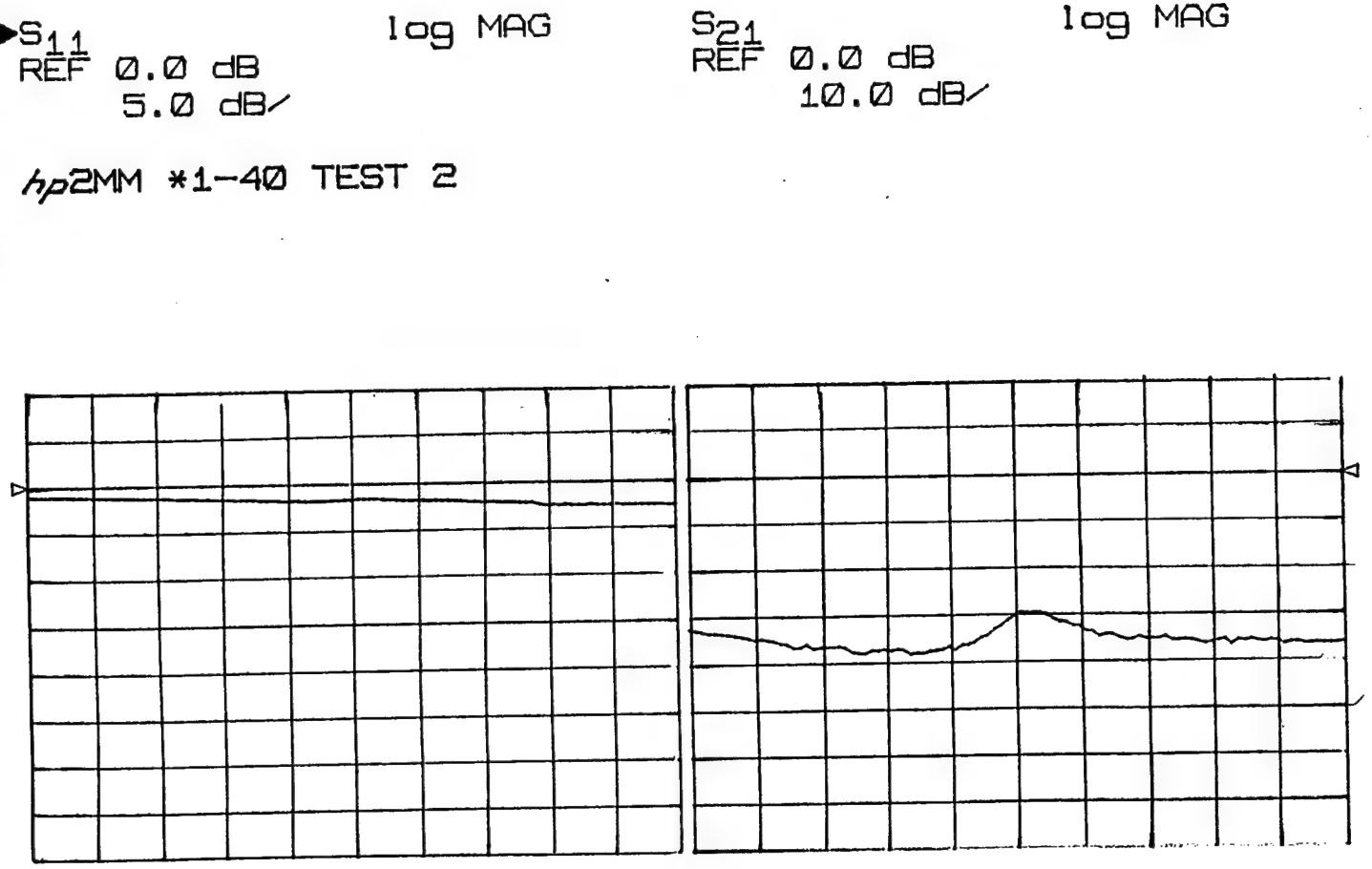
▶S11
log MAG
REF 0.0 dB
5.0 dB/
S21
log MAG
REF 0.0 dB
10.0 dB/
hp2MM *1-40 TEST 2
*
C
START
0.500000000 GHz
STOP
2.000000000 GHz
31 JUL 96
09:18:02

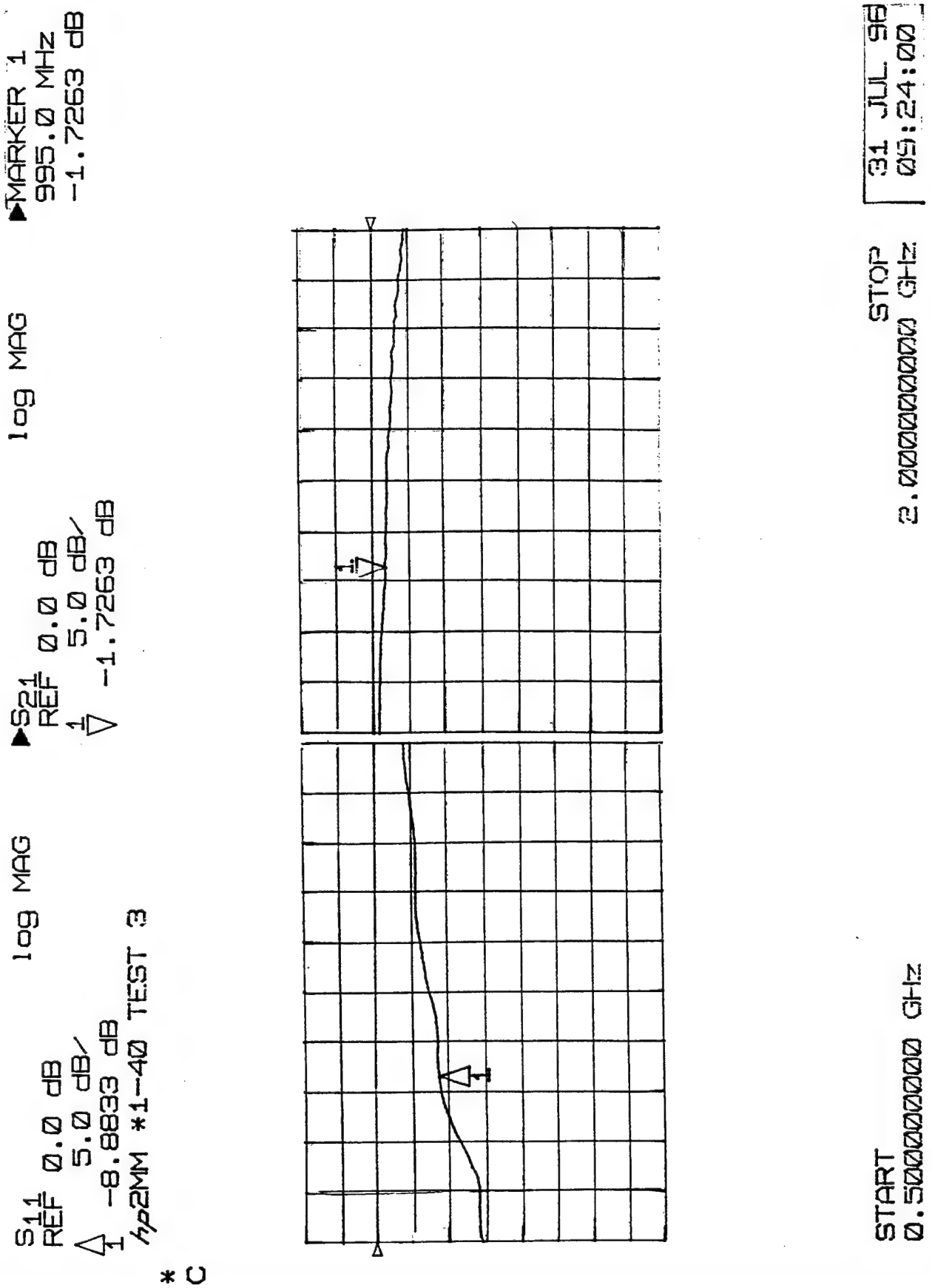
S11
REF 0.0 dB
5.0 dB/
1 -8.8833 dB
hp2MM *1-40 TEST 3
log MAG
S21
REF 0.0 dB
5.0 dB/
1 -1.7263 dB
log MAG
MARKER 1
995.0 MHz
-1.7263 dB
START
0.500000000 GHz
STOP
2.000000000 GHz
31 JUL 96
09:24:00

*C

$S_{11}$ log MAG
REF 0.0 dB
5.0 dB/
1 -11.295 dB
hp2MM *1-40 TEST 4

$S_{21}$ log MAG
REF 0.0 dB
1 1.0 dB/
1 -1.3332 dB

MARKER 1
995.0 MHz
-1.3332 dB

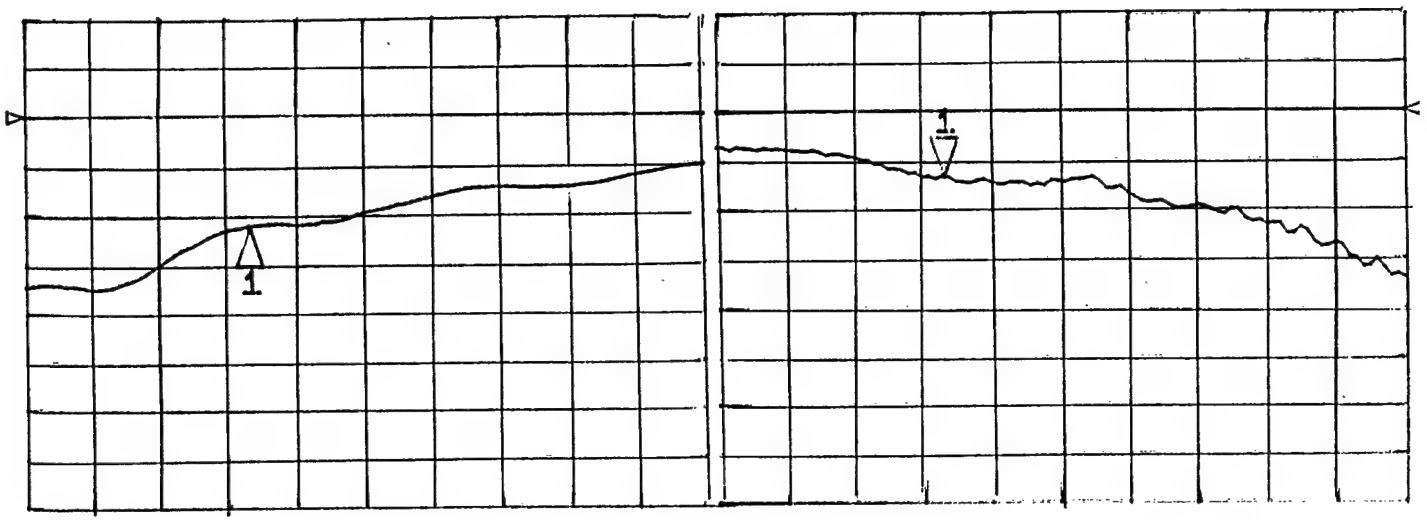


START
0.500000000 GHz

STOP
2.000000000 GHz

31 JUL 96
09:28:31

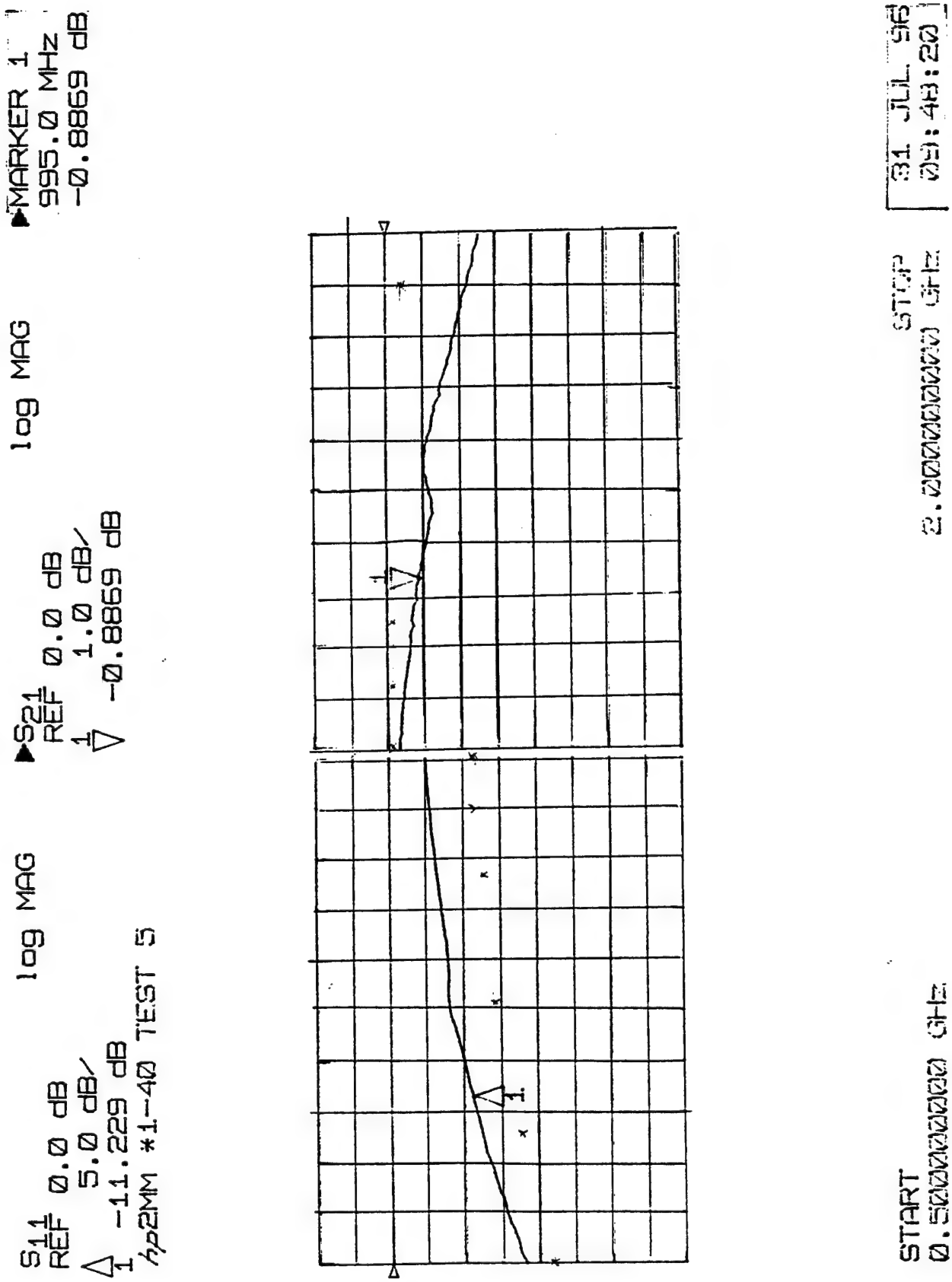
S11
REF 0.0 dB
5.0 dB/
1 -11.229 dB
log MAG
#p2MM *1-40 TEST 5
S21
REF 0.0 dB
1.0 dB/
1 -0.8869 dB
log MAG
MARKER 1
995.0 MHz
-0.8869 dB
START
STOP
31 JUL 96
09:48:20

$S_{11}$ log MAG
REF 0.0 dB
5.0 dB/
1 -8.873 dB
hp2MM *1.-40 TEST 6 7 8

$S_{21}$ log MAG
REF 0.0 dB
1 5.0 dB/
-1.2538 dB

MARKER 1
995.0 MHz
-1.2538 dB

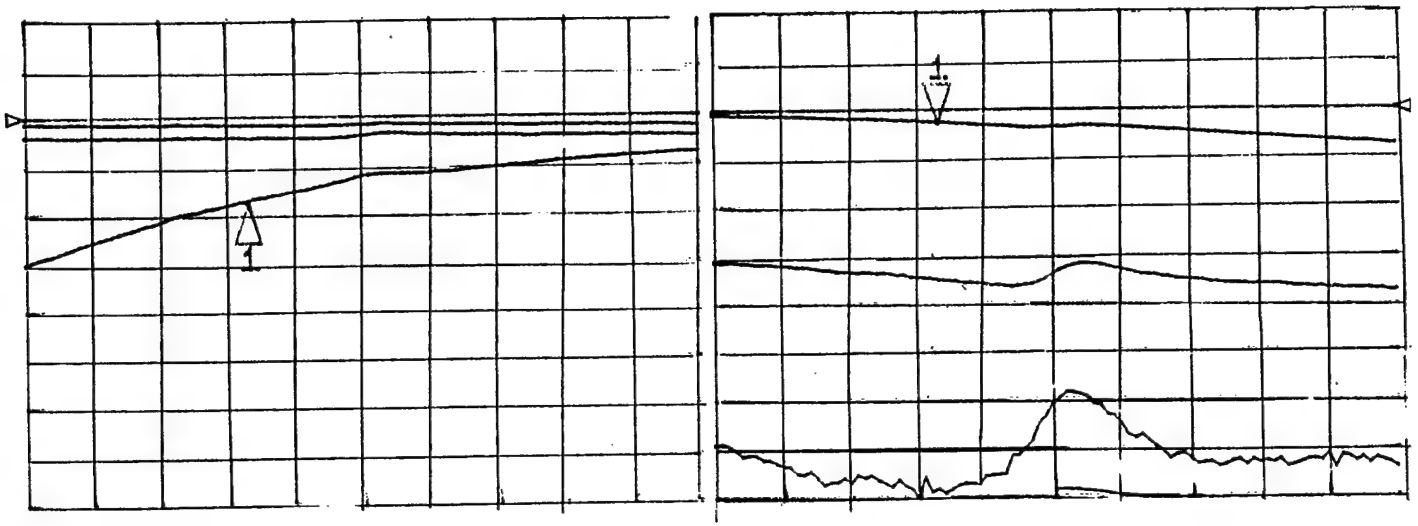

START
0.500000000000 GHz

STOP
2.000000000000 GHz

31. JUL. 96
09:51:03

$S_{11}$ log MAG
REF 0.0 dB
5.0 dB/
1 -1.4276 dB

$S_{21}$ log MAG
REF 0.0 dB
1 5.0 dB/
-24.297 dB

MARKER 1
995.0 MHz
-24.297 dB

hp2MM *1-40 TEST 9 1.0 1.1

*
C

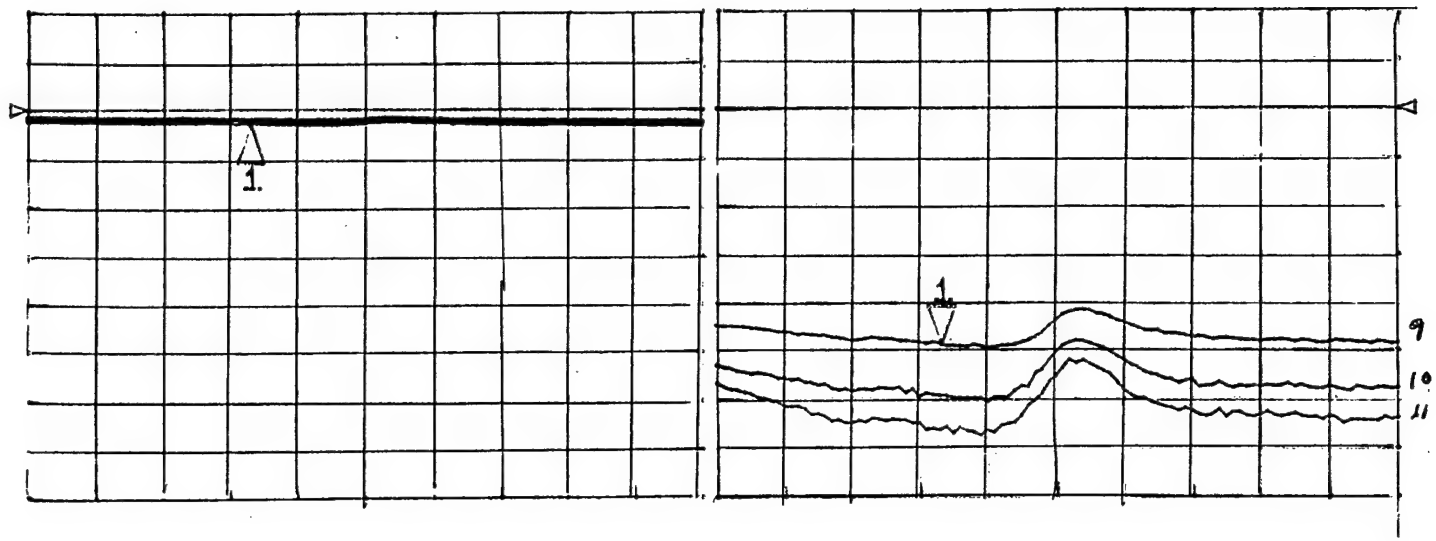


START
0.500000000000 GHz

STOP
2.000000000000 GHz

31. JUL 96
09:55:54

$S_{11}$ log MAG
REF 0.0 dB
5.0 dB/
1 -1.3228 dB
hp2MM *1.-40 TEST 1.2 1.3 1.4

$S_{21}$ log MAG
REF 0.0 dB
1 5.0 dB/
-26.037 dB

MARKER 1
995.0 MHz
-26.037 dB

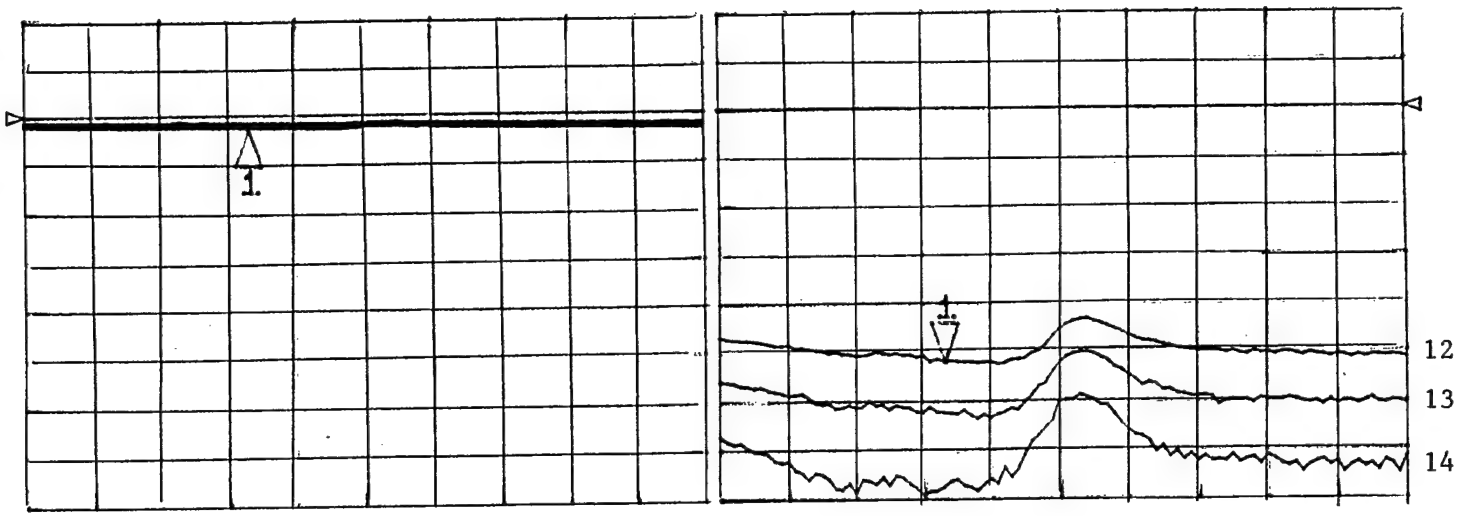


START
0.500000000000 GHz

STOP
2.000000000000 GHz

31. JUL. 96
10:00:29

$S_{11}$ log MAG
REF 0.0 dB
5.0 dB/
1 -1.0853 dB
Hp2MM *1-40 TEST 1.5 1.6 1.7

$S_{21}$ log MAG
REF 0.0 dB
1 5.0 dB/
-30.876 dB

MARKER 1
995.0 MHz
-30.876 dB

*
C

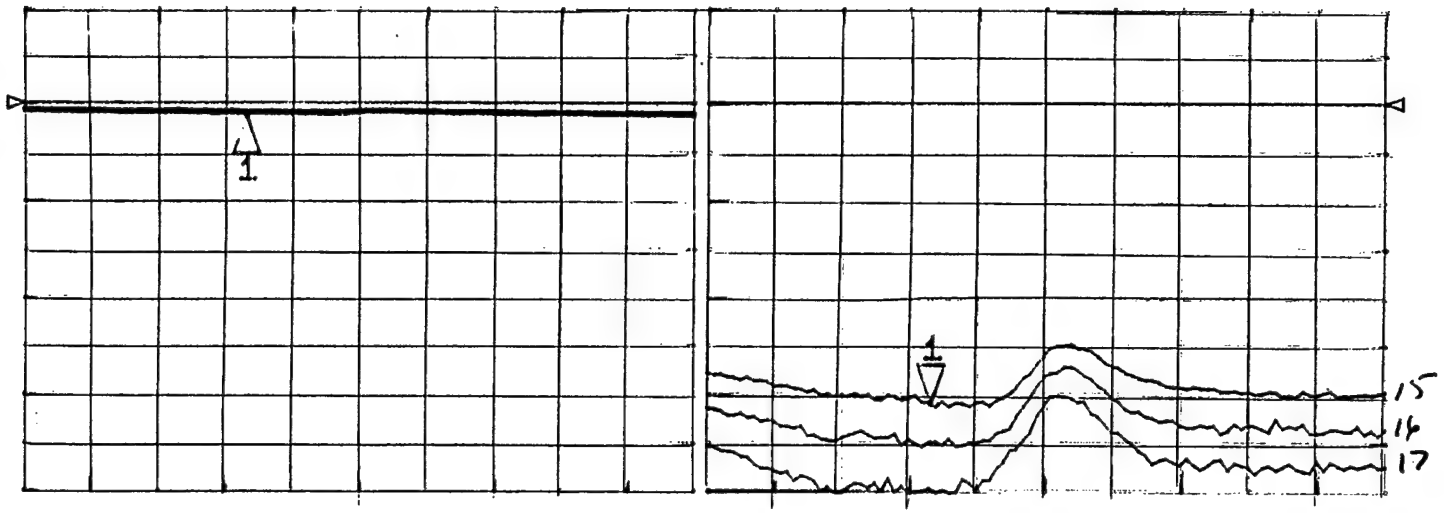


START
0.500000000000 GHz

STOP
2.000000000000 GHz

31 JUL 96
10:04:12

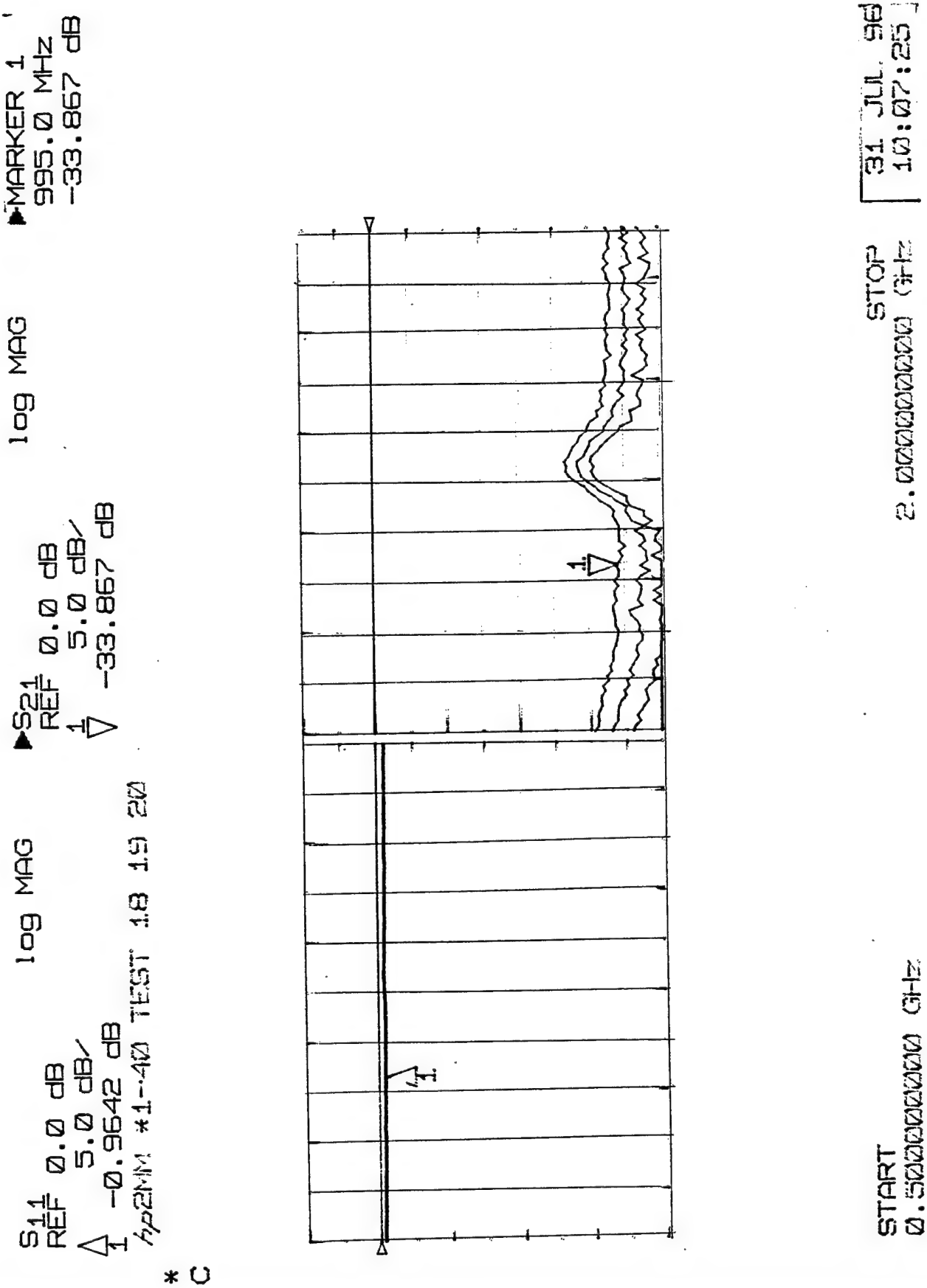
log MAG
S11
REF 0.0 dB
5.0 dB/
1 -0.9642 dB
log MAG
S21
REF 0.0 dB
5.0 dB/
1 -33.867 dB
MARKER 1
995.0 MHz
-33.867 dB
START
0.500000000000 GHz
STOP
2.000000000000 GHz
31 JUL 96
10:07:25

## Appendix D

### NRL TEST RESULTS ON CONDUCTUS CIRCUITS

SUMMARY REPORT OF NRL RESULTS OBTAINED ON CONDUCTUS TEST CIRCUITS BY V.M. BROWNING, CODE 6344, NRL, WASHINGTON, DC.

This report summarizes results obtianed at NRL on test circuits manufactured by Conductus and received via NAWCWPNS, China Lake. These circuits were provided as part of the Navy's high temperature superconducting antenna program and were to be used to test various methods for fast switching of high $T_c$ circuits. Each circuit consists of two patterened superconducting $YBa_2Cu_3O_{7-\delta}$ (YBCO) microstrips which have been deposited on one side of an $LaAlO_3$ substrate. The other side of the substrate contains a layer of either gold or YBCO that comprises the device ground plane. Each microstrip has a switching segment that consists of a narrowed region 10-millimeters wide and ion milled to a thickness of 1000 Å. The four circuits tested at NRL were intended for studying the films response to a resistive heater and were provided with heaters deposited on top of the narrowed region with winding spacings of 40 and 80 millimeters. The heaters were electrically isolated from the superconducting fims through the use of a thin polyimide layer.

The tests conducted included resistive R(T) measurements on the microstrips as well as inductive measurements on the superconducting ground planes. Both measurements yield information concerning the quality of the superconducting films in terms of superconducting transition temperature $T_c$, transition width $\Delta T_c$, and resistivity values at essentially zero frequency. It is hoped that comparision of the dc results with those obtained at rf frequencies will help to determine whether these circuits can be considered thin film resistors for modeling purposes when designing switches that can be inserted in a superconducting antenna device.

The resistive measurements used to characterize the patterned microstrips were performed using a drive current of 1 μA applied at a frequency of 18 Hz by monitoring the in-phase (resistive) response of the sample signal using a dual-phase lock-in amplifier. Typically this measurement is performed using a four-probe configuration consisting of separate current and voltage leads. Unforturately, the circuits as provided did not allow a true four-probe measurement and, therefore, the contact resistances of the wires attached to the circuits contributed to the measured signal. However, the contact resistances were typically less than 1% of the normal state resistance of the microstrips, hence the error induced in the measurement is negligible.

The ac susceptibility measurements used to characterize circuits that had superconducting ground planes involve the use of two mutually inductive coils, one primary coil for inducing a small magnetic field and one secondary coil for monitoring the sample response. Again a lock-in amplifier is used both to drive the primary coil

(I = 100 μA, f = 10 kHz) and to monitor the out-of-phase (inductive) component of the secondary coil that is sensitive to the films response to the applied oscillating field.

Table D-1 summarizes the results obtained on the four circuits. Details can be found in the accompanyuing plots. Of note is that the superconducting ground planes contained in three out of four of the circuits all exhibited high, sharp superconducting transition temperatures indicating that Conductus deposition techniques of YBCO yielded films of consistent high quality. The resistive measurements, however, exhibited a high degree of variability suggesting that the patterning of the films has not yet been perfected. Note: the onset of the superconducting transition as measured by ac susceptibility typically occurs near the R = O point in the resistive transition, hence the 3 to 4 K discrepancy between resistive and inductive Tc values is not unexpected. Although, the resistive Tc and Dtc values were all consistent with good quality patterened films, the variability seeen in the normal state resistivity values is disturbing and suggests that the geometry of the microstrips is not well controlled. In particular, since it is unlikely that the patterning techniques used used to narrow the films will produce variable geometries, it is more likely that the ion milling process used to thin the films produces geometries of varying thickness.

Any questions concerning the results reported here or the measurement techniques used should be directed either to Valerie Browning (202) 767-6186 or Robert Soulen, Jr. (202) 767-6175 at NRL.

TABLE D-1. Summary of Results Obtained From Conductus Switching Circuits.

| | Ground plane | | Strip w/40 windings | | | | Strip/w 80 μ windings | | | |
|---|---|---|---|---|---|---|---|---|---|---|
| Film | $T_c$(K) | $\Delta t_c$ (K) | $T_c$(K) | $\Delta t_c$ (K) | R @ 300K (Ω) | R @ 100 K (Ω) | $T_c$(K) | $\Delta T_c$ (K) | R @ 300 K (Ω) | R @ 100 K (Ω) |
| 1 | 85.5 | 0.5 | 89.9 | 4.5 | 3900 | 1600 | 89.8 | 5.5 | 8700 | 3800 |
| 2 | 85.5 | 0.5 | 89.8 | 5 | 4200 | 1700 | 91 | 2 | 4000 | 1700 |
| 3 | 87.5 | 0.9 | 89.9 | 0.5 | 6400 | 2750 | 89.7 | 5.5 | 6200 | 2750 |
| 4 | | | 90.5 | 1.4 | 4500 | 1900 | 90.5 | 1.3 | 3200 | 1400 |

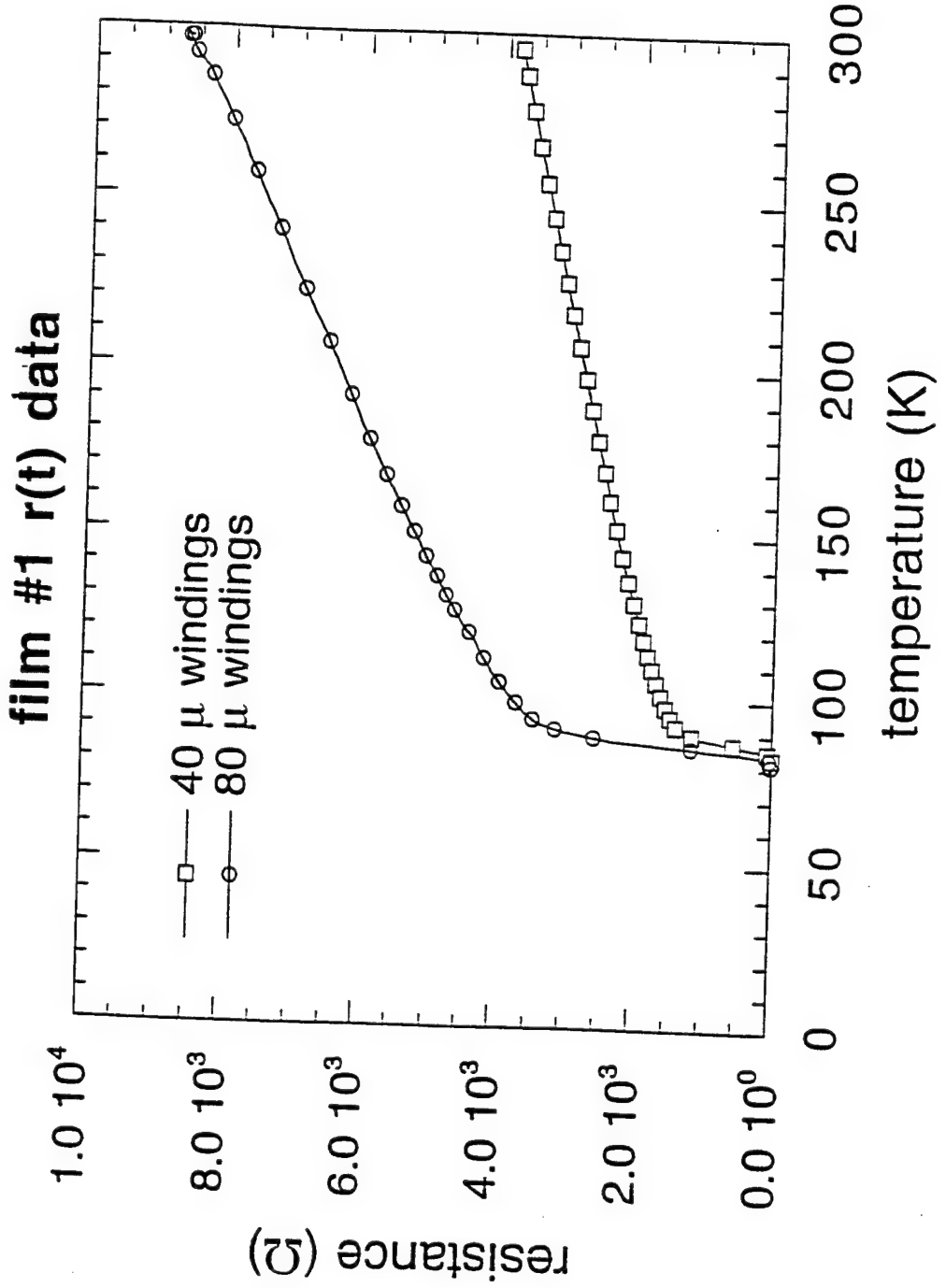
film #1 r(t) data
40 μ windings
80 μ windings
resistance (Ω)
1.0 10^4
8.0 10^3
6.0 10^3
4.0 10^3
2.0 10^3
0.0 10^0
0
50
100
150
200
250
300
temperature (K)

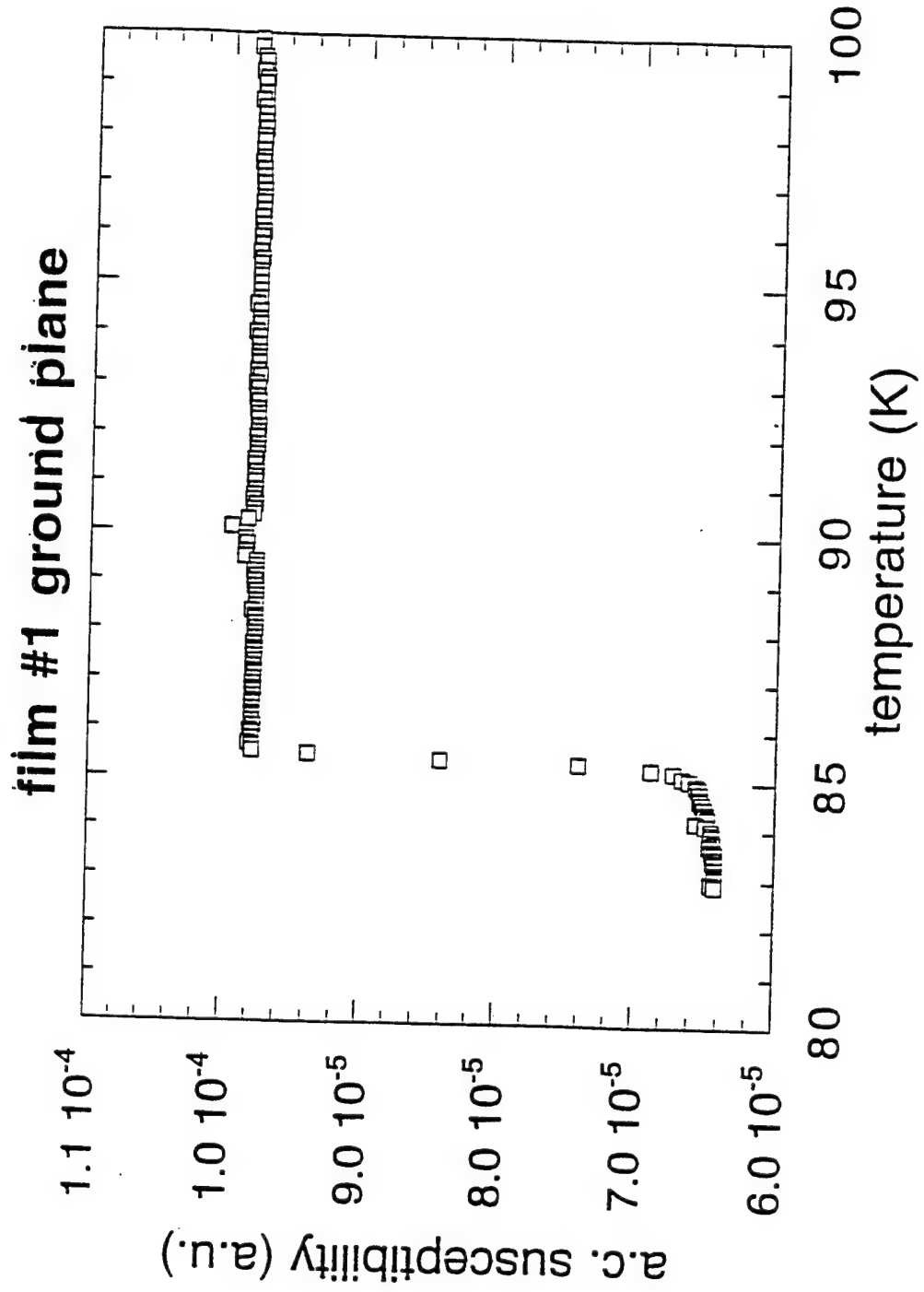
film #1 ground plane
a.c. susceptibility (a.u.)
1.1 10-4
1.0 10-4
9.0 10-5
8.0 10-5
7.0 10-5
6.0 10-5
80
85
90
95
100
temperature (K)

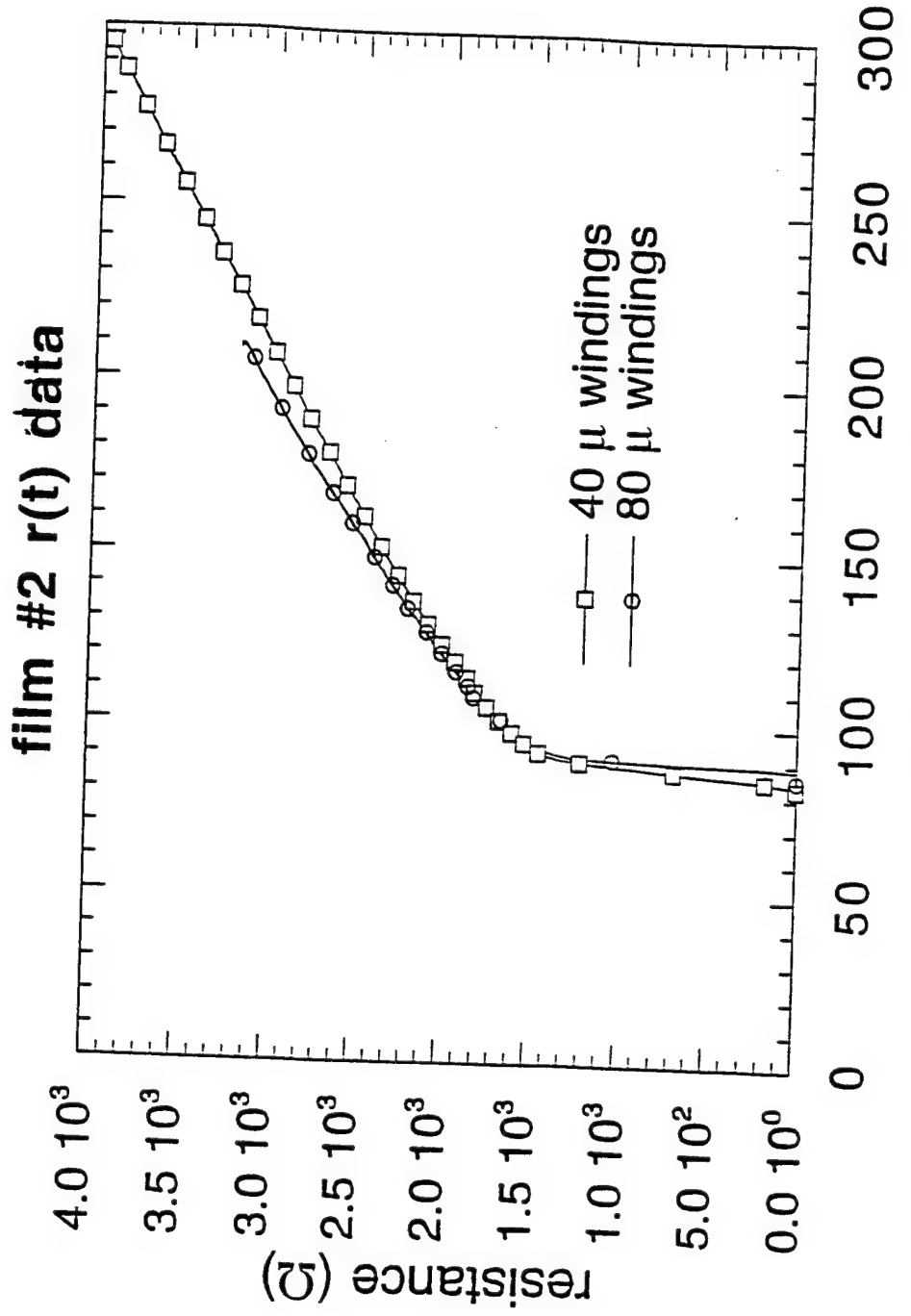
film #2 r(t) data
resistance (Ω)
4.0 10^3
3.5 10^3
3.0 10^3
2.5 10^3
2.0 10^3
1.5 10^3
1.0 10^3
5.0 10^2
0.0 10^0
0
50
100
150
200
250
300
temperature (K)
40 μ windings
80 μ windings

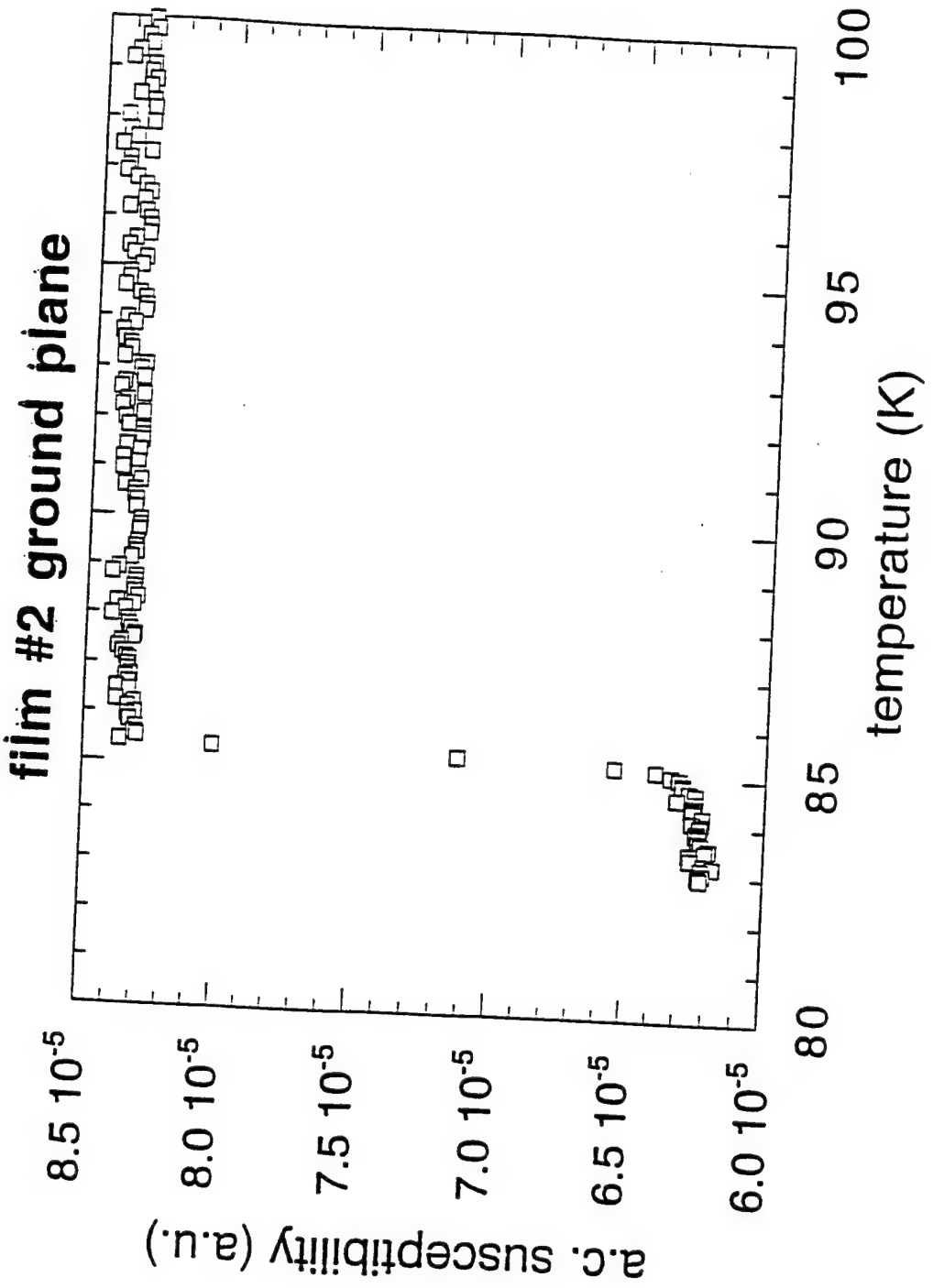
film #2 ground plane
a.c. susceptibility (a.u.)
8.5 10-5
8.0 10-5
7.5 10-5
7.0 10-5
6.5 10-5
6.0 10-5
80
85
90
95
100
temperature (K)

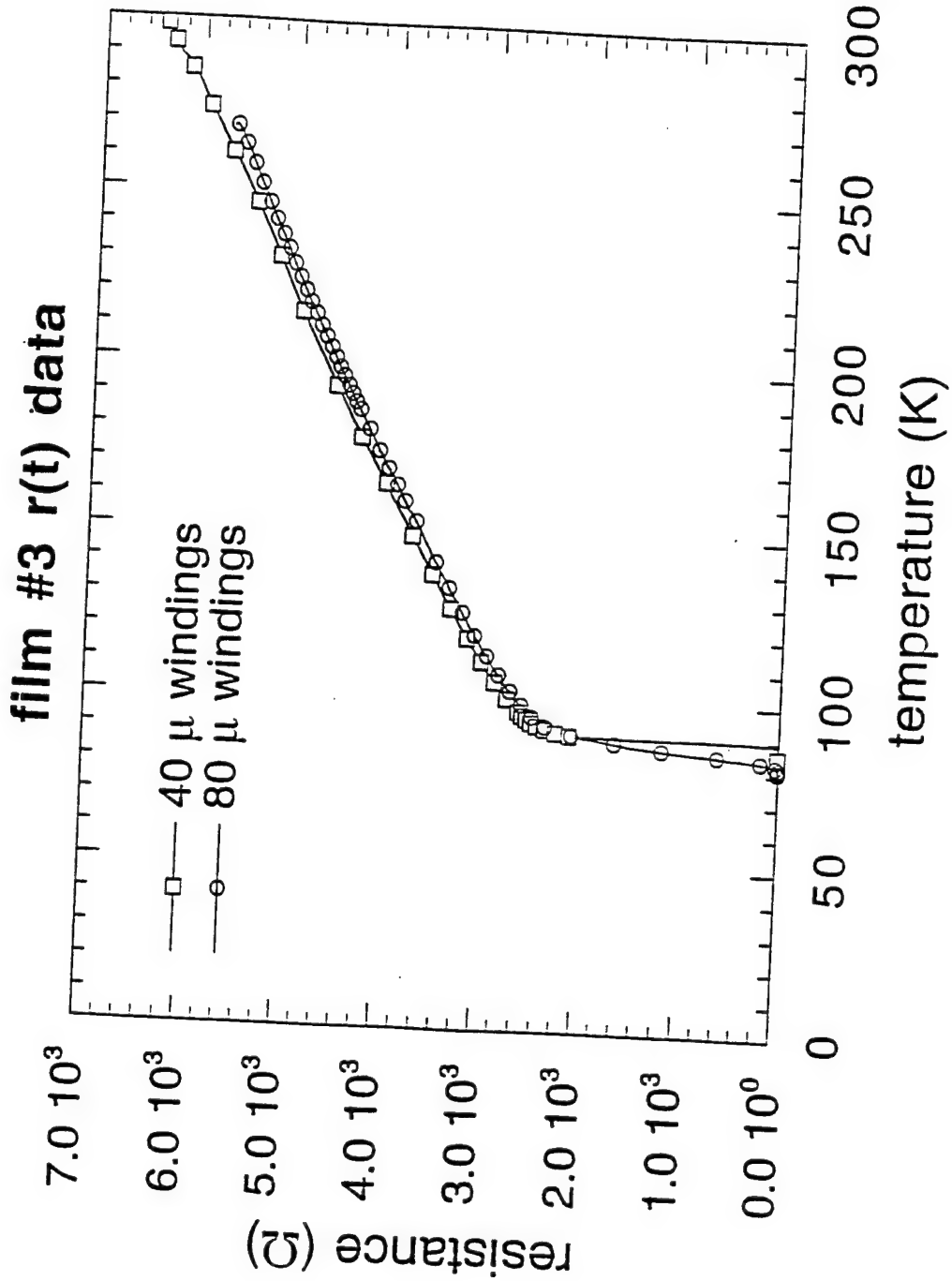
film #3 r(t) data
40 μ windings
80 μ windings
resistance (Ω)
7.0 10^3
6.0 10^3
5.0 10^3
4.0 10^3
3.0 10^3
2.0 10^3
1.0 10^3
0.0 10^0
0
50
100
150
200
250
300
temperature (K)

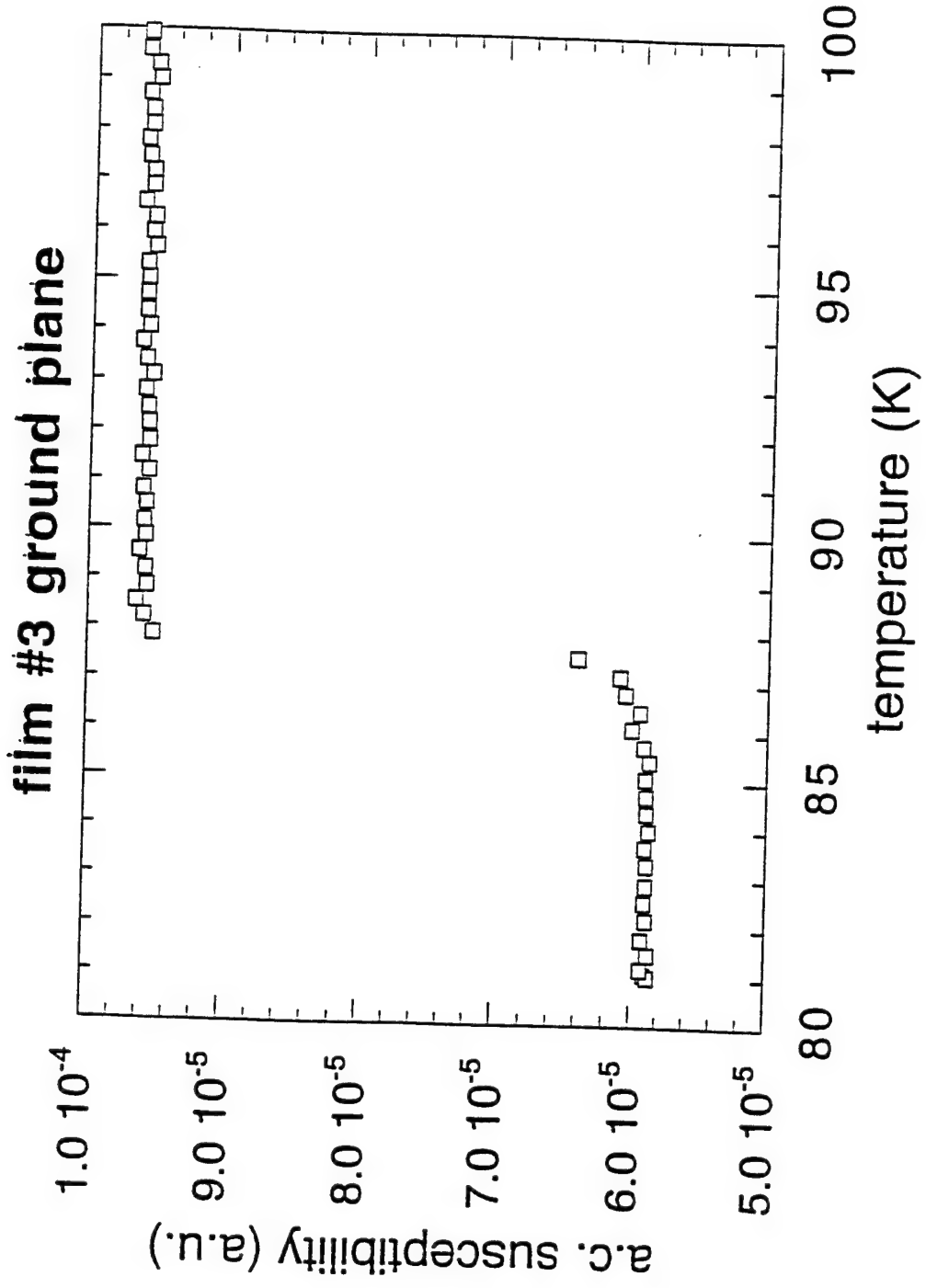
film #3 ground plane
a.c. susceptibility (a.u.)
1.0 10-4
9.0 10-5
8.0 10-5
7.0 10-5
6.0 10-5
5.0 10-5
80
85
90
95
100
temperature (K)

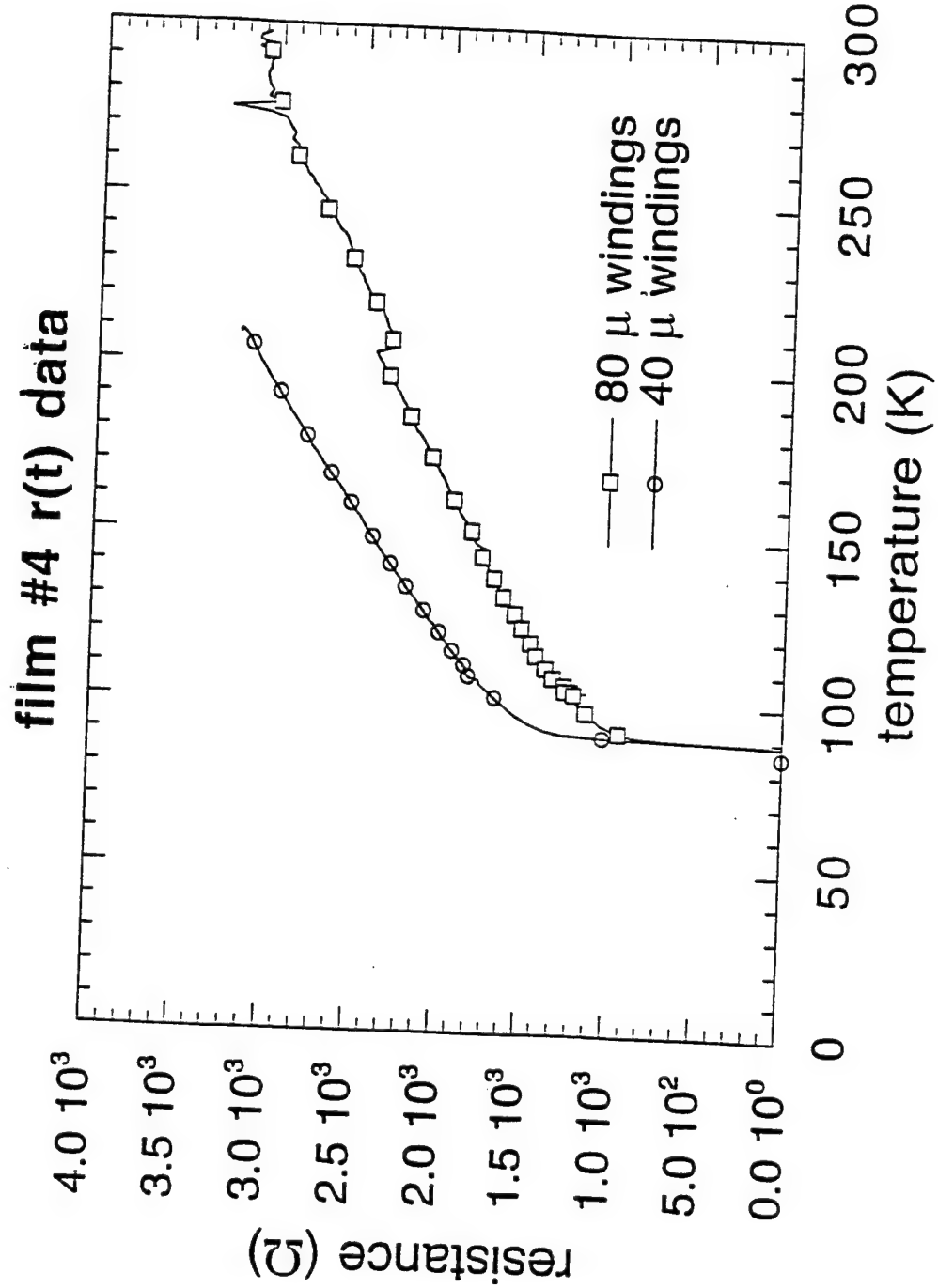
film #4 r(t) data
resistance (Ω)
4.0 10^3
3.5 10^3
3.0 10^3
2.5 10^3
2.0 10^3
1.5 10^3
1.0 10^3
5.0 10^2
0.0 10^0
0
50
100
150
200
250
300
temperature (K)
80 μ windings
40 μ windings

## Appendix E

LASER ILLUMINATED SWITCH RESULTS

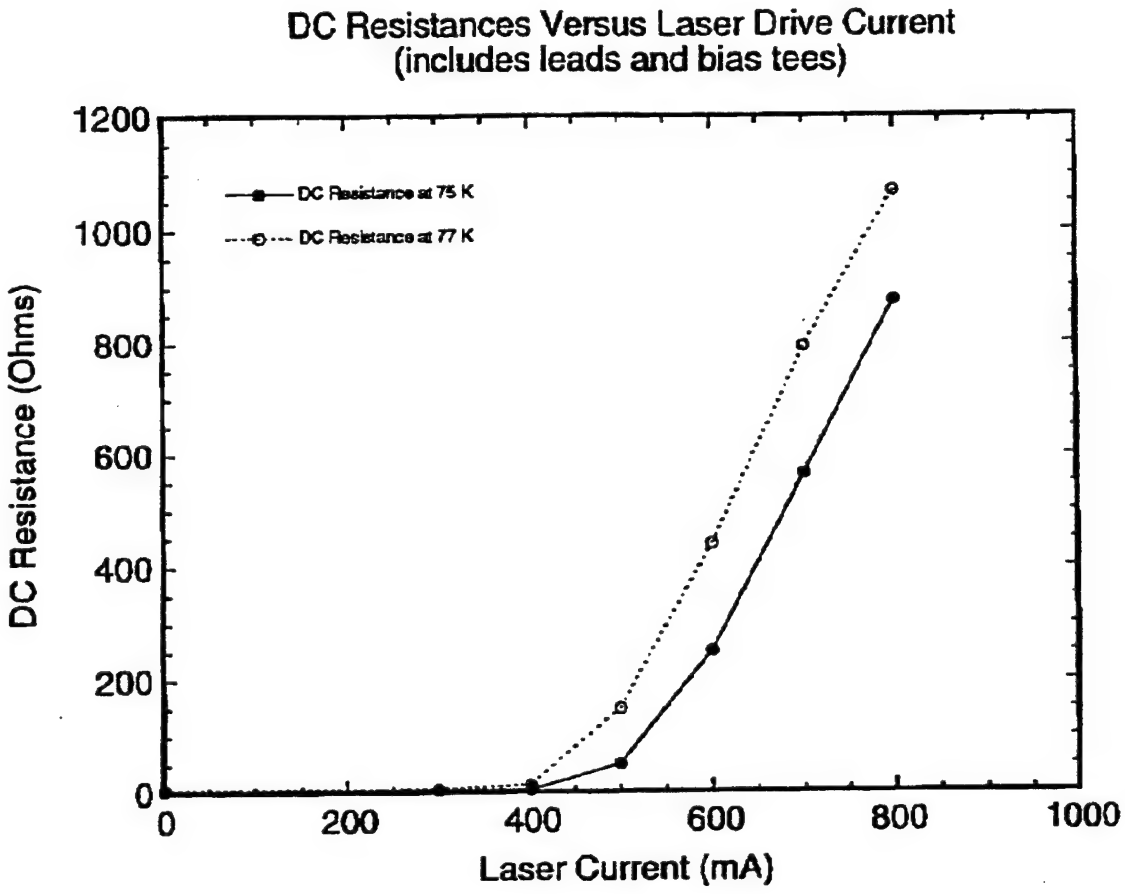


FIGURE E-1. 2-Millimeter Switch Circuit.

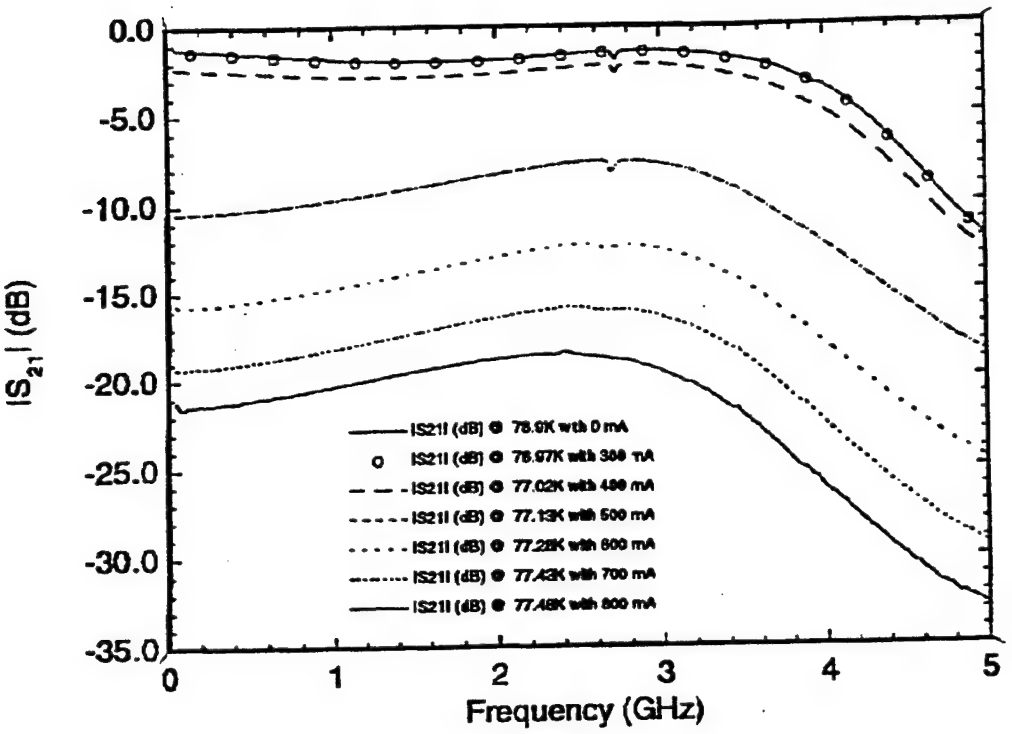


FIGURE E-2. Switch Circuit. $S_{21}$ versus laser power supply current, 2-Millimeter circuit at 77 K.

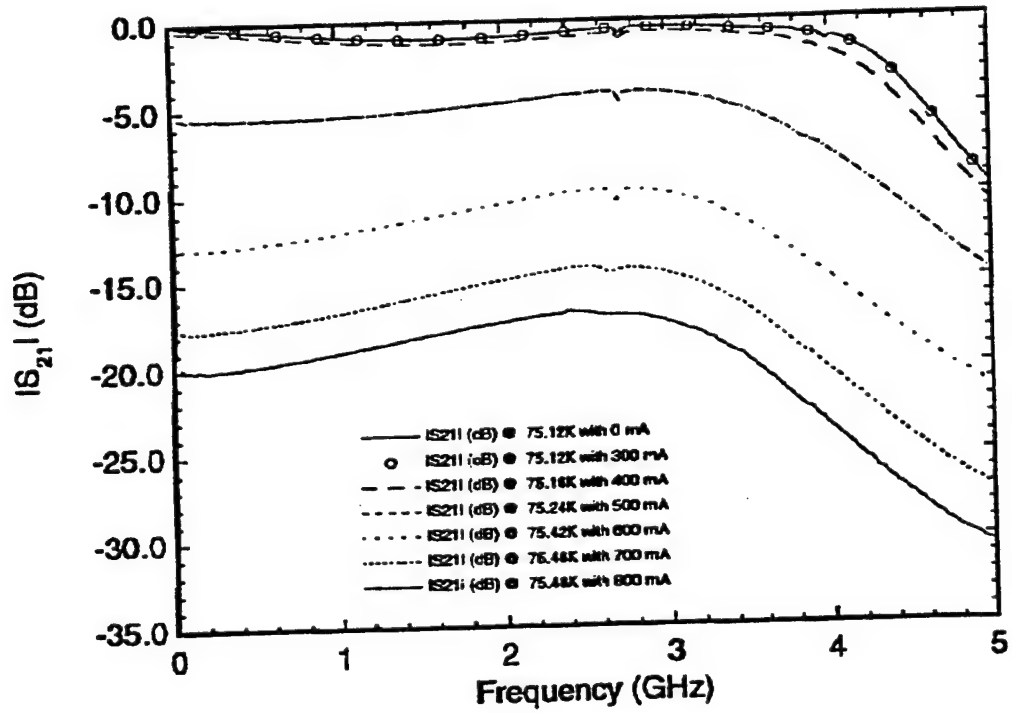


FIGURE E-3. Switch Circuit. $S_{21}$ versus laser power supply current, 2-Millimeter circuit at 75 K.

## Appendix F

PULSED SWITCHING RESULTS

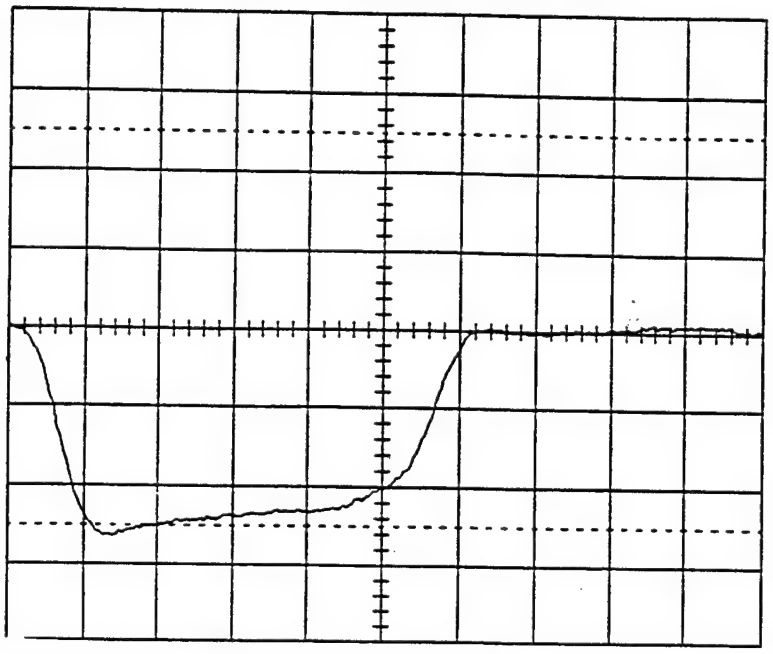

5 ns/division time scale
20 mv/division amplitude

FIGURE F-1. Detected Pulsed Output of RF Generator. Measured rise time of RF generator.

**MEASURED RISE TIME OF MODULATED RF GENERATOR OUTPUT THROUGH BIAS TEES.**

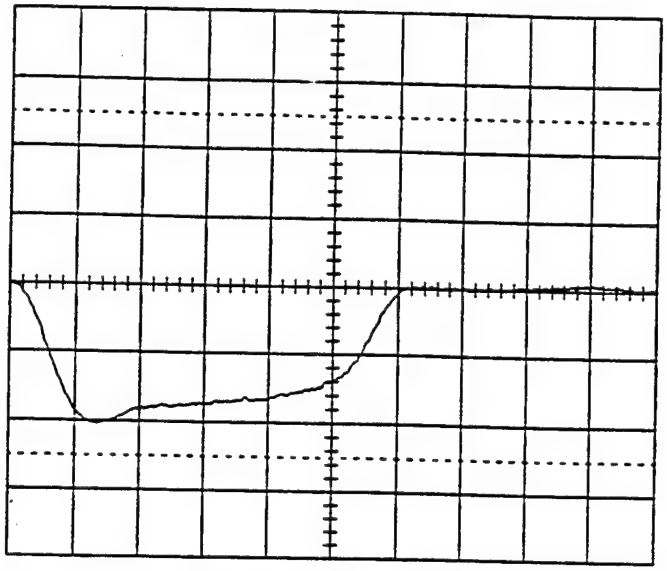

5 ns/division time scale
1 v/division amplitude

FIGURE F-2. Pulse Out of Bias Tees.

**MEASURED RISE TIME OF PULSE MEASUREMENT CIRCUIT**

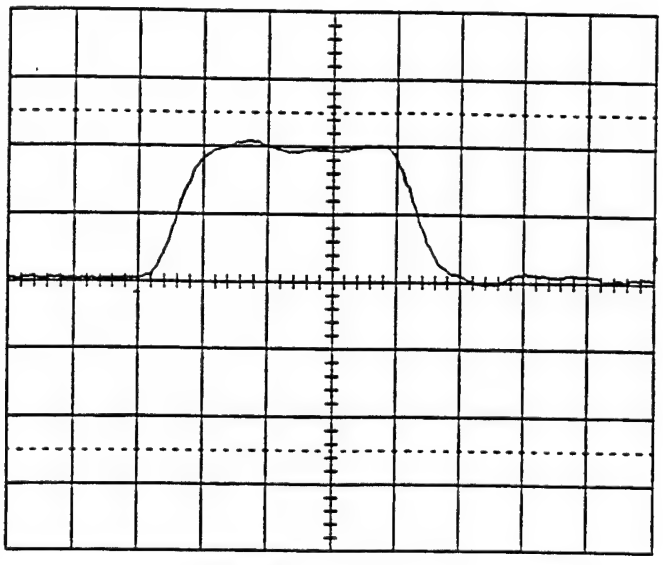

5 ns/division time scale
20 mv/division amplitude

FIGURE F-3. Detected Output of Generator Signal Through Bias Tees and Coax Cable.

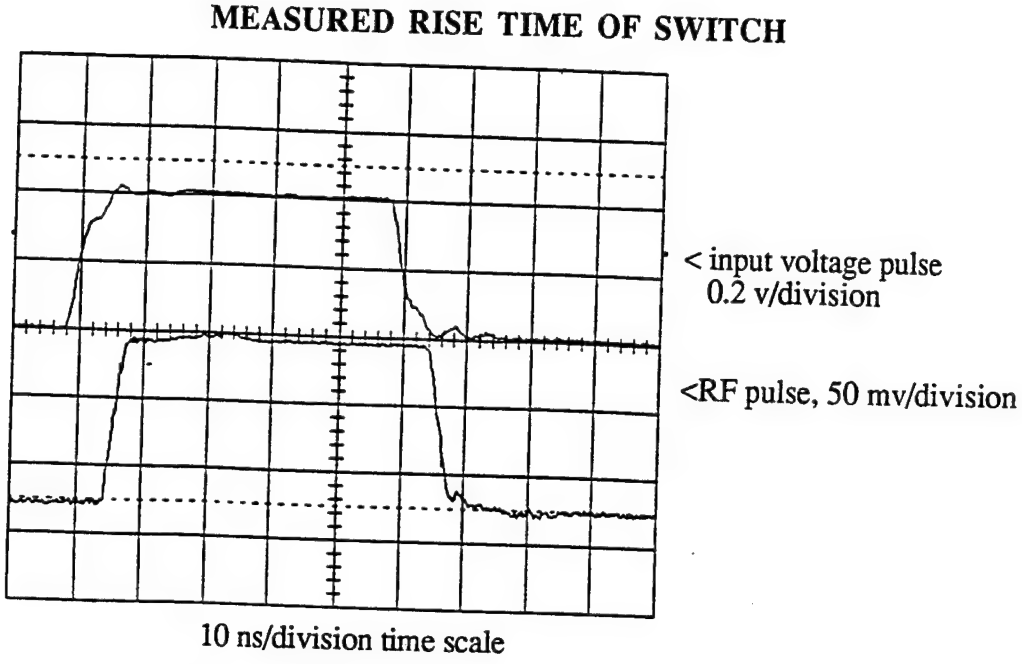


FIGURE F-4. Detected RF Pulse Out of 2-Millimeter Switch #1, 0.4 V, 50 ns wide pulse, and 500 ns period.

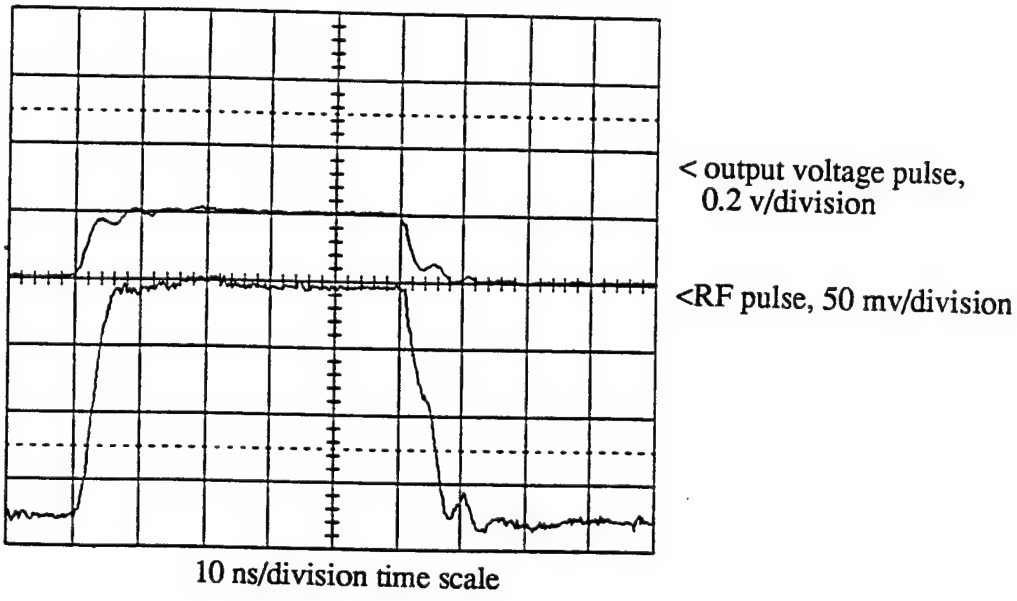


FIGURE F-5. Detected RF Pulse Out of 2-Millimeter Switch #1. 0.45 volt, 50 ns wide, 100 ns period.

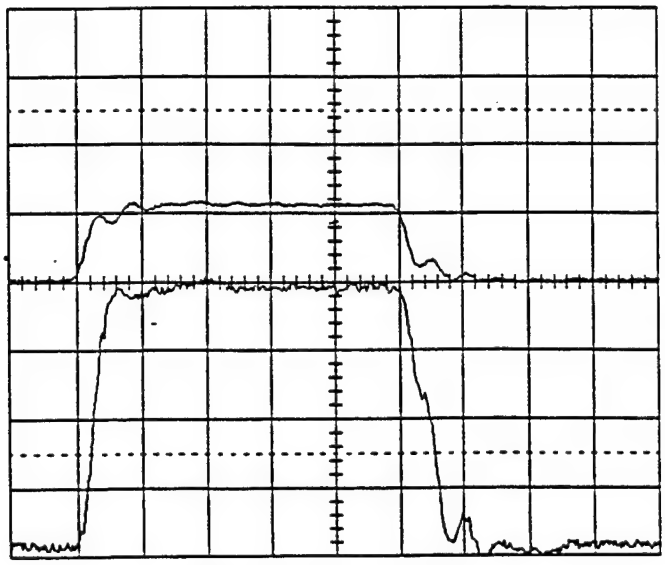


FIGURE F-6. Detected RF Pulse Out of 2- Millimeter Switch #1. 0.5 volt, 50 ns wide, 100 ns period.

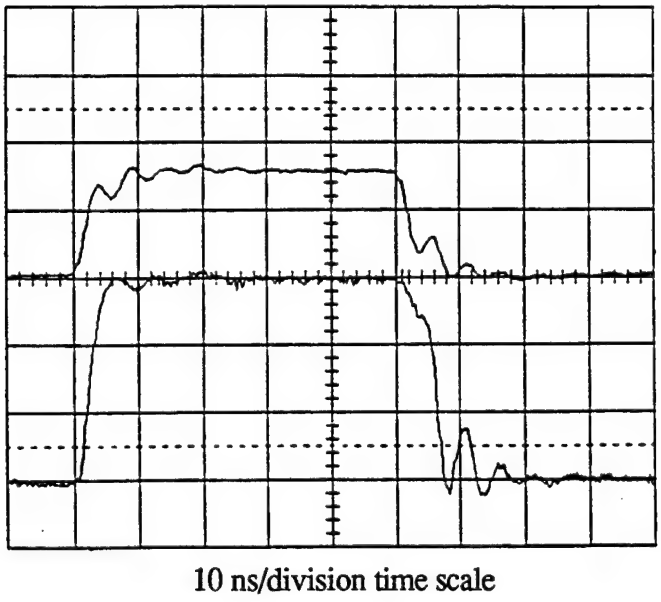


FIGURE F-7. Detected RF Pulse Out of 2- Millimeter Switch #1. 1.0 volt, 50 ns wide, 100 ns period.

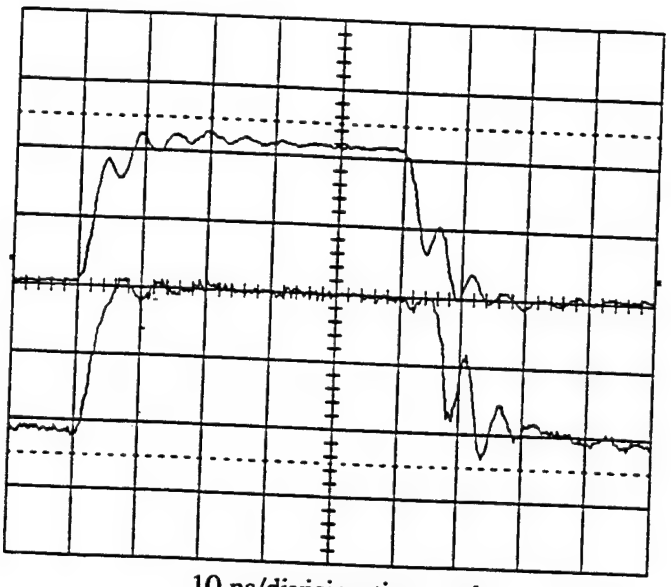


FIGURE F-8. Detected RF Pulse Out of 2- Millimeter Switch #1. 2.0 volt, 50 ns wide, 100 ns period.

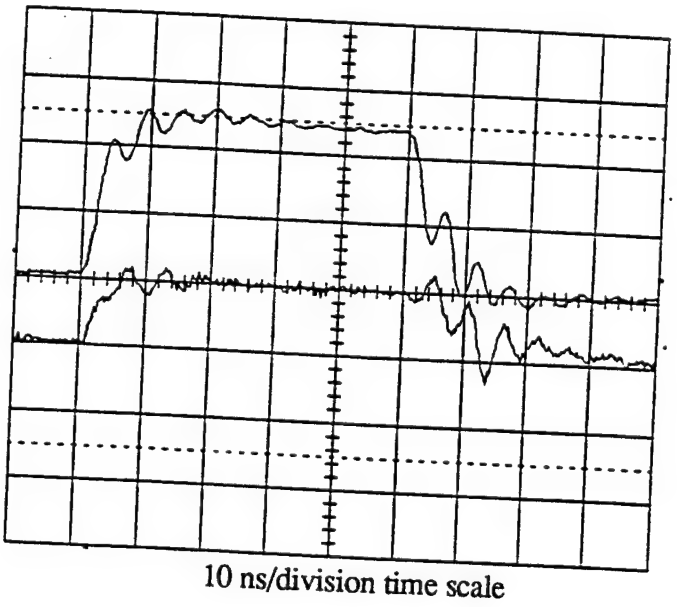


FIGURE F-9. Detected RF Pulse Out of 2-Millimeter Switch #1. 3.0 volt, 50 ns wide, 100 ns period.

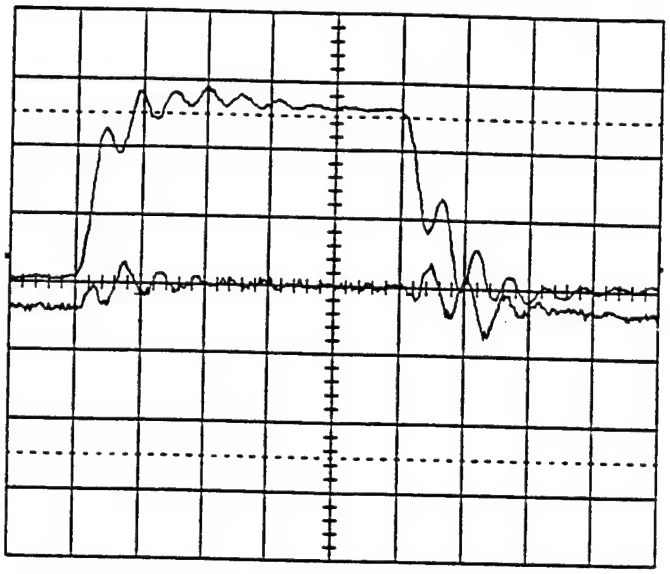


FIGURE F-10. Detected RF Pulse Out of 2-Millimeter Switch #1. 4.0 volt, 50 ns wide, 100 ns period.

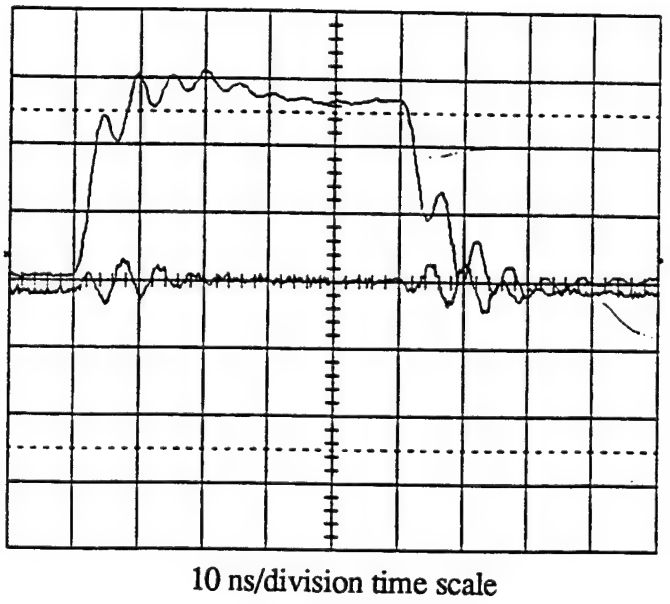


FIGURE F-11. Detected RF Pulse Out of 2-Millimeter Switch #1. 5.0 volt, 50 ns wide, 100 ns period.

## MEASURED INPUT CURRENT PULSE TO SWITCH

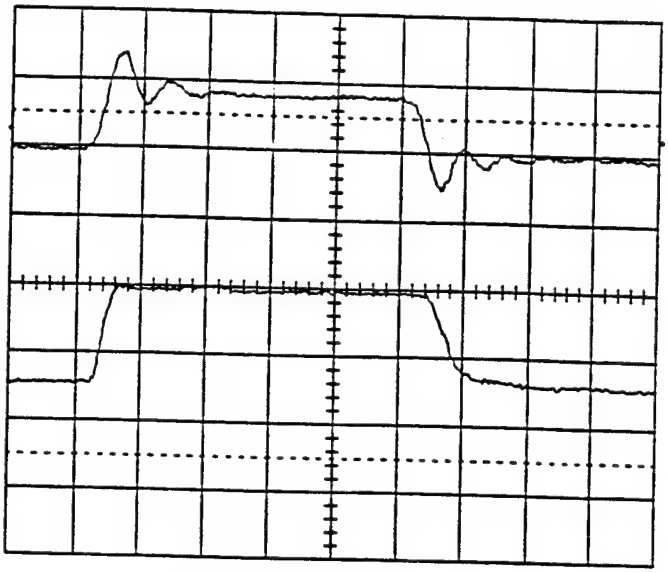


FIGURE F-12. Measured Input Current into and RF Pulse Out of 2-Millimeter Switch #1. 0.5 volt, 50 ns wide pulse, and 500 ns period.

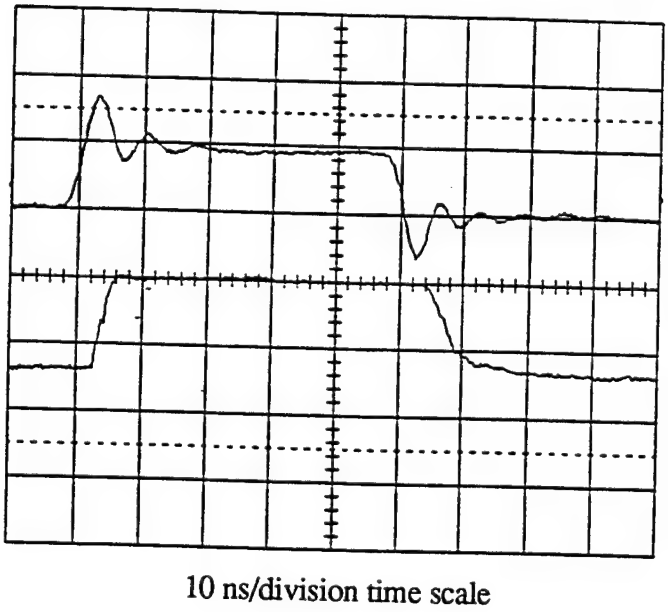


FIGURE F-13. Measured Input Current into and RF Pulse Out of 2-Millimeter Switch #1. 0.71 volt, 50 ns wide, 1000 ns period.

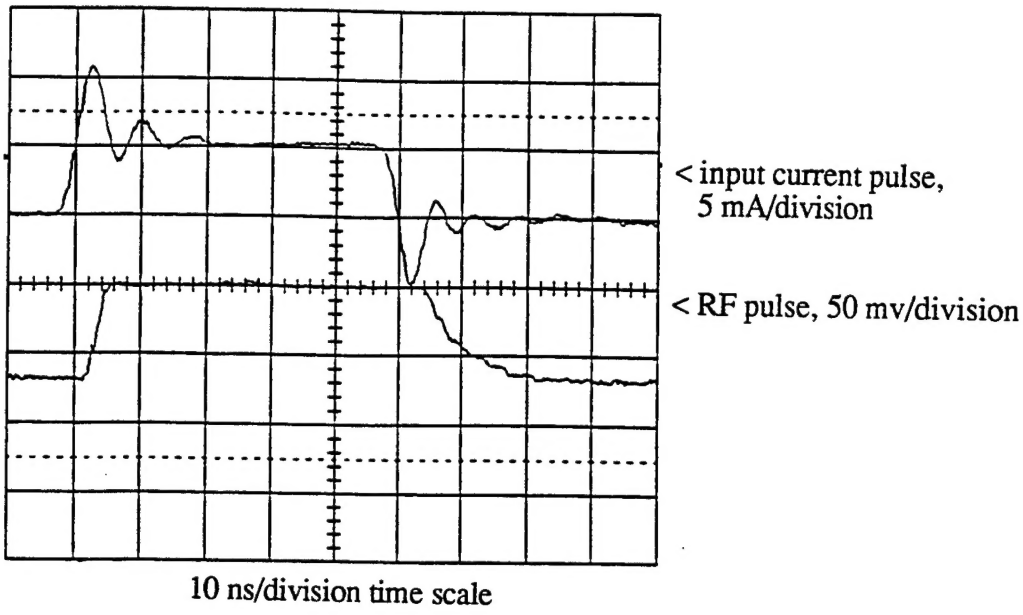


FIGURE F-14. Measured Input Current into and RF Pulse Out of 2-Millimeter Switch #1. 0.8 volt, 50 ns wide pulse, and 1000 ns period.

**MEASURED INPUT CURRENT AND VOLTAGE PULSE TO SWITCH**

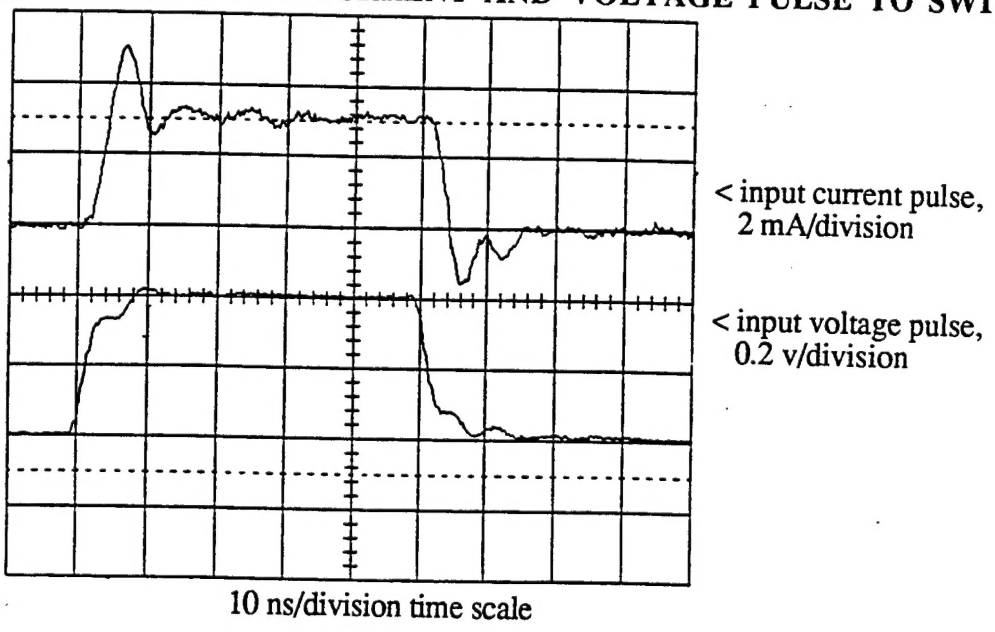


FIGURE F-15. Measured Input Current and Voltage Pulse to 2-Millimeter Switch #1. 0.5 volt, 50 ns wide, 1000 ns period.

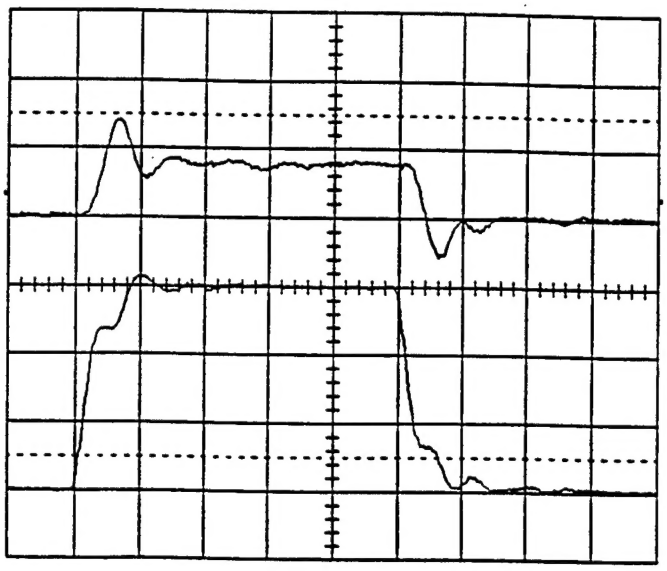


FIGURE F-16. Measured Input Current into and RF Pulse Out of 2-Millimeter Switch #1. 0.71 volt, 50 ns wide pulse, and 500 ns period.

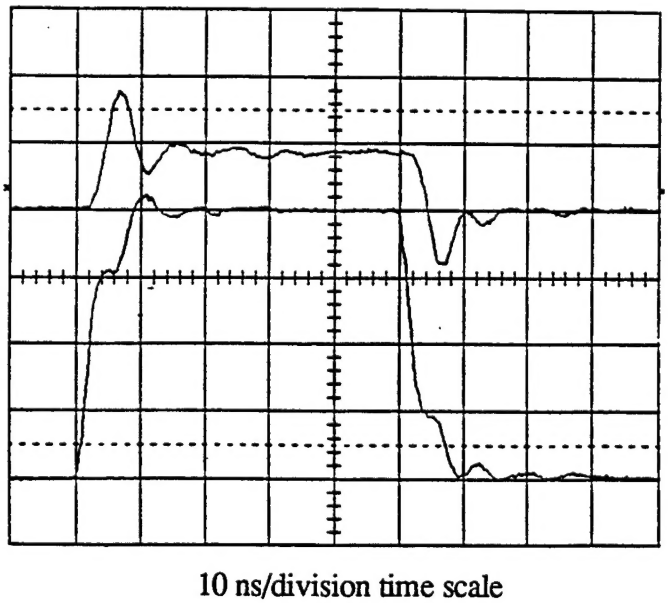


FIGURE F-17. Measured Input Current and Voltage Pulse to 2-mm Switch #1. 0.94 volt, 50 ns wide pulse, and 1000 ns period.

## INITIAL DISTRIBUTION

1 Office of Naval Research, Arlington (Code 312, Dr. D. Van Vechten)
2 Naval Research Labortory
    Code 6300, Dr. D. Gubser (1)
    Code 6850, Dr. M. Nissenoff (1)
2 Army Communications-Electronics Command, Fort Monmouth
    AMSEL-RD-Iew-TAS-M, S. Sahba (1)
    IEWD Directoate, M. Caprario (1)
1 Air Force Wright Laboratories, Dynamics Directorate, Wright-Patterson Air Force Base
  (WL/AAWW-1, P. Ryan)
2 Advanced Research Projects Agency, Arlington, VA
    Dr. F. Patten (1)
    Dr. S. Wolf (1)
4 AEL Defense Corporation, Lansdale, PA
    F. Euchler (1)
    D. Martin (1)
    J. Schuchardt (1)
    G. Sun (1)
2 Dupont, Central Research and Development Experimental Station, Wilmington, DE
    Dr. D. Laubacher (1)
    Dr. A. Lauder (1)
1 Megawave Corporation, Boylston, MA (J. Benham)
1 Strategic Analysis, Incorporated, Arlington, VA (D. Treger)
1 Superconductor Technologies, Santa Barbara, CA (J. Madden)
1 University of Houston, Houston, TX (Deptartment of Electrical Engineering, Dr. J. William)
1 WEO Corporation, Marietta, GA (Dr. J. J. H. Wang)

## ON-SITE DISTRIBUTION

4 Code 4BL000D (3 plus Archives Copy)
3 Code 4B1100D
    D. Banks (1)
    D. Bowling (1)
    A. Martin (1)
1 Code 4B1120D, P. Overfelt
1 Code 4B4000D, S. Chesnut
2 Code 455560D
    W. Katzenstein (1)
    J. Otto (1)
1 Code 472000D, K. Higgins
6 Code 472200D
    C. Hauser (1)
    T. Hoppus (1)
    B. Joy (1)
    J. McCammon (1)
    D. Stapelton (1)
    D. Wagner (1)
2 Code 472230D
    D. Paolino (1)
    F. Schieffen (1)
15 Code 472310D, M. Neel